CONTRACT NO. A832-132
FINAL REPORT
NOVEMBER 1993

Particulate and Gaseous Organic Receptor Modeling for the Southern California Air Quality Study

CALIFORNIA ENVIRONMENTAL PROTECTION AGENCY

AIR RESOURCES BOARD
Research Division

PARTICULATE AND GASEOUS ORGANIC RECEPTOR MODELING FOR THE SOUTHERN CALIFORNIA AIR QUALITY STUDY

Final Report
Contract No. A832-132

Prepared for:

California Air Resources Board
Research Division
2020 L Street
Sacramento, California 95814

Prepared by:

John G. Watson
Judith G. Chow
Zhiqiang Lu
and
Alan W. Gertler

Desert Research Institute
P. O. Box 60220
Reno, Nevada 89506

NOVEMBER 1993

DISCLAIMER

The statements and conclusions in this report are those of the contractor and not necessarily those of the California Air Resources Board. The mention of commercial products, their source or their use in connection with material reported herein is not to be construed as either an actual or implied endorsement of such products.

ABSTRACT

The Chemical Mass Balance (CMB) receptor model was applied to the chemically-speciated diurnal particulate matter samples and volatile organic compound (VOC) acquired during the summer and fall campaigns of the Southern California Air Quality Study (SCAQS). Source profiles applicable to the Los Angeles area were used to apportion $PM_{2.5}$ and PM_{10} to primary paved road dust, primary construction dust, primary motor vehicle exhaust, primary marine aerosol, secondary ammonium nitrate, and secondary ammonium sulfate. Nonmethane hydrocarbon was apportioned to motor vehicle exhaust, liquid fuel, gasoline vapor, gas leaks, architectural and industrial coatings, and biogenic emissions. Suspended dust was the major contributor to PM_{10} during the summer, while secondary ammonium nitrate and primary motor vehicle exhaust contributions were high in the fall. Motor vehicle exhaust was the major contributor to nonmethane hydrocarbons, ranging from 30% to 70% of the total. Liquid fuel, gasoline vapor, and gas leaks were also significant contributors, while contributions from architectural coatings and other emitters were negligible.

ACKNOWLEDGEMENT

The authors wish to acknowledge the secretarial and technical staff at DRI for its indispensable help in producing this manuscript. Ms. Kim Snow, Ms. Bridget Ball, Ms. Sandra Chandra, Ms. Dana Dondero, and Ms. Arlee Fisher typed and edited most of the text and assembled the report. Ms. Barbara Hinsvark prepared figures and captions and supervised copying and binding. The authors are grateful to project officer Dr. Lowell Ashbaugh, Dr. Eric Fujita, Dr. Douglas Lawson, and Mr. Bart Croes of the California Air Resources Board. Mr. Croes assembled the SCAQS aerosol data and provided it in computer compatible formats. Dr. Ashbaugh provided valuable technical guidance during the project. Dr. Fujita provided much help with data validation and quality assurance. His knowledge of the volatile organic compound data base and ARB source profiles for volatile organic compounds was indispensable.

Table of Contents

Table of Contents (continued)

Table of Contents (continued)

Table of Contents (continued)

List of Tables

List of Tables (continued)

List of Tables (continued)

List of Tables (continued)

List of Figures

List of Figures (continued)

List of Figures (continued)

List of Figures (continued)

List of Figures (continued)

List of Figures (continued)

List of Figures (continued)

S.0 EXECUTIVE SUMMARY

The Southern California Air Quality Study (SCAQS) aerosol data set has been extensively evaluated in this study. The spatial and temporal distributions of $PM_{2.5}$ (particles with aerodynamic diameters less than 2.5 μm), and PM_{10} (particles with aerodynamic diameters less than 10 μm) mass have been studied, as have variations in nitrate and carbon species. Source profiles for the dominant particulate and organic emissions sources in the South Coast Air Basin (SoCAB) were assembled, and the Chemical Mass Balance (CMB) receptor model was applied to $PM_{2.5}$, PM_{10}, and volatile organic compound (VOC) data sets. Conclusions are drawn with regard to six of the SCAQS objectives and issues.

The first objective was to evaluate the validity of methods for measuring $PM_{2.5}$, PM_{10}, and precursor species. Findings with respect to this objective are:

- Carbon and elemental measurements in the SCAQS aerosol data are negatively biased by $\sim$20% owing to inhomogeneous aerosol deposits on the filters and analysis methods which were applied to a portion of the filters. These biases seem relatively consistent and do not affect overall study conclusions.

- The organic to elemental carbon ratios during SCAQS differ from those found in earlier studies. This is due to differences in analytical methods rather than changes in aerosol composition.

- Significant fractions (30% to 60%) of ammonium nitrate volatilize during sampling when temperatures are high during the summer. Less than 10% typically volatilizes during the fall when temperatures are lower.

The second objective was to describe the spatial, temporal, size distributions, and chemical and physical characteristics of suspended particles less than 10 μm in aerodynamic diameter. Findings related to this objective are:

- The 24-hour federal PM_{10} standard was exceeded only at the Rubidoux site during the summer campaign. This 164 $\mu g/m^3$ PM_{10} exceedance occurred on August 28, 1987. Daily PM_{10} exceedances were more widespread during the fall campaign, and occurred at five sites on December 3, 1987: 162 $\mu g/m^3$ at the Burbank site; 157 $\mu g/m^3$ at the Downtown Los Angeles site; 194 $\mu g/m^3$ at the Long Beach site; 203 $\mu g/m^3$ at the Anaheim site; and 229 $\mu g/m^3$ at the Rubidoux site. The $PM_{2.5}$ fraction exceeded 150 $\mu g/m^3$ on December 3, 1987 at every site except Downtown Los Angeles and Hawthorne.

- $PM_{2.5}$ constituted one-half to two-thirds of PM_{10} at all sampling sites. The $PM_{2.5}$ portion of PM_{10} was higher during fall than during summer.

- The most abundant species (generally >1 $\mu g/m^3$) in PM_{10} at all sites were chloride, nitrate, sulfate, ammonium, sodium, organic carbon, elemental carbon, calcium, and iron.

- Sodium, aluminum, silicon, calcium, and iron were abundant only in the PM_{10} fraction, consistent with their presence in marine aerosol (sodium) and suspended dust (aluminum, silicon, calcium, and iron).

- Average concentrations for all species were generally higher in the fall than in the summer. The exception is sulfate, where the summer averages are nearly twice the fall averages at the six sites which operated during both seasons.

The third objective was to determine the contribution of trace metals to atmospheric aerosols in source and receptor areas as a function of particle size. Findings related to this objective are:

- Potentially toxic trace metal concentrations measured during SCAQS were low. The maximum 24-hour concentrations observed at all sites in the PM_{10} fraction were: 1) 0.019 $\mu g/m^3$ of vanadium at the Hawthorne site; 2) 0.064 $\mu g/m^3$ of chromium at the Hawthorne site; 3) 0.137 $\mu g/m^3$ of manganese at the Rubidoux site; 4) 0.033 $\mu g/m^3$ of nickel at the Anaheim site and 0.031 $\mu g/m^3$ at the Hawthorne site; 5) 0.38 $\mu g/m^3$ of copper at the Hawthorne site; 6) 0.667 $\mu g/m^3$ of zinc at the Hawthorne site; 7) 0.032 $\mu g/m^3$ of arsenic at the Downtown Los Angeles site; 8) 0.023 $\mu g/m^3$ of selenium at the Burbank site; 9) 0.042 $\mu g/m^3$ of strontium at the Burbank and Hawthorne sites; 10) 0.020 $\mu g/m^3$ of barium at the Downtown Los Angeles site; 11) 0.02 to 0.03 $\mu g/m^3$ of mercury at all sites; and 12) 0.46 $\mu g/m^3$ of lead at the Long Beach site. Many of these maxima were at or near instrumental detection limits. All of these maximum concentrations occurred during the fall campaign.

- The quarterly lead standard of 1.5 $\mu g/m^3$ was never exceeded on any of the SCAQS samples.

The fourth objective was to determine which chemical and physical properties of ambient concentrations and source emissions are most useful for source attribution of receptor concentrations. This applies to the source attribution of $PM_{2.5}$, PM_{10}, and VOCs. Findings from this study are:

- SCAQS chemical measurements were sufficient to resolve $PM_{2.5}$ and PM_{10} source contributions of primary geological material, primary motor vehicle exhaust,

primary marine aerosol, primary lime/gypsum/construction dust, and secondary sulfates and nitrates.

- SCAQS chemical measurements were sufficient to determine that industrial sources and vegetative burning were not major contributors to suspended particles during summer and fall.

- SCAQS chemical measurements were insufficient to: 1) separate secondary organic aerosols and cooking contributions from other source types; 2) allow different types of fugitive dust to be resolved; and 3) distinguish gasoline-fueled vehicle exhaust from diesel-fueled vehicle exhaust.

- Ratios of ethene to ethyne in the vehicle exhaust profiles are twice the ethene/ethyne ratios in ambient samples collected during the morning when exhaust is fresh and photochemical reactions are minimal. This discrepancy can significantly affect the receptor model source contribution estimates for vehicle exhaust.

- Hydrocarbons with reactivity equal to or less than toluene are sufficiently stable to be used as fitting species in the CMB analysis. More reactive species should not be used.

- There were significant amounts of propane in the western part of the basin (especially at the Hawthorne site) which are not related to gasoline or vehicle exhaust. Source profiles containing propane are needed to explain these concentrations.

- Vehicle exhaust contains some liquid gasoline and these profiles are partially collinear. The ability to resolve these two sources depends upon the relative abundance of ethyne (combustion products) in the source profile relative to species associated with uncombusted gasoline.

- Profiles derived from gasoline headspace vapors reflect evaporative emissions due to refueling, diurnal emissions, and running loss. Profiles for vehicle exhaust, liquid gasoline, gasoline vapor, and geogenic natural gas are partially collinear.

- Using commercial natural gas, geogenic natural gas, and liquefied petroleum gas together provides better model performance than any one of the profiles alone.

The fifth objective was to quantify the amounts and uncertainties of source contributions estimated by receptor models as a function of chemical and physical properties used to characterize sources. This applies to $PM_{2.5}$, PM_{10}, and VOCs. The major findings of this study are:

- Primary geological material was the major contributor to PM_{10} during summer at the eastern sites, and its average source contributions at the Rubidoux and Azusa sites were approximately five times the primary geological material contribution at the Hawthorne site. Primary geological material contributions were significantly lower during the fall, with the exception of contributions at the Rubidoux site. The primary lime/gypsum (construction) contribution nearly equals the primary geological contribution during the fall. Rubidoux was the only site with the lime/gypsum contribution. The overwhelming source of primary geological material is paved road dust. The largest primary geological material contribution of 51 ± 5 $\mu g/m^3$ was found at the Azusa site on August 28, 1987 when 24-hour PM_{10} was 120 $\mu g/m^3$.

- Primary motor vehicle exhaust was generally the second largest contributor, except at the Rubidoux, Hawthorne, and Long Beach sites during summer. The average contributions at the Burbank, Downtown Los Angeles, Rubidoux, Azusa, and Claremont sites were two to three times the average contributions at the Hawthorne, Long Beach, and Anaheim sites. Primary motor vehicle exhaust was the major contributor at all sites, even at the Hawthorne, Long Beach, and Anaheim sites which showed much lower contributions from this source during the summer. The largest primary motor vehicle exhaust contribution of 74 ± 31 $\mu g/m^3$ was found at the Long Beach site on December 3, 1987 when 24-hour PM_{10} was 194 $\mu g/m^3$.

- During summer, secondary ammonium sulfate contributions were fairly uniform across the SoCAB. During fall, secondary ammonium sulfate contributed uniformly across the SoCAB, but its average contribution was less than half that found during summer. The largest secondary ammonium sulfate contribution of 27 ± 9 $\mu g/m^3$ was measured at the Hawthorne site on June 24, 1987 when 24-hour PM_{10} was 75 $\mu g/m^3$.

- Primary marine aerosol also showed a fairly homogeneous distribution across the SoCAB during summer, including its contribution at the San Nicolas Island site. During fall, the primary marine aerosol contribution was lower than during summer and was substantially lower at the inland sites relative to the sites near the coast. The largest primary marine aerosol contribution of 11 ± 2 $\mu g/m^3$ was found at the Long Beach site on September 2, 1987 when 24-hour PM_{10} was 65 $\mu g/m^3$.

- Secondary ammonium nitrate at the Rubidoux site was five to ten times larger than averages measured at the other sites during summer. During fall, secondary ammonium nitrate was the second largest contributor at all sites. The largest secondary ammonium nitrate contribution of 96 ± 18 $\mu g/m^3$ was found at the Anaheim site on December 3, 1987 when 24-hour PM_{10} was 203 $\mu g/m^3$.

- Temporal and spatial uniformity in ratios of hydrocarbons normally associated with vehicle exhaust and gasoline with carbon monoxide and nonmethane hydrocarbon (NMHC) indicate that vehicle-related emissions were the major source of NMHC in the SoCAB.

- Vehicle exhaust was the main source of NMHC at all sites and time periods, ranging from 30% to 70% of NMHC. The relative contributions of vehicle exhaust were greater during fall, particularly for the morning samples (66% to 71% in the fall versus 42% to 65% in the summer). This seasonal difference is consistent with the reactive organic gas emissions inventory, which shows higher relative contribution from vehicle exhaust during the fall than during the summer.

- The contribution of liquid gasoline was generally greater in the morning samples at most sites during summer, and was higher in the central part of the basin (15% to 23%) and lower in the afternoon in the eastern part of the basin (2% to 5%). The relative contribution of liquid gasoline is more uniform, spatially and temporally, during fall.

- Contributions from gasoline vapor were higher in the western part of the basin during the morning and mid-day periods (15% to 24%), lowest in the central basin (2% to 12%), and higher in the afternoon in the eastern basin (10% to 15%). The combined contributions of commercial natural gas, geogenic natural gas, and liquefied petroleum gas showed the same pattern as gasoline vapor.

- Contributions from architectural and industrial coatings were negligible, consistent with the strong correlation in the ambient data between toluene and carbon monoxide.

- The sum of the individual calculated source contributions and the measured ambient NMHC indicates that all major source types were included in the calculations, that the ambient and source profile measurements are reasonably accurate, and that the source profiles are reasonably representative of actual emissions.

The final objective was to determine the portions of $PM_{2.5}$ and PM_{10} which are of primary and secondary origin.

- On average, secondary ammonium sulfate and secondary ammonium nitrate contributed 20% to 32% of the PM_{10} during summer and 20% to 38% of PM_{10} during fall. These secondary contributors typically accounted for one-half to two-thirds of $PM_{2.5}$.

- Secondary organic carbon was not detectable in the SCAQS aerosol data set. Other studies performed during SCAQS showed that up to 40% of the organic

carbon measured in the afternoon sample might be of secondary origin. This is expected only during summer episodes with intense photochemistry and in the eastern SoCAB. If they exist, secondary organic carbon contributions to 24-hour PM_{10} are small.

- During the summer, secondary ammonium nitrate contribution appears to be ammonia-limited at every site except Rubidoux. This is not the case during the fall, when it is not known whether the secondary ammonium nitrate is limited by ammonia or nitric acid precursors.

1.0 INTRODUCTION

1.1 Background and Objectives

The Southern California Air Quality Study (SCAQS) was conducted by the California Air Resources Board (ARB) during the summer and fall of 1987 to better understand the causes of excessive pollution concentrations in California's South Coast Air Basin (SoCAB, Lawson *et al.*, 1990). SCAQS was carefully planned (Blumenthal *et al.*, 1987) and executed (Hering and Blumenthal, 1989) to acquire measurements of pollutant and meteorological variables which influence ozone and suspended particulate matter concentrations.

SCAQS acquired simultaneous meteorological, air quality, and visibility measurements at more than forty measurement locations throughout the SoCAB. Additional measurements were made for five episodes of one- to three-days duration (eleven days total) between 6/19/87 and 9/3/87 (termed the "summer" campaign) and for three episodes of one- to three-days duration (six days total) between 11/11/87 and 12/11/87 (termed the "fall" campaign). The summer episodes were selected according to forecasts of elevated ozone and particulate matter concentrations while fall episodes were selected to correspond to meteorological stagnation.

Extensive particulate and volatile organic compound (VOC) measurements were acquired during these episodes at nine locations during the summer and at six locations during the fall. This report analyzes these particulate and VOC concentrations to accomplish several of the objectives and sub-objectives identified by Blumenthal *et al.* (1989). These objectives include:

- Evaluate the validity of methods for measuring $PM_{2.5}$ (particles with aerodynamic diameters less than 2.5 μm), PM_{10} (particles with aerodynamic diameters less than 10 μm), and precursor species.

- Describe the spatial, temporal, size-distribution, and chemical and physical characteristics of suspended particles less than 10 μm aerodynamic diameter.

- Determine the contribution of trace metals to atmospheric aerosols in source and receptor areas as a function of particle size.

- Determine which chemical and physical properties of ambient concentrations and source emissions are most useful for source attribution of receptor concentrations.

- Quantify the amounts and uncertainties of source contributions estimated by receptor models as a function of chemical and physical properties used to characterize sources.

- Determine the portions of PM_{10} and $PM_{2.5}$ which are of primary and secondary origin.

The approach taken in this report is receptor-oriented rather than source-oriented. Both source-oriented dispersion models and receptor models have been used to apportion atmospheric constituents to sources. Receptor models use the chemical and physical characteristics of gases and particles measured at source and receptor to both identify sources and quantify their contributions to the receptor. The characteristics used for these purposes must be such that: 1) they are present in different proportions in different source emissions; 2) these proportions remain relatively constant for each source type; and 3) changes in these proportions between source and receptor are negligible or can be accounted for. Spatial and temporal differences in source contributions are often used to validate receptor model outputs and to increase the specificity of the apportionment.

The SCAQS data set includes two subsets, the chemically-speciated aerosol measurements for $PM_{2.5}$ and PM_{10} (Collins and Fujita, 1989; Countess, 1989; Hering and Blumenthal, 1989; Hering, 1990), and the chemically-speciated VOC measurements (Fujita *et al.*, 1992; Lurmann and Main, 1992), which are appropriate for the application of receptor models. Both of these data sets are examined in this report.

1.2 Relationships to Other SCAQS Studies

This project is one of several which have examined different components of the suspended particulate and VOC data sets. Other relevant studies include:

- Size-Time-Compositional Analyses of Aerosols During SCAQS (Cahill *et al.*, 1990). This study describes elemental concentration data acquired by the Interagency Monitoring of PRQtected Visual Environments (IMPROVE) and Davis Rotating-drum Unit for Monitoring (DRUM) samplers coupled with elemental analysis by Proton Induced X-ray Emission (PIXE) spectroscopy. Measurements taken by the University of California Davis (UCD) at the SCAQS Long Beach, Claremont, and Rubidoux sites during summer and at the Long Beach and Downtown Los Angeles sites during fall show particle size distributions of different chemical species and how these distributions change with time.

- Descriptive Analysis of Organic and Elemental Carbon Concentrations (Huntzicker and Turpin, 1991; Turpin and Huntzicker, 1991). This study examined particulate organic and elemental carbon concentrations, measured with a continuous thermal/optical transmission carbon analyzer during summer at the Claremont site and during the fall at the Long Beach site, to determine diurnal variations in these aerosol components. Changes in the ratio of organic to elemental carbon were interpreted as varying influence of secondary organic carbon aerosol formation.

- Acidic Aerosol Size Distributions (John *et al.*, 1989; 1990). This study examined chemically-specific size distributions acquired with cascade impactors at the Long Beach, Claremont, and Rubidoux sites during summer, and at the Long Beach and Downtown Los Angeles sites during fall. Size distributions were plotted for chloride, sulfate, nitrate, ammonium, and sodium for each of the four samples taken on each episodic day. Different particle size modes were identified and classified according to formation mechanisms.

- Long-Term Chemical Characterization of PM_{10} in Claremont (Summer) and Long Beach (Fall) (Wolff *et al.*, 1991). This study acquired daytime and nighttime samples of 12-hours duration for the full 59 days of the summer campaign and the full 23 days of the fall campaign. Average concentrations for the most abundant chemical species from the entire sampling periods were compared with those acquired during the SCAQS episodes.

- Analysis of Ambient Volatile Organic Compound Data (Fujita *et al.*, 1992; Lurmann and Main, 1992). This study examined the relative abundances of different organic species present in the gas phase at 0600, 1100, and 1500 PDT (PST in the fall) and compared them with those anticipated from emissions inventories.

Other aerosol and visibility data sets, specified by Lawson (1990), were acquired and are undergoing interpretation by other investigators, and they are not examined here. This study performs a detailed examination of the SCAQS aerosol data which were acquired as five sequential samples per day at nine sites in the summer and six sites in the fall. An extensive examination of measurement methods and an evaluation of the data is made as a prelude to attributing aerosol concentrations to sources. This study builds on the work of Fujita (1992) and Lurmann and Main (1992) by applying more specific source apportionment methods to the VOC data which have already been subjected to detailed examination in these prior studies. Results from the studies cited above, and from previous aerosol and VOC source apportionment efforts in the SoCAB, are related to the receptor modeling source apportionment results of this study.

1.3 Guide to Report

This section states the objectives of this study and its relationship to other SCAQS data analysis efforts. Section 2 describes the physical and meteorological setting in which the measurements were conducted and identifies known or hypothesized relationships between emissions, meteorology, atmospheric transformations, and ambient concentrations of suspended particles and VOCs. Section 3 documents the measurement methods applied during SCAQS and describes the extensive validation of the SCAQS gas/aerosol sampler measurements. Essential information from several SCAQS measurement reports has been unified in this section as part of the aerosol data evaluation. Since extensive VOC data validation was completed by Lurmann and Main (1992), only a brief summary of their findings is given in this report.

Section 4 presents a descriptive analysis of aerosol data, examining average and maximum concentrations of chemical components in $PM_{2.5}$ and PM_{10} and their gaseous precursors, variations of individual chemical concentrations with time, and covariational relationships among chemical concentrations at different sampling locations. Aerosol and VOC source profiles are assembled and examined in Section 5. Emphasis is placed on understanding the VOC profiles, since the $PM_{2.5}$ and PM_{10} profiles have been extensively evaluated in previous source apportionment studies in the SoCAB and elsewhere. Section 6 presents the methodology and results for receptor model source apportionment of aerosol measurements while Section 7 describes the source apportionment of ambient VOCs. Overall conclusions from this study are stated in Section 8 while Section 9 presents a comprehensive bibliography of related studies.

2.0 PARTICULATE AND ROG EMISSIONS, METEOROLOGY, AND CONVERSION MECHANISMS IN THE SOUTH COAST AIR BASIN

The primary purpose of this study is to explain the sources which contribute to ambient concentrations of suspended particles and reactive organic gases (ROG). A conceptual understanding of those sources, their emissions, and the changes which these emissions undergo between source and receptor is a prerequisite for this type of analysis.

The South Coast Air Basin (SoCAB) occupies more than 16,000 km^2 of the non-desert portions of Los Angeles, San Bernardino, Riverside, and Orange counties in Southern California. The 1990 census lists the population for the three standard metropolitan statistical areas (SMSAs) in the region as 13.8 million, a 25% increase over the 1980 census; five percent of the entire U.S. population lives in the SoCAB. It is estimated that an average of 267 million vehicle miles is traveled daily within the SoCAB. Major commercial activities include tourism, aerospace manufacturing, light manufacturing, oil production and refining, power generation (natural gas combustion), and agriculture (livestock, orchards, and crops). As the population has grown, much agricultural land has been replaced with housing developments, shopping malls, highways, and recreation areas. Figure 2-1 identifies the boundaries of the SoCAB and the locations of long-term monitoring sites operated by the South Coast Air Quality Management District (SCAQMD).

The SoCAB is located on the Pacific Coast in an area of complex terrain. It is bounded to the west and south by the Pacific Ocean, to the north by the San Gabriel and San Bernardino Mountains, and to the east by the San Bernardino and San Jacinto Mountains. The northern and eastern mountain ranges typically exceed 2,000 m in altitude, often rising above the surface mixed layer of the atmosphere. Mount San Jacinto is the tallest peak (3,293 m above MSL). The mountains are populated with chaparral at the lower elevations and Ponderosa Pine and other conifers at the higher elevations ($>1,500$ m).

The SoCAB includes three major sub-basins, the Coastal Plain, the San Fernando Valley, and the San Gabriel/San Bernardino Valleys. The Coastal Plain rises gently from the coast and includes the major cities of Los Angeles, Torrance, Anaheim, Long Beach, Garden Grove, Anaheim, Fullerton, and Santa Ana. It is separated from the San Fernando Valley on the northwest by the Santa Monica Mountains and the Hollywood Hills, and from the San Gabriel/San Bernardino Valleys to the east and northeast by the Chino Hills and the Santa Ana Mountains. Major passes which punctuate the northern and eastern boundaries include Tejon Pass (1,256 m ASL) to the San Joaquin Valley, Soledad Canyon ($\sim$1,000 m ASL) and Cajon Pass ($\sim$1,000 m ASL) to the Mojave Desert, and San Gorgonio Pass ($\sim$750 m ASL) to the Coachella and Imperial Valleys.

Both primary and secondary compounds contribute to PM_{10} and gaseous organic precursors for PM_{10} and ozone. Primary compounds are those which are emitted directly from sources. These compounds undergo few changes between sources and receptors, and atmospheric concentrations are usually proportional to the quantities which are emitted. Secondary compounds are those which form in the atmosphere from primary emittants.

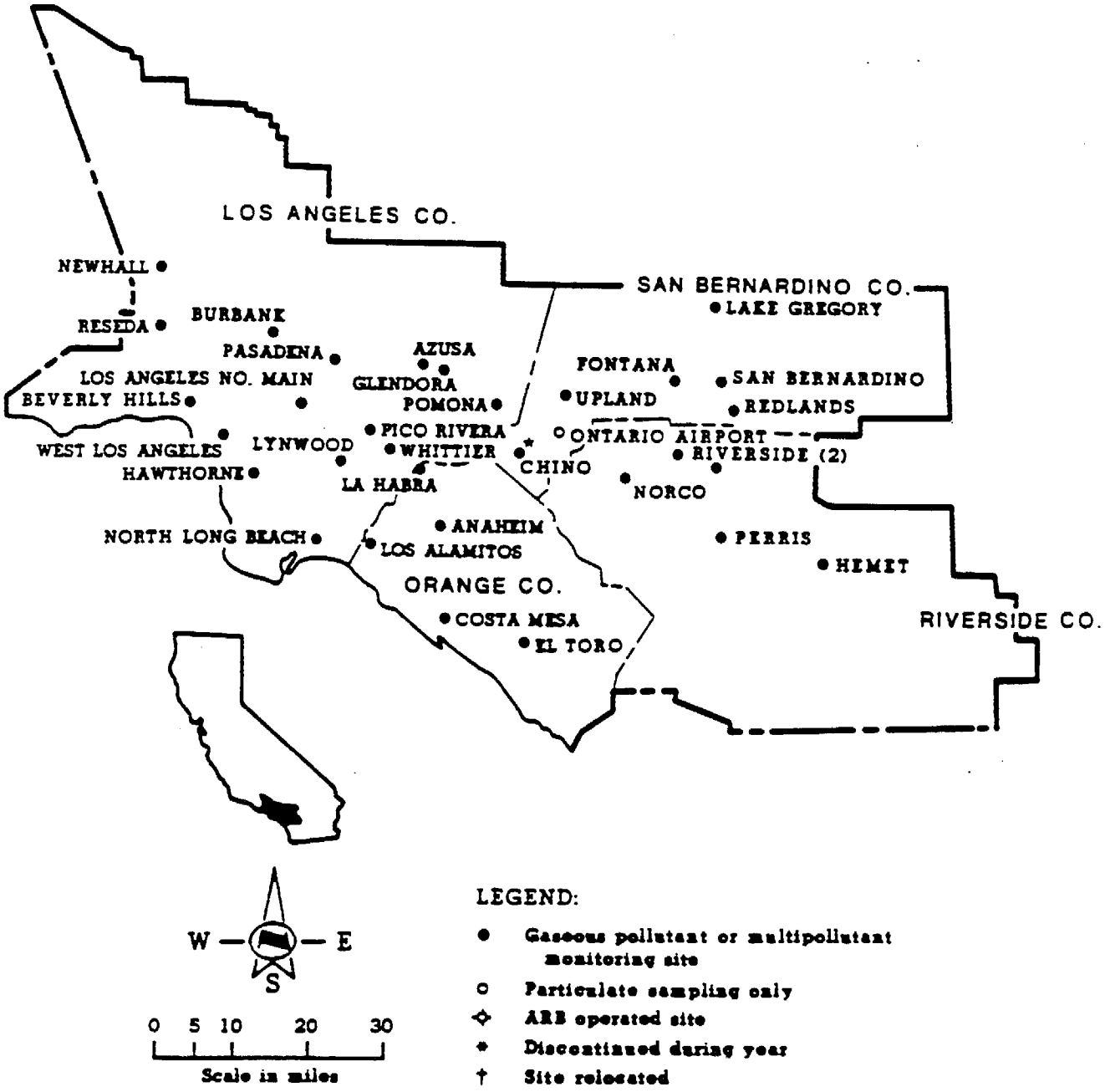

Figure 2-1. Locations of the Ambient Monitoring Sites in the South Coast Air Basin (California Air Resources Board, 1988)

Ammonium sulfate, ammonium nitrate, and sodium nitrates are common secondary particles found in the SoCAB. Carbonyl compounds (ketones and aldehydes), carboxylic acids, dicarboxylic acids, peroxyacetylnitrate (PAN), and organonitrates are secondary organic materials which are often found in abundance. Some of these may be partially present in the particulate phase.

Emissions of primary particles, sulfur dioxide, oxides of nitrogen, ammonia, and organic gases must be coupled with transport and transformation to understand the causes of elevated PM_{10} and VOC levels in the SoCAB.

2.1 Emissions

Air pollution emission rates in the SoCAB are higher than those in any other California Air Basin (California Air Resources Board, 1990). Daily emissions of 2,130 tons of total organic gases (TOG), 1,286 tons of reactive organic gases (ROG), 1,088 tons of nitrogen oxides (NO_x), 124 tons of sulfur oxides (SO_x), 1,180 tons of PM_{10}, and 4,970 tons of carbon monoxide (CO) were estimated to be released into the atmosphere during the year in which SCAQS was conducted. Table 2-1 summarizes the 1987 emissions (California Air Resources Board, 1990) for each county in the SoCAB. These estimates were supplemented during SCAQS by day-specific, hourly, 5 × 5 km gridded emission estimates suitable for modeling studies (Mirabella and Nazemi, 1989; Yotter and Wade, 1989). Fujita *et al.* (1992) have evaluated the SCAQS emissions inventory for ROG.

Table 2-1 shows that Los Angeles and Orange counties account for 82% of TOG, 85% of ROG, 92% of SO_x, 74% of primary PM_{10}, and 85% of CO emissions. The western portion of the SoCAB accounts for the majority of SoCAB emissions, owing to its greater area, higher population density, and concentration of industries and highways. Examining source categories shows that mobile sources, both on-road and off-road, account for 53% of ROG, 74% of NO_x, 59% of SO_x, and only 6% of PM_{10} emissions. Light duty passenger cars and light and medium duty trucks emit the majority of each pollutant for on-road vehicles. With respect to on-road vehicles, 63% of PM_{10} is emitted by gasoline-fueled vehicles with the remainder from diesel-fueled vehicles, primarily heavy-duty trucks. The largest mobile source (on-road and off-road) contributor to SO_x is ship traffic in the ocean and in Los Angeles harbors; ships contribute 47% of the SO_x from mobile sources and 27% of the basin-wide SO_x emissions.

Other significant ROG emitters include architectural and other surface coatings (18% of total), consumer products (5% of total), oil and gas extraction and refining (5% of total), farming operations and pesticides (4% of total), petroleum marketing (3% of total), and degreasing/industrial solvents (3% of total). The remaining sub-categories (e.g., dry cleaning, industrial emissions) do not contribute more than 1% to 2% of ROG according to the 1987 ARB inventory.

Table 2-1
Summary of 1987 Emissions Inventory for the South Coast Air Basin[a] (annualized tons/day)

		Species[b]					
Source	County	TOG	ROG	NO_x	SO_x	CO	PM_{10}
Stationary Fuel Combustion (agricultural, oil & gas production, petroleum refining, other manufac./ industrial, electric util., other services & commerce, residential)	Los Angeles	33	12	190	18	58	11
	Orange	9.0	3.2	36	3.3	9.2	1.3
	Riverside	0.8	0.4	7.7	0.8	3.9	0.4
	San Bernardino	1.6	0.8	21	1.5	6.3	1.0
	All	44.4	16.4	254.7	23.6	77.4	13.7
Stationary Waste Burning (agricultural debris, range and forest management, incineration)	Los Angeles	1.0	0.7	1.6	0.4	2.2	0.8
	Orange	11	8.3	0	0	0.2	0
	Riverside	0.1	0.1	0	0	0.7	0.1
	San Bernardino	0.3	0.2	0	0	0	0.4
	All	12.4	9.3	1.6	0.4	3.1	1.3
Stationary Solvent Use (dry cleaning, degreasing architectural coating, asphalt paving, printing, consumer prod., industrial solvent use)	Los Angeles	310	270	0.2	0	0	1.1
	Orange	86	74	0	0	0	0.2
	Riverside	20	18	0	0	0	0
	San Bernardino	29	28	0	0	0	0.1
	All	445	390	0.2	0	0	1.4
Stationary Petroleum Processing, Storage, and Transfer (oil & gas extraction, petroleum refining and marketing)	Los Angeles	250	69	7.8	17	5.9	2.8
	Orange	48	15	0.4	2.0	0.1	0
	Riverside	7.1	1.5	0	0	0.1	0
	San Bernardino	17	3.7	0.1	0	0.2	0
	All	322.1	89.2	8.3	19.0	6.3	2.8

Table 2-1 (continued)
Summary of 1987 Emissions Inventory for the South Coast Air Basin[a] (annualized tons/day)

		Species[b]					
Source	County	TOG	ROG	NO_x	SO_x	CO	PM_{10}
Stationary Industrial Processes (chemical, food, agricultural, mineral and metal processing, wood and paper industries)	Los Angeles	33	26	8.6	6.8	0.8	31
	Orange	13	10	2.3	0.6	3.7	6.8
	Riverside	2.8	2.2	0.2	0	1.3	2.9
	San Bernardino	3.8	3.0	0.4	0	0.9	4.1
	All	52.6	41.2	11.5	7.4	6.7	44.8
Stationary Miscellaneous Processes (pesticide appl., farming, construction and demolition, road dust, unplanned fires, waste disposal, natural sources)	Los Angeles	110	19	1.4	0	66	550
	Orange	230	9.6	0.9	0	14	210
	Riverside	85	19	0.6	0.1	23	160
	San Bernardino	110	19	0.5	0	22	130
	All	535	66.6	3.4	0.1	125	1050
Mobile On-Road Vehicles (light duty passenger, light and med. duty trucks, heavy duty gas and diesel trucks, motorcycles, and buses)	Los Angeles	430	400	420	20	2800	36
	Orange	140	130	130	6.4	890	12
	Riverside	35	33	51	2.4	250	4.8
	San Bernardino	52	49	64	3.0	350	6.4
	All	657	612	665	31.8	4290	59.2
Other Mobile Sources (off road vehicles, trains, ships, aircraft, mobile and utility equipment)	Los Angeles	42	40	94	36	310	7.1
	Orange	12	12	22	3.4	92	2.4
	Riverside	13	12	9.1	0.9	51	2.3
	San Bernardino	12	12	16	1.6	61	2.1
	All	79	76	141.1	41.9	514	13.9

Table 2-1 (continued)
Summary of 1987 Emissions Inventory for the South Coast Air Basin[a] (annualized tons/day)

		Species[b]					
Source	County	TOG	ROG	NO_x	SO_x	CO	PM_{10}
All Sources	Los Angeles	1200	830	720	98	3200	640
	Orange	540	260	200	16	1000	230
	Riverside	160	86	68	4.2	330	170
	San Bernardino	230	110	100	6.2	440	140
	All	2130	1286	1088	124.4	4970	1180

[a] California Air Resources Board, 1990a.
[b] Species:

TOG: Total Organic Gases include compounds containing hydrogen and carbon in combination with one or more other elements. These include aldehydes, ketones, organic acids, esters, and ethers.

ROG: Reactive Organic Gases include all organic gases except non-reactive species such as methane and low molecular weight halocarbons. ROGs are relatively reactive and are the most likely precursors of photochemical aerosol.

NO_x: Nitrogen Oxides, reported as equivalent amounts of NO_2, include nitric oxide (NO) and nitrogen dioxide (NO_2) gases.

SO_x: Sulfur Oxides, reported as equivalent amounts of SO_2, include sulfur dioxide (SO_2) and sulfur trioxide (SO_3).

CO: Carbon Monoxide, a pure species that is reported as equivalent amounts of CO.

PM_{10}: Primary PM_{10}, particles in the 0 to 10 μm aerodynamic size range that are emitted in a liquid or solid phase. This includes dust, sand, salt spray, metallic and mineral particles, pollen, smoke, mist, and acid fumes.

Fuel burning at industrial point sources (oil and gas production, refining, manufacturing, and electric utilities) constitutes 17% of non-mobile NO_x emissions. Many emissions originate from stacks ranging from 30 to 100 m in height above ground level. These same point sources are also significant SO_x emitters, constituting 17% of total SoCAB SO_x emissions.

PM_{10} emissions are dominated by miscellaneous processes, most of which can be characterized as fugitive dust emissions. Eighty-five percent of the total PM_{10} emissions are estimated to originate in fugitive dust, with 59% of the total deriving from paved road dust, 19% from construction and demolition, and 7% from agricultural tilling and travel on unpaved roads. Table 2-1 shows that sources other than primary vehicle exhaust and fugitive dust are minor emitters of PM_{10}.

The 1987 ARB inventory in Table 2-1 served as a basis for calculating the gridded, hourly average, day-specific inventory used for SCAQS modeling (Harley *et al.*, 1993). Day-specific adjustments reflect changes in motor vehicle hydrocarbon emissions with changes in ambient temperature, and this causes slight differences between summer and fall inventories. Allocations to modeling grids are based on estimates of vehicle miles travelled, locations of known point sources, and census data.

Yotter and Wade (1989) show the spatial distribution of ROG and NO_x emissions in the SoCAB from mobile sources in the SCAQS emissions inventory. Every grid square shows substantial emissions from vehicular sources, though the highest peaks are found in downtown Los Angeles and correspond to major interchanges of the freeway system.

Temporal variations of ROG and NO_x in the SCAQS inventory are illustrated in Figures 2-2 and 2-3, respectively, from Fujita (1992). The majority of ROG and NO_x emissions occur between 0600 and 1800 PST, which usually corresponds to daylight hours in the summer. The diurnal cycle for NO_x is largely driven by on-road motor vehicle sources and varies little between summer and winter. The ROG cycle is only partially driven by on-road motor vehicle emissions, which constitute the majority of ROG during morning and evening rush hours, and somewhat less than half of all ROG emissions during other hours.

Figure 2-2 breaks down the on-road motor vehicle source emissions into functional rather than vehicle-type categories (as is done by California Air Resources Board, 1990). Hot exhaust, diesel, and cold start in Figure 2-2 refer to tailpipe emissions. Hot exhaust and diesel refer to ROG tailpipe emissions when a gasoline- or diesel-fueled vehicle is fully warmed up. Cold start emissions are additional emissions from gasoline-fueled vehicle tailpipes which occur when the engine and catalyst are at less than normal operating temperatures. Notice that this fraction is most significant in the morning, and especially winter mornings, when ambient temperatures are expected to be lowest. The remaining mobile source categories refer to evaporative emissions, with diurnal losses arising from vaporization and escape of liquid fuel in the gas tank as the daily temperature rises, hot soak emissions from evaporation of gasoline in the fuel system (e.g., the carburetor) at the end of a trip, and running losses from fuel system leaks during the trip. The evaporation of gasoline during transfer operations at service stations and refineries is not

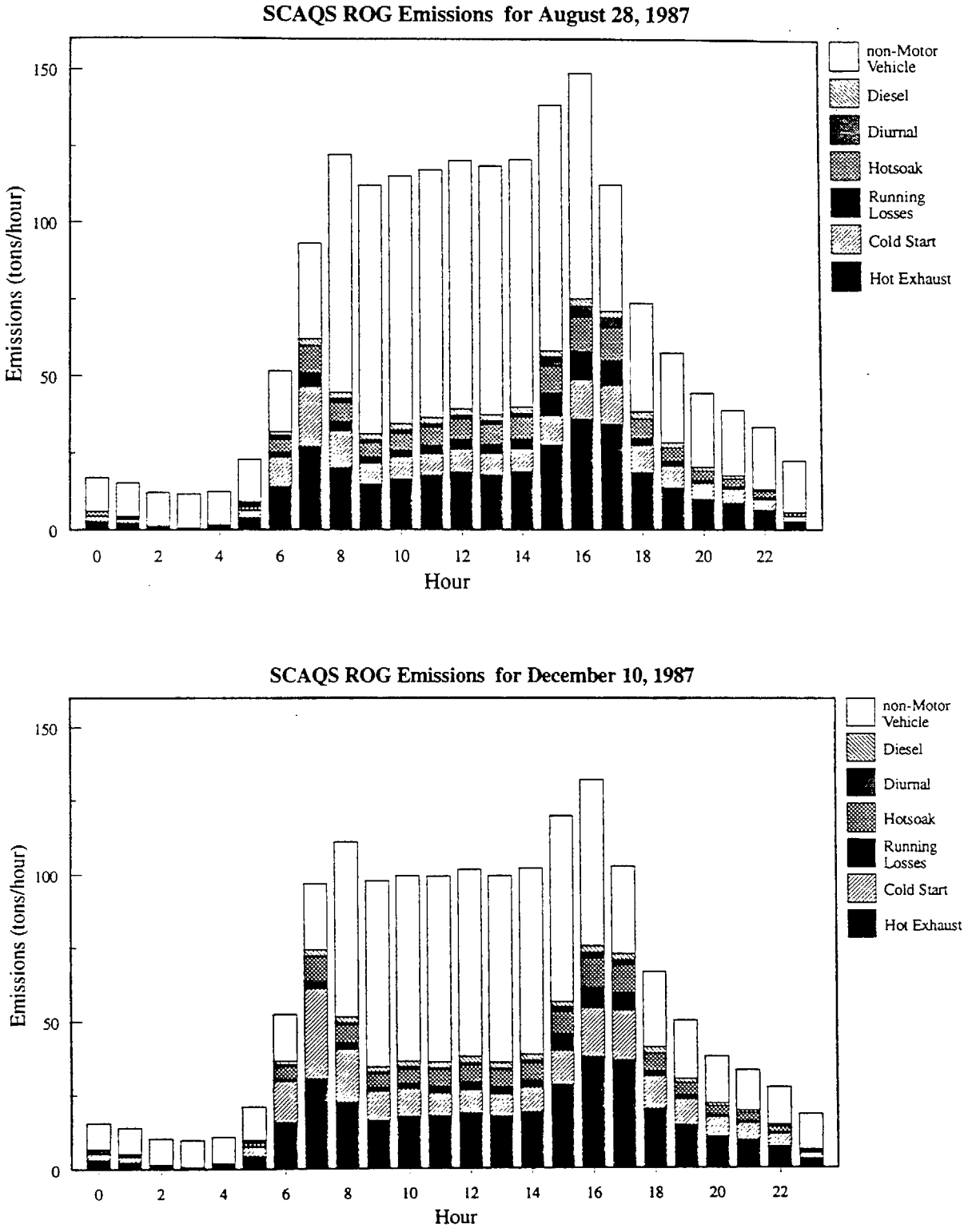

Figure 2-2. Hourly Reactive Organic Gas Emissions for the SoCAB Modeling Domain

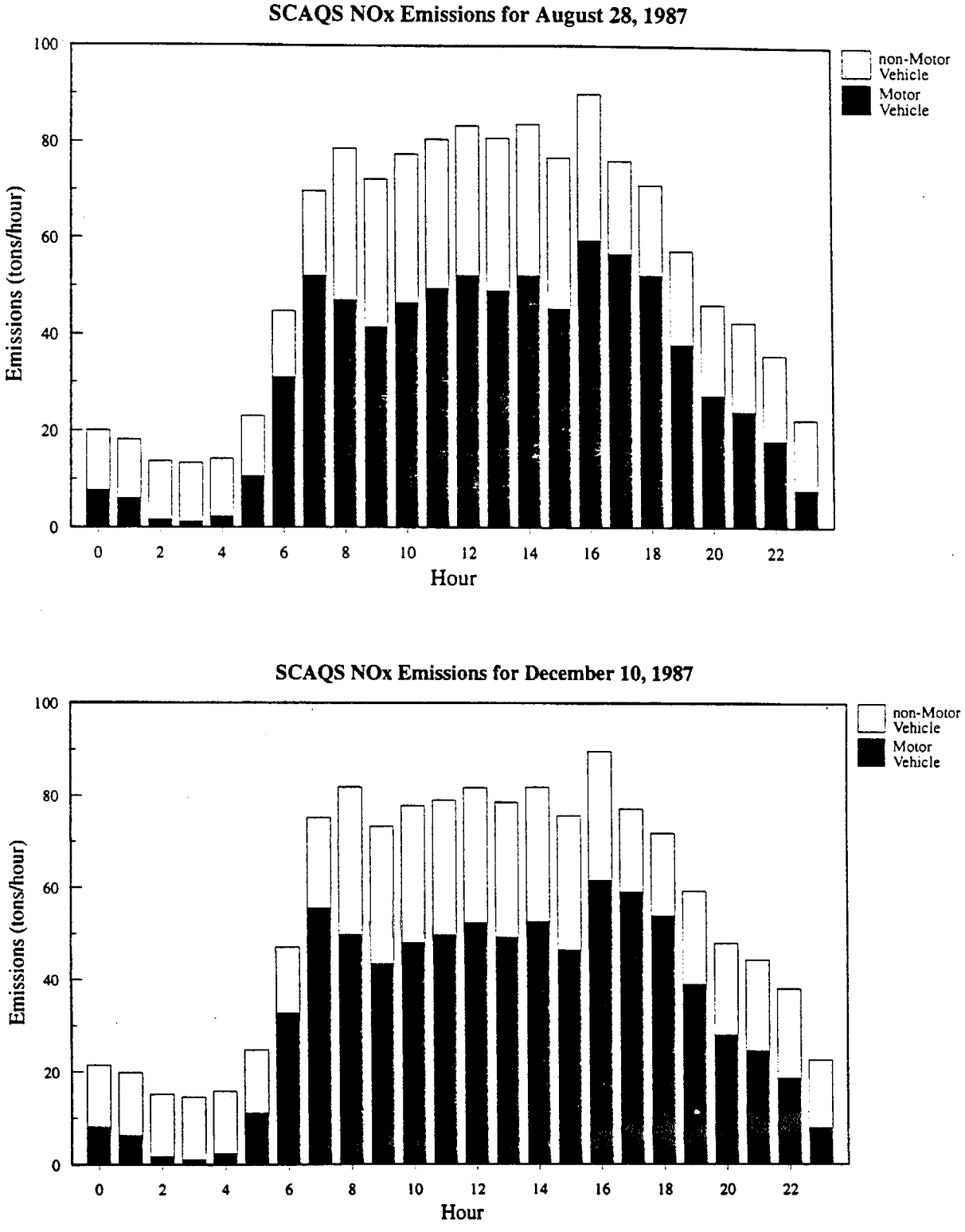

Figure 2-3. Hourly Nitrogen Oxide Emissions for the SoCAB Modeling Domain

included in the motor vehicle category, though its chemical characteristics are similar to those of mobile source evaporative emissions.

Several other emissions which are not listed in Table 2-1 are important for understanding particulate and ozone concentrations in the SoCAB. Biogenic and geogenic emission rates are not included, and they can be significant. Biogenic ROG emissions in the SoCAB have been estimated to be 100 to 200 tons/day (Winer *et al.*, 1983; Horie *et al.*, 1990; Causley and Wilson, 1991), with substantial dependence on plant type, leaf biomass, wind speed, and temperature. Harley *et al.* (1993) use a value of 117 tons/day of biogenic ROG for ozone modeling of the August 27-29, 1987, SCAQS episode. This emission rate is comparable to those of many other source types in Table 2-1. Geogenic hydrocarbon gases might be expected in areas where oil is extracted, but estimates of their magnitudes are not available.

Ammonia (NH_3) emissions are known to be important components of secondary sulfate and nitrate compounds, and these rates are not contained in the 1987 ARB emissions inventory, though Dickson *et al.* (1989) describe plans to enhance the earlier inventory of Gharib and Cass (1984). Russell and Cass (1986) estimated 164 tons/day of ammonia emitted, with 2 tons/day from industrial point sources, 3 tons per day from stationary fuel combustion, 3 tons/day from mobile sources, 9 tons/day from fertilizer, 15 tons/day from sewage treatment, 23 tons/day from humans and pets, 24 tons/day from exposed soil, and 85 tons/day from livestock. The spatial distribution shows peaks corresponding to dairies and feedlots, with a large concentration of ammonia emissions in the Chino area.

Hildemann *et al.* (1991) have recently identified charbroiling and frying of meat in both restaurants and homes as a potential source of particulate matter which has been neglected in previous PM_{10} inventories. Their studies show that almost all of these emissions are in the $PM_{2.5}$ size fraction. Emissions rates measured for regular and extra-lean hamburger meat which was charbroiled or fried on a restaurant-style grill (with commonly used grease traps) showed emissions rates of 40 g/kg charbroiled regular meat, 7.1 g/kg charbroiled extra-lean meat, 1.1 g/kg fried regular meat, and 1.4 g/kg fried extra-lean meat. If one assumes that average daily meat consumption is 0.1 kg/meat-eater times 10,000,000 meat-eaters in the SoCAB times 5 g/kg emissions, the organic particle emissions would be on the order of 5 tons/day, which is comparable to the particulate emissions estimates from motor vehicle exhaust.

The emissions values reported in Table 2-1 are especially limited by incomplete knowledge of pollution emissions factors for: 1) ROG; 2) primary particles from mobile sources; and 3) primary particles from fugitive dust.

Ingalls *et al.* (1989) showed that on-road emissions of ROG and CO during SCAQS were significantly larger than those calculated by the ARB mobile source emissions model (EMFAC7E) for Table 2-1. Pierson *et al.* (1990) demonstrated that the SCAQS tunnel results were consistent with observations from other on-road studies, and that the SCAQS tunnel experiment could not be dismissed as an indicator that the emissions factors might be wrong. Fujita *et al.* (1992) found significant discrepancies between the ratios of different ROG species

in the SCAQS emissions inventory and the concentrations of those species in ambient air. Harley *et al.* (1993) could predict ambient ozone and hydrocarbon measurements with a photochemical model only when motor vehicle exhaust emissions in the SCAQS emissions inventory were doubled.

Further evidence using remote sensing of individual tailpipe emissions for CO (Stedman, 1989; Bishop *et al.*, 1989; Bishop and Stedman, 1990; Ashbaugh *et al.*, 1992; Knapp, 1992) has shown that approximately 20% of the on-road vehicles emit nearly 80% of the CO. Remote sensing methods take the ratio of CO to CO_2 in vehicle exhaust gases. This ratio is proportional to the amount of CO emitted per quantity of fuel consumed. A pilot study by Lawson *et al.* (1990) in Southern California indicates that the high- and super-emitters cannot necessarily be identified by model year or by the time which has elapsed since their most recent inspection and maintenance. These variables are not treated in the current inventory.

Hansen and Rosen (1990) provide some of the few measurements to date on the variability of primary particle emissions from on-road vehicles, and their results apply only to the ratio of light-absorbing carbon to CO_2. They found a factor of 250 between the highest and lowest ratio of light-absorbing carbon to CO_2 for 60 gasoline-fueled vehicles. They did not categorize vehicles by weight and age.

ARB uses the best emission factors available for fugitive dust, but none of these are very reliable. The most important one for PM_{10} in the SoCAB is that associated with paved road dust, and the uncertainties associated with this factor illustrate the problem in general. The emissions factors consider: 1) silt content of road dust; 2) quantity of road dust; and 3) vehicle miles travelled (VMT) on the road. Silt contents typically range from 1% to 20%, depending on the type of road dust and the extent to which it has been ground up by traffic. Dust loadings on different streets can range over two or three orders of magnitude, and there is no guarantee that dust loadings taken at a single time represent dust loadings throughout the year. Fugitive dust emissions estimates are further complicated by their episodic nature in space and time. The construction and demolition emissions estimates in Table 2-1 may be reasonable on a yearly basis for the entire SoCAB, but their contributions to specific PM_{10} concentrations will be highly dependent on their proximity to a sampling site on a sampling day.

Another limitation of the PM_{10} and ROG emissions estimates in Table 2-1 is that they deal with total mass emissions rather than with individual species (as is the case for SO_2, CO, and NO_x). This makes it much harder to relate chemical species measured in the atmosphere to their emissions sources. ARB (California Air Resources Board, 1991) has assigned organic species profiles to the different emitters of ROG which can be superimposed on the Table 2-1 mass emission rates, and this process has been evaluated for the SCAQS emissions inventory (Harley *et al.*, 1992a). Houck *et al.* (1989) have compiled particulate chemical profiles for the ARB which represent several parts of California, but not the SoCAB. Cooper *et al.* (1987) provide the closest estimates for particulate profiles in southern California. Since an accurate specification of these profiles is essential to the analyses performed in this report, they will be examined in greater detail in Section 5.

Though the emissions in Table 2-1 provide qualitative estimates of major and minor contributors to ambient PM_{10} and ROG, they cannot be relied upon to fully explain the source contributions to measurements at a particular time and location.

2.2 Meteorology

Southern California is in the semi-permanent high pressure zone of the eastern Pacific. Summers are hot (average temperature ~25°C, with maximum daily readings which often exceed 35°C, 1993 World Almanac and Book of Facts) and precipitation events are rare. Winters are cooler (average temperature ~15°C with minimum temperatures which are normally ~5°C but can drop below freezing at inland locations on clear, windless nights following a cold frontal passage. Precipitation is frequent from December through March, with monthly averages of 5 to 8 cm. Summertime sunrise and sunset are approximately 0500 and 1900 PST, and wintertime sunrise and sunset are approximately 0700 and 1700 PST.

Frequent and persistent temperature inversions are caused by subsidence of descending air which warms when it is compressed over cool, moist marine air. These inversions often occur during periods of maximum solar radiation which create daytime mixed layers of ~1,000 m thickness, though the top of this layer is often lower during ozone episodes (Blumenthal *et al.*, 1978). Afternoon relative humidities depend on the origin of the air mass and the time of day. As might be expected, relative humidities are higher near the coast than farther inland (Smith *et al.*, 1984).

Smith *et al.* (1972), Keith and Selik (1977), and Hayes *et al.* (1984) have examined wind flow patterns in the SoCAB, and these separate analyses show the same types of patterns, illustrated in Figures 2-4 and 2-5 for summer and winter periods, respectively. During the summertime, the sea breeze is strong during the day and there is a weak land-mountain breeze at night. Owing to the high summer temperatures and extensive urbanization in the SoCAB, the land surface temperature does not usually fall below the water temperature at night, and the nocturnal and morning winds are much less vigorous than the daytime winds. The land surface does cool sufficiently to create a surface inversion with a depth as low as ~50 m. This surface layer usually couples to the mixed layer within a few hours after sunrise each day. Summertime flow patterns are from the west and south during the morning, switching to predominantly westerly winds by the afternoon.

During the winter, land surface temperatures fall below those of the ocean, and easterly nocturnal winds are more pronounced than during the summer. A mild sea breeze is only established later in the day when temperatures approach their maxima. Wintertime trajectories are much less predictable than summertime trajectories and are often influenced by frontal passages punctuated by periods of stagnation. In the absence of a strong synoptic-scale pressure gradient, wintertime flows are from the east and north at night, switching to westerly trajectories by afternoon.

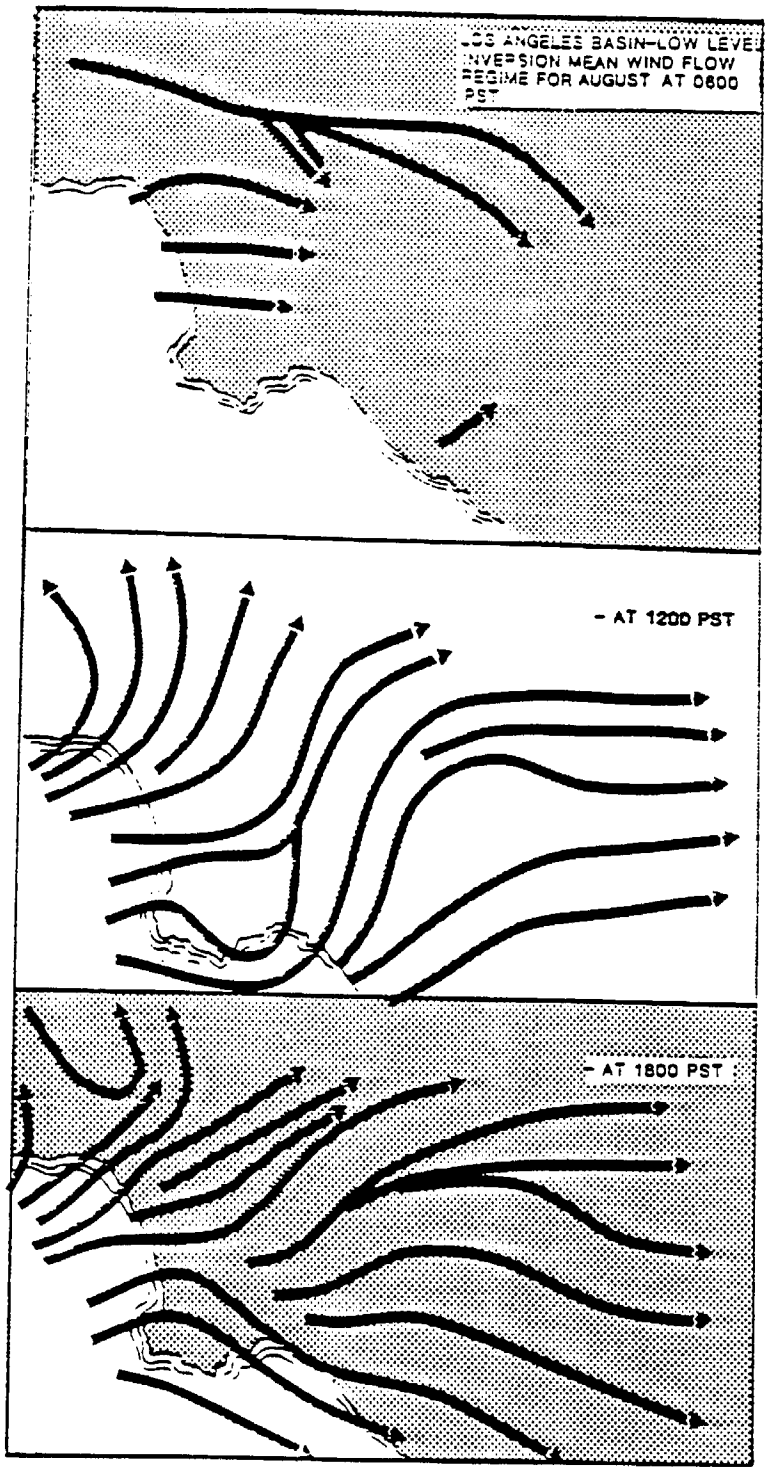

Figure 2-4. Summer Variation in Surface Wind Flow Patterns Throughout the Day in the South Coast Air Basin (Smith *et al.*, 1972)

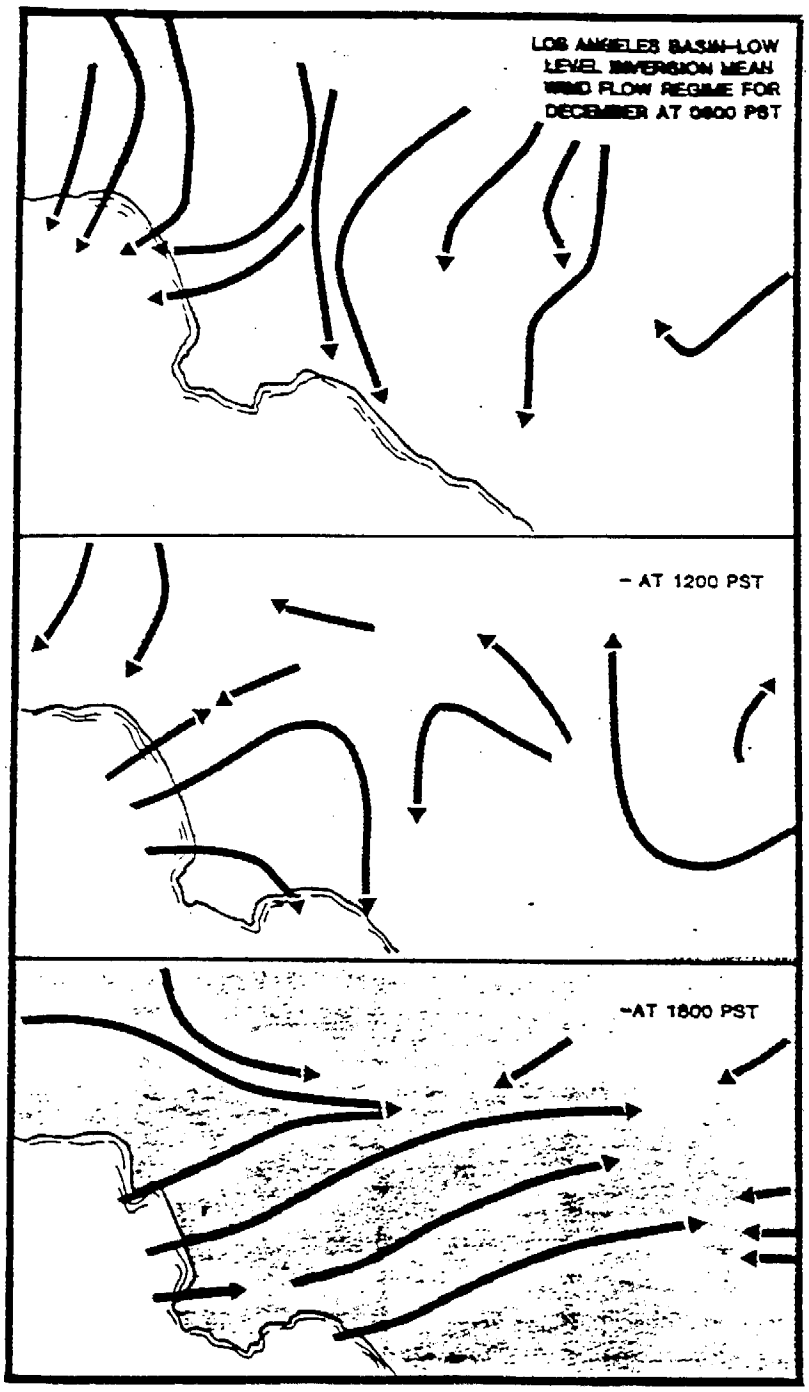

Figure 2-5. Winter Variation in Surface Wind Flow Pattern Throughout the Day in the South Coast Air Basin (Smith *et al.*, 1972)

The land/sea breeze circulation transfers air back and forth between the SoCAB and the Pacific Ocean. Cass and Shair (1984) estimated that up to 50% of the sulfate measured at Lennox was due to emissions which had been transported to sea on the previous day. When wind speeds are low, air tends to slosh back and forth within the SoCAB itself. The SoCAB is ventilated when air exits to the Mojave Desert and the Coachella Valley. Using tracer gas releases, Smith and Shair (1983) found transport routes through Soledad Canyon, Cajon Pass, and San Gorgonio Pass. They also found evidence of transport aloft from the San Fernando Valley into eastern Ventura County under certain circumstances.

In addition, there are many less significant features which affect pollutant movement in the SoCAB. Heating of the San Gabriel and San Bernardino Mountains during the daytime engenders upslope flows which can transport pollutants from the surface into the upper parts of, and sometimes above, the mixed layer. When the slopes cool after sunset, the denser air flows back into the SoCAB with pollutants entrained in it. Convergence zones occur where terrain and pressure gradients direct wind flow in opposite directions, resulting in an upwelling of air. Smith *et al.* (1984) have identified convergence zones at Elsinore (McElroy *et al.*, 1982; Smith and Edinger, 1984), the San Fernando Valley (Edinger and Helvey, 1961), El Mirage, the Coachella Valley, and Ventura.

Blumenthal *et al.* (1978) describe the meteorology for a July 24 to 26, 1973 ozone case study during which the maximum hourly ozone average reached 630 ppb. During this episode, a strong high pressure ridge near the coast induced a cap of warm air over the SoCAB which limited the mixing depth of surface emissions. Nighttime surface inversions were strong and stable with little transport until late morning. Ozone above the surface layer was not ventilated, but was carried over to the following day. The afternoon sea breeze was weak. On the second day, coupling of the surface layer to the rest of the mixed layer entrained the ozone aloft with ozone generated from fresh emissions. When the high pressure system weakened, the mixing depth increased and more vigorous on-shore winds ventilated the SoCAB.

Chow *et al.* (1992) describe the meteorology for several cases in which high PM_{10} concentrations were measured at the Rubidoux sampling site during 1988. More than 60% of the highest SoCAB PM_{10} (243 $\mu g/m^3$) at Rubidoux was composed of ammonium nitrate and ammonium sulfate on October 24, 1988. This day and the days preceding it were characterized by stratus clouds, patchy morning ground fogs, and stagnant winds. Another high PM_{10} concentration at Rubidoux (159 $\mu g/m^3$) occurred on September 9, 1988, with nearly 70% contributed by geological material. This day experienced limited vertical mixing during the morning, with restricted penetration of the marine layer to the eastern part of the SoCAB. Without cooling intrusion of the marine layer, the surface temperature at Rubidoux exceeded 32°C by early afternoon, which engendered vigorous vertical mixing. The sea breeze developed by mid-afternoon, and wind speeds exceeding 5.5 m/s were recorded for several hours. These speeds often correspond to those needed for the entrainment and transport of fugitive dust (Gillette *et al.*, 1982; Gillette and Passi, 1988).

General meteorological conditions and trajectories during SCAQS episodes have been examined by Douglas *et al.* (1991). Flows during the summertime were generally westerly, and residence times were typically less than 12 hours. The backward trajectories from Claremont and Riverside on August 27 and 28, 1987 show an upper level recirculation in the middle of the SoCAB which probably led to the build-up of ozone and precursors during this episode. The fall trajectories show less distinct transport patterns. Backward trajectories at Riverside show short eastward transport on November 12 and 13, 1987, northwestward transport on December 3, 1987, and southeastward transport on December 10 and 11, 1987. The trajectories during SCAQS episodes are consistent with the conditions desired for selecting episodes. Summer episodes showed the west to east transport with potential for pollutant carryover aloft which typifies high ozone levels. The fall episodes show low surface wind speeds and meandering trajectories which typify the high particulate concentrations measured during that period.

2.3 Secondary Particle Formation

Both primary and secondary particles contribute to suspended particles in the SoCAB, and especially to PM_{10} concentrations which exceed standards. Primary particles are those which are directly emitted by sources. These particles undergo few changes between source and receptor, and the atmospheric concentrations are, on average, proportional to the quantities which are emitted. Secondary particles are those which form in the atmosphere from gases which are directly emitted by sources. Sulfates and nitrates are the most common secondary particles, though a fraction of organic carbon can also result from volatile organic compounds (VOCs) via atmospheric reactions.

Suspended particles congregate in different sub-ranges according to the method of formation (Whitby *et al.*, 1972). The "nuclei" range consists of particles <0.08 μm in aerodynamic diameter which are emitted directly from combustion sources. In polluted areas, the lifetimes of particles in the nuclei range are usually less than one hour because they rapidly coagulate with large particles or serve as nuclei for cloud or fog droplets. This size range is generally detected only when fresh emissions sources are close to the measurement site.

The "accumulation" range consists of particles of 0.08 to ~ 2 μm in aerodynamic diameter. These particles generally result from the coagulation of smaller primary particles emitted from combustion sources, from condensation of volatile species, from gas-to-particle conversion, and from finely ground dust particles. The nuclei and accumulation ranges comprise the $PM_{2.5}$ size fraction measured in SCAQS, and this size range includes contributions from primary as well as secondary particles. The majority of sulfates, nitrates, ammonium, organic carbon, and elemental carbon are found in this $PM_{2.5}$ size fraction. SCAQS measurements by John *et al.* (1991) and those from earlier studies in the SoCAB by Hering and Friedlander (1982) show the accumulation range consists of several modes. One of these which peaks at ~ 0.2 μm is interpreted as a "condensation" mode containing gas-phase reaction products. A ~ 0.7 μm peak is interpreted as a "droplet" mode which forms as the "condensation" mode accumulates water.

The "coarse" particles (PM_{10} minus $PM_{2.5}$) consist of particles between 2.5 μm and 10 μm. Coarse particles result from grinding activities and are generally dominated by material of geological origin. Pollen and spores are also in this size range, as are ground up trash, leaves, tire wear, other detritus, and sea salt. Coarse particles at the low end of the size range may result when clouds and fog droplets form in a polluted environment, then dry out after having scavenged other particles and gases.

The gaseous precursors of most particulate sulfates and nitrates are sulfur dioxide (SO_2) and oxides of nitrogen (NO and NO_2, the sum of which is designated NO_x), respectively. Ambient concentrations of sulfate and nitrate are not necessarily proportional to quantities of emissions since the rates at which they form may be limited by factors other than the concentration of the precursor gas. The majority of secondary sulfates are found as a combination of sulfuric acid (H_2SO_4), ammonium bisulfate (NH_4HSO_4), and ammonium sulfate ($(NH_4)_2SO_4$). Previous sulfate measurements in the SoCAB (e.g., Gray *et al.*, 1986; Solomon *et al.*, 1989; Watson *et al.*, 1991a; Chow *et al.*, 1992) have found sufficient ammonium to attribute all sulfate to ammonium sulfate. The majority of secondary nitrates in PM_{10} are found as ammonium nitrate (NH_4NO_3), though a portion of the nitrate is also found in the coarse particle fraction, usually in association with sodium (this is presumed to be sodium nitrate [$NaNO_3$] derived from the reaction of nitric acid with the sodium chloride [NaCl] in sea salt).

Secondary organic compounds in particulate matter include aliphatic acids, aromatic acids, nitro-aromatics, carbonyls, esters, phenols, and aliphatic nitrates (Grosjean and Seinfeld, 1989; Grosjean, 1992). The exact precursors of these secondary organics are not well understood, but they are generally assumed to be heavier hydrocarbons (i.e., molecules which contain more than seven or eight carbon atoms). Many of the suspected precursors of secondary organic particles are not measured by the usual VOC sampling and analysis methods.

Atmospheric gases can become suspended particles by absorption, solution, condensation, or chemical transformation. Several of these mechanisms may operate in series in the process of secondary particle formation. In absorption, gas molecules are attracted to and adhere to existing particles. Sulfur dioxide and many organic gases have an affinity for graphitic carbon (e.g., activated charcoal is often used as a scrubbing agent for these gases), and most graphitic carbon particles in the atmosphere are found in association with an organic component. Most gases are somewhat soluble in water, and liquid particles will rapidly become saturated with sulfur dioxide, nitrogen dioxide, and certain organic gases when these gases are present. Many hydrocarbons are emitted as gasses at elevated temperatures which result from combustion; these condense rapidly upon cooling to ambient temperatures. These are usually considered to be primary emissions if the condensation takes place rapidly, but the particles formed can be sensitive to changes in temperature and the surrounding gas concentrations.

Chemical transformation and equilibrium processes for inorganic secondary aerosols are complicated, depend on many meteorological and chemical variables, and are not completely understood. Lurmann *et al.* (1988) and Lurmann (1989) summarize the different pathways from gas to particle. Calvert and Stockwell (1983) have studied the gas-phase chemistry. Stelson and

Seinfeld (1982a; 1982b; 1982c), Russell *et al.* (1983), Russell and Cass (1984; 1986), Bassett and Seinfeld (1983; 1984), Saxena *et al.* (1986), Pilinis and Seinfeld (1987), Wexler and Seinfeld (1991; 1992) provide good explanations of the equilibrium between gas and particle phases in polluted environments. Much of the current understanding of secondary particle formation has resulted from air pollution monitoring and modeling in the SoCAB.

Sulfur dioxide gas changes to particulate sulfate through gas- and aqueous-phase transformation pathways. In the gas-phase pathway, sulfur dioxide reacts with hydroxyl radicals in the atmosphere to form hydrogen sulfite. This species rapidly reacts with oxygen and small amounts of water vapor to become sulfuric acid gas. Sulfuric acid gas has a low vapor pressure, and it either condenses on existing particles, nucleates at high relative humidities to form a sulfuric acid droplet, or, in the presence of ammonia gas, becomes neutralized as ammonium bisulfate or ammonium sulfate. Though there are other gas-phase pathways, this one with the hydroxyl radical is usually the dominant one. Calvert and Stockwell (1983) show a wide range of gas-phase transformation rates from less than 0.01%/hr to about 5%/hr. The transformation rate appears to be controlled more by the presence or absence of the hydroxyl radical and competing reactions of other gases than by the sulfur dioxide concentration. Hydroxyl radical concentrations are related closely to photochemistry, and gas-phase sulfur dioxide transformation rates are highest during daytime and drop to less than 0.1%/hr at night (Calvert and Stockwell, 1983).

When fogs or clouds are present, sulfur dioxide can be dissolved in a droplet where it experiences aqueous reactions which are much faster than gas-phase reactions. If ozone and hydrogen peroxide are dissolved in the droplet, the sulfur dioxide is quickly oxidized to sulfuric acid. If ammonia is also dissolved in the droplet, the sulfuric acid is neutralized to ammonium sulfate. As relative humidity decreases below 100% (i.e., the fog or cloud evaporates), the sulfate particle is present as a small droplet which includes a portion of liquid water. As the relative humidity further decreases below 70%, the droplet evaporates and a small, solid sulfate particle remains. The reactions within the fog droplet are very fast, and the rate is controlled by the solubility of the precursor gases. Aqueous transformation rates of sulfur dioxide to sulfate are 10 to 100 times as fast as gas-phase rates.

Zeldin *et al.* (1989) observed no daytime fog occurrences during SCAQS from daytime satellite photographs. However, Pandis *et al.* (1992a) observed that an early morning coastal fog occurred on the morning of December 11, 1987 during a SCAQS episode, and that inland sulfate concentrations doubled from the levels measured on the previous day. Their gas-phase and liquid aerosol chemical models could not account for the measured sulfate concentrations, even when extreme values for mixing depth, deposition rate, and oxidant levels were selected. Only when sufficient residence of primary sulfur dioxide emissions in the fog was assumed could the measured sulfate concentrations be accounted for by known chemical mechanisms.

Emitted nitric oxide converts to nitrogen dioxide, primarily via reaction with ozone. The nitrogen dioxide can follow several pathways: 1) it can change back to nitric oxide in the presence of ultraviolet radiation; 2) it can change to short-lived radical species which take place in other chemical reactions; 3) it can form organic nitrates such as peroxyacetyl nitrate (PAN);

or 4) it can oxidize to form nitric acid. The major pathway to nitric acid is reaction with the same hydroxyl radicals which transform sulfur dioxide to sulfuric acid. Nitric acid deposits from the atmosphere fairly rapidly but, in the presence of ammonia, it is neutralized to particulate ammonium nitrate. Calvert and Stockwell (1983) show a wide range of conversion rates for nitrogen dioxide to nitric acid, ranging from less than 1%/hr to 90%/hr. Though they vary throughout a 24-hour period, these rates are significant during both daytime and nighttime hours, in contrast to the gas-phase sulfate chemistry which is most active during daylight hours. Nitrate is also formed by aqueous-phase reactions in fogs and clouds in a manner analogous to aqueous-phase sulfate formation.

While ammonium sulfate is a fairly stable compound, ammonium nitrate is not. Its equilibrium with gaseous ammonia and nitric acid is strongly influenced by temperature and relative humidity. Russell *et al.* (1983) show that lower temperatures and higher relative humidities favor the particulate phase of ammonium nitrate. Their sensitivity tests demonstrate that the equilibrium is most sensitive to changes in ambient temperature and gaseous ammonia concentrations. The gas phase is highly favored when ambient temperatures approach or exceed 35°C, while the particulate ammonium nitrate phase is highly favored when temperatures are less than 15°C. When gaseous ammonia or nitric acid concentrations are reduced, some of the particulate ammonium nitrate evaporates to regain equilibrium with the gas phase. This phenomenon makes accurate measurements of particulate nitrate and nitric acid exceedingly difficult, since ammonium nitrate particles on a filter may disappear during sampling or between sampling and analysis with changes in temperature and gas concentrations.

As noted above, gaseous nitric acid can also react with basic materials such as sodium chloride (from sea salt) and possibly alkaline dust particles. The products of these reactions (e.g., sodium nitrate) are usually stable and are often observed as coarse particles, since the original sea salt or dust was in that size range. Coarse particle nitrate accompanied by sodium and a deficit of chloride is a good indicator that this reaction has taken place.

Sulfur dioxide to particulate sulfate and nitrogen oxide to particulate nitrate reactions compete with each other for available hydroxyl radicals and ammonia. Ammonia is preferentially scavenged by sulfate to form ammonium sulfate and ammonium bisulfate, and the amount of ammonium nitrate formed is significant only when the total ammonia exceeds the sulfate by a factor of two or more on a mole basis. In an ammonia-limited environment, reducing ammonium sulfate concentrations by one molecule would increase ammonium nitrate concentrations by two molecules. This implies that sulfur dioxide, oxides of nitrogen, and ammonia must be treated as a coupled system and cannot be dealt with separately. Reducing sulfur dioxide emissions might actually result in ammonium nitrate increases which exceed the reductions in ammonium sulfate where the availability of ammonia is limited.

Atmospheric water is another important component of suspended particulate matter. The liquid water content of ammonium nitrate, ammonium sulfate, sodium chloride, and other soluble species changes with relative humidity (Charlson *et al.*, 1969; Covert *et al.*, 1972), and this is especially important when relative humidity exceeds 70%. Liquid water has been found to be

a significant component of suspended particles in the SoCAB (Ho *et al.*, 1974), in addition to its role in fomenting aqueous-phase oxidation of sulfur dioxide and nitrogen dioxide.

While the mechanisms and pathways for inorganic secondary particles are fairly well-known, those for secondary organic aerosol are not well understood. Hundreds of precursors take place in these reactions, and the rates at which these particles form are highly dependent on the concentrations of other pollutants and meteorological variables. Secondary organics are formed in the atmosphere by gas-phase reactions involving reactive organic gases and oxidizing species such as ozone, hydroxyl radicals, and nitrate radicals. Particles are formed when gaseous reaction products achieve concentrations which exceed their saturation concentrations. This means that chemical transformations must be rapid enough to increase concentrations faster than they decrease by deposition and atmospheric dilution, and that the saturation concentrations of the products must be lower than those of the gaseous precursors. Grosjean and Seinfeld (1989) note that only reactive organic gases containing more than seven carbon atoms meet these conditions for reactivity and saturation vapor pressure. Toluene and higher aromatics meet these conditions.

Grosjean and Seinfeld (1989) outline an empirical model for addressing secondary organic formation and Grosjean (1992) demonstrates this model for reactive organic emissions in the SoCAB. Fraction conversion factors, based on experimental data taken in smog chamber experiments, relate the aerosol products of selected precursors to the original quantities of those precursors. Applying these factors to chemically-speciated emissions inventories provides an approximate estimate of the equivalent emissions of secondary organic particles. Grosjean (1992) shows that these equivalent emissions are comparable to primary emissions from other carbon-containing sources such as motor vehicle exhaust in the Los Angeles area. While this empirical model provides an order-of-magnitude estimate of the VOC impacts on PM_{10}, and while these impacts appear to be significant in southern California, quantitative estimates are imprecise.

Ultimately, one desires an organic transformation model based on fundamental principles. The structure for such models already exists in photochemical mechanisms which are applied in grid-based models for ozone prediction. Unfortunately, these models are highly simplified with respect to organic chemistry. Ozone mechanisms assign all hydrocarbons to five to eight groups having similar reactive properties. While these groupings have been shown to be effective for ozone, they have little to do with the tendency of reactions to create products which might achieve saturation in the atmosphere. Pandis *et al.* (1992b) have divided these groups into sub-groups which are more conducive to aerosol formation and have added reactions for alcohols, pinenes, isoprene, toluene, acetylene, heptane, octene, and nonene. When Pandis *et al.* (1992b) modeled the SCAQS August 27-29, 1987 episode with double the ROG emissions in the SCAQS emissions inventory, they found reasonable comparisons between calculated secondary organic aerosol and that inferred by Turpin and Huntzicker (1991) from time-resolved organic to elemental carbon ratios.

Secondary sulfates and nitrates are fairly easy to identify because there are few primary emitters of these species. Secondary organic particles are more difficult to identify because only

organic carbon, and not its chemical constituents, is usually measured and there are many primary emitters of organic material. Gray *et al.* (1986) propose that evidence of secondary organic carbon contributions to suspended particles is found when: 1) the ratio of total (elemental plus organic) to elemental carbon exceeds that in source emissions (which can be as high as 4:1 but are typically between 2:1 and 3:1); 2) ambient ratios of total to elemental carbon are higher in summer and during the afternoon (when the products of photochemistry are most influential); and 3) when the ratio of total to elemental carbon is larger at sites which receive aged aerosol (i.e., downwind sites) than at sites which receive unaged aerosol.

Gray *et al.* (1986) did not find conclusive evidence of secondary organic aerosol formation in the 24-hour samples taken in 1982. Turpin and Huntzicker (1991) did observe total to elemental carbon ratios as high as 5.6 at the Claremont site on the afternoon of August 28, 1987 and they interpreted a portion of this increase to contributions from secondary organic carbon. Though they monitored organic carbon at two-hour intervals every day during SCAQS, Turpin and Huntzicker (1991) definitively observed this phenomenon only between June 22 and 28, July 11 and 13, July 25 and 29, and August 27 and 31, 1987. Elevated total to elemental carbon ratios were not found during fall monitoring at the Long Beach site.

Particulate receptor models require certain species in the source emissions which retain their relative proportions to each other between source and receptor. This is straightforward for primary particles, since these are not expected to change. In cases such as sea salt, where there is one primary particle precursor (NaCl) and one end-product ($NaNO_3$), and where reactions with nitric acid are anticipated, profiles which represent various degrees of reaction (i.e., different proportions of sodium chloride and sodium nitrate) can be constructed. For substances such as ammonium nitrate and ammonium sulfate, current receptor model technology only allows attribution to the particulate end-product, and not to the directly-emitted gaseous precursors. Examination of the spatial and temporal distribution of these secondary contributions, and their relationships to precursor measurements does allow some inferences to be made about the sources of their precursors.

2.4 Volatile Organic Compounds

In this report, VOC refers to all gaseous organic compounds that may be present in the ambient air. Non-methane hydrocarbons (NMHC) and non-methane organic gases (NMOG) refer to specific VOC data sets. The definitions of NMHC and NMOG are operational, and reflect the selectivity and sensitivity of the analytical methods that were applied. In this report, NMHC refers to C_2 through C_{12} hydrocarbons that were collected in stainless steel canisters and measured by gas chromatography with flame ionization detection (GC-FID). NMHC plus methane equals total hydrocarbons (THC). NMOG refers to NMHC plus C_1 through C_7 carbonyl compounds measured by collection of samples on acidified 2,4-dinitrophenylhydrazine (DNPH)-impregnated C_{18} cartridges and analysis of the carbonyl derivatives by high performance liquid chromatography with UV detection (HPLC/UV). NMOG plus methane equals TOG.

ROG refers to emission inventory estimates, and includes all organic gases except methane and a number of organic compounds such as low molecular weight halogenated organic compounds that have been identified by the Environmental Protection Agency as essentially non-reactive.

The main purpose for measuring VOCs during SCAQS was to assess their contributions to elevated ozone levels rather than to particulate matter. Grosjean (1992) notes that most of the compounds in SCAQS hydrocarbon samples were those with less than seven carbon atoms, and many of the heavier species which might provide condensible end-products were not quantified. The majority of measured VOC precursors and end-products measured during SCAQS will remain in the gaseous phase, and their major chemical role is in ozone formation rather than particulate formation.

The role of VOCs in the formation of tropospheric ozone has been well established (Seinfeld, 1986). The only significant chemical reaction producing ozone in the atmosphere is the reaction of atomic and molecular oxygen. While molecular oxygen (O_2) is abundant in the atmosphere, free oxygen (O) atoms are not. At high altitudes (above 20 km) free oxygen atoms are produced by photodissociation of molecular oxygen by radiation in the deep ultraviolet. At lower altitudes, where only radiation with wavelengths greater than 280 nm is present, the only significant oxygen atom production is from photodissociation of nitrogen dioxide into nitrogen oxide and atomic oxygen. The nitrogen oxide reacts rapidly with ozone to regenerate nitrogen dioxide. In the lower atmosphere, these three reactions occur rapidly, establishing a steady-state equilibrium ozone concentration that depends on the ratio of nitrogen dioxide to nitrogen oxide. One ozone molecule is required to regenerate nitrogen dioxide from nitrogen oxide, so these reactions are insufficient, by themselves, to create excessive ozone levels.

A reaction path that converts nitrogen oxide back to nitrogen dioxide without consuming a molecule of ozone is provided by the presence of reactive organic gases. The organic radicals produced in the oxidation of organic gases react with nitrogen oxide to form nitrogen dioxide, thereby shifting the equilibrium, which allows ozone to accumulate. Aside from meteorology and transport, emissions of nitrogen oxides and ROG are the main factors that affect ozone levels in urban areas, and are the primary focus of control programs that have been developed to attain federal and state air quality standards for ozone. Without anthropogenic nitrogen oxides emissions, the hourly concentration of ozone in the troposphere would not exceed background levels of 20 to 50 ppb. Even with the presence of nitrogen oxides, ozone would not reach the levels that now occur in California's major urban areas (as high as 350 ppb on the worst days) if it were not for the effects of ROG.

This study focuses on the origins of ambient VOC concentrations rather than the fates of their end-products. As noted in Section 1, a prerequisite for using receptor models is that the relative proportions of chemical species change little between source and receptor. For the majority of organic compounds emitted from anthropogenic and biogenic sources, reaction with the hydroxyl radical is the sole chemical sink process, and typical atmospheric residence times can be estimated from typical and maximum reaction rates for different ROG when the hydroxyl is present at urban concentrations.

Typical lifetimes of some VOCs which result from reaction with the hydroxyl radical are given in Table 2-2. This table shows that acetylene, most of the alkanes, benzene, and toluene have lifetimes which exceed the typical summer residence time of air masses during SCAQS ($\sim$ 12 hours according to SCAQS trajectories). These species should be appropriate for use as fitting species in Chemical Mass Balance (CMB) receptor model calculations. Most of the other species in Table 2-2 would be appropriate fitting species when emissions are fresh (i.e., sampled within a few hours after release) but will have substantially changed in proportion to the other species after the air mass containing them has aged for a few hours. Since photochemical production of the hydroxyl radical is substantially lower in the fall and winter compared to the summer, the lifetimes are expected to be three to four times as long, and the ratios of species concentrations should be relatively constant for typical aging times, as shown in Table 2-2, between source emissions and receptor measurement.

2.5 Previous Aerosol Studies

Air pollution has been more completely studied in the SoCAB than in any other area. A large part of current knowledge about the interaction between pollutants derives from research performed in the SoCAB. This review restricts itself to past studies of ambient concentrations and source contributions to suspended particles.

The SCAQMD has measured PM_{10} mass and several of its chemical constituents for several years. PM_{10} is a regulated pollutant with a federal 24-hour standard of 150 $\mu g/m^3$ which is not to be exceeded more than three times in three years and an annual arithmetic average standard of 50 $\mu g/m^3$ which is never to be exceeded. California has more stringent standards of 50 $\mu g/m^3$ for a 24-hour period and an annual geometric average of 30 $\mu g/m^3$; no exceedances of these levels are allowed.

Table 2-3 summarizes PM_{10} concentrations from the SCAQMD's sixth-day monitoring at eleven sites in the SoCAB between 1986 and 1988 (California Air Resources Board, 1987; 1988; 1989). The 24-hour federal standard was exceeded 18 times at 7 sites in 1986, 18 times at 6 sites in 1987, and 17 times at 5 sites in 1988. The California standards were exceeded at all sites during the three years.

Annual average PM_{10} sulfate concentrations are typically 5 to 6 $\mu g/m^3$, though the basin-wide maxima often exceed 20 $\mu g/m^3$ at the Rubidoux and Fontana sites. Both the average and maximum concentrations are nearly twice as high as those commonly observed in the San Francisco Bay Area and San Joaquin Valley air basins (Chow *et al.*, 1993a). Annual average PM_{10} nitrate concentrations vary from 3 to 16 $\mu g/m^3$ from county to county within the SoCAB, and the maximum nitrate concentrations are much higher than the maximum sulfate levels, exceeding 90 $\mu g/m^3$ at the Rubidoux site.

Table 2-4 lists PM_{10} mass, sulfate, and nitrate concentrations for the 53 samples that exceeded the 150 $\mu g/m^3$ PM_{10} standard during the three-year period. PM_{10} exceedances were reported on 8 days in 1986, 7 days in 1987, and 11 days in 1988. Approximately 70% of the

Table 2-2

Lifetimes of Some Hydrocarbons Due to Reaction with OH Radical

Compound	10E12 x k cm3/mol-sec @ 298 K	Lifetimes Daytime 12-hour mean Low	Lifetimes Daytime 12-hour mean High	Midday Peak
	OH/cm3	5.0E+05	5.0E+06	1.0E+07
Alkanes				
Methane	0.01	15.2 years	1.5 years	
Ethane	0.27	173 days	17.3 days	
Propane	1.15	40 days	4 days	
n-Butane	2.54	18 days	1.8 days	
2-Methylpropane (i-Butane)	2.34	20 days	2 days	
n-Pentane	3.94	12 days	1.2 days	
2-Methylbutane (i-Pentane)	3.9	12 days	1.2 days	
n-Hexane	5.61	8.3 days	9.9 hours	5 hours
2-Methylpentane	5.6	8.3 days	9.9 hours	5 hours
3-Methylpentane	5.7	8.1 days	9.7 hours	4.9 hours
2,4-Dimethylpentane	5.1	9.1 days	10.9 hours	5.4 hours
Heptane	7.2	6.5 days	7.8 hours	3.9 hours
Methylcyclohexane	10.4	4.5 days	5.3 hours	2.7 hours
Alkenes				
Ethylene	8.5	5.4 days	6.5 hours	3.3 hours
Propene	26.3	1.8 days	2.1 hours	1.1 hours
Butene	31.4	1.5 days	1.8 hours	0.9 hours
cis-2-Butene	56.1	9.9 hours	1 hours	0.5 hours
trans-2-Butene	63.7	8.7 hours	0.9 hours	0.4 hours
3-Methyl-1-Butene	31.8	1.5 days	1.7 hours	0.9 hours
Cyclohexene	67.4	8.2 hours	0.8 hours	0.4 hours
Isoprene	101	5.5 hours	0.6 hours	0.3 hours
Alkynes				
Acetylene	0.9	51.4 days	5.1 days	
Aromatics				
Benzene	1.2	37.6 days	3.8 days	
Toluene	6	7.8 days	9.3 hours	4.7 hours
m-Xylene	23.6	2 days	2.4 hours	1.2 hours
p-Xylene	14.3	3.2 days	3.9 hours	1.9 hours
o-Xylene	13.7	3.4 days	4.1 hours	2 hours
Ethylbenzene	7.1	6.5 days	7.8 hours	3.9 hours
1,2,4-Trimethylbenzene	32.5	1.4 days	1.7 hours	0.9 hours

Lifetimes are for summer conditions. Lifetimes in winter are about 3-4 times longer.

Table 2-3

Annual Statistics for PM_{10} Concentrations in South Coast Air Basin, California

Basin/ County/Site	PM_{10} Mass						PM_{10} Sulfate					PM_{10} Nitrate				
	Maximum 24-Hour ($\mu g/m^3$)	Geo-metric Average ($\mu g/m^3$)	Arith-metic Average ($\mu g/m^3$)	No. of Values ($\mu g/m^3$) >150	>50	No. of Obser-vations	Maximum 24-Hour ($\mu g/m^3$)	Geo-metric Average ($\mu g/m^3$)	Arith-metic Average ($\mu g/m^3$)	No. of Values >10 $\mu g/m^3$	No. of Obser-vations	Maximum 24-Hour ($\mu g/m^3$)	Geo-metric Average ($\mu g/m^3$)	Arith-metic Average ($\mu g/m^3$)	No. of Values >20 $\mu g/m^3$	No of. Obser-vations
1986[a]																
Los Angeles																
Azusa	183	53.5[b]	60.3[b]	2	33	55	15.1	4.20[b]	5.75[b]	12	55	37.6	4.63[b]	5.90[b]	2	55
Burbank	211	55.4[b]	61.3[b]	1	37	56	19.1	4.85[b]	6.37[b]	13	56	43.3	4.83[b]	6.39[b]	1	56
L.A. North Main	178	53.2	57.9	1	37	57	19.0	4.84	6.35	15	57	19.7	4.24	5.45	0	56
North Long Beach	136	50.5[b]	55.7[b]	0	21	52	23.3	5.90[b]	7.03[b]	11	52	35.7	4.26[b]	6.09[b]	2	52
Orange																
El Toro	109	33.9	36.9	0	5	59	16.2	3.82	4.80	4	59	11.2	2.24	2.71	0	59
Los Alamitos-Orange	124	43.6[b]	48.0[b]	0	18	57	22.0	4.94[b]	6.07[b]	8	57	30.3	3.32[b]	4.90[b]	1	57
Riverside																
Rubidoux	294	74.1	86.0	5	48	61	23.5	4.43	5.79	9	61	106.7	10.87	16.47	17	61
San Bernardino																
Fontana-Arrow Hwy	275	62.0	74.3	3	37	55	19.5	3.84	5.24	6	55	90.6	7.32	11.04	4	55
Ontario Airport	272	63.6[b]	74.3[b]	4	42	57	21.9	4.73[b]	6.03[b]	9	57	79.5	8.16[b]	11.98[b]	5	57
San Bernardino-E3R	136	111.2[b]	112.3[b]	0	6	6	12.1	9.93[b]	10.03[b]	2	6	24.5	17.21[b]	17.65[b]	1	6
San Bernardino-Four	285	66.4[b]	78.7[b]	2	20	29	18.4	3.51[b]	5.16[b]	3	29	95.8	6.89[b]	11.93[b]	5	29
1987[a]																
Los Angeles																
Azusa	188	58.7	68.2	2	38	59	15.2	3.95	5.45	10	59	27.5	3.87	5.43	2	59
Burbank	147	53.7	60.2	0	36	59	16.9	4.42	5.76	10	58	26.5	2.97	4.76	3	59
L.A. North Main	158	51.2	57.1	1	36	57	15.8	4.47	5.61	8	57	38.3	3.22	4.55	1	57
North Long Beach	113	44.7[b]	49.0[b]	0	16	53	17.4	4.61[b]	5.74[b]	6	53	14.5	2.25[b]	3.23[b]	0	53

Table 2-3 (continued)

Annual Statistics for PM_{10} Concentrations in South Coast Air Basin, California

Basin/ County/Site	PM_{10} Mass						PM_{10} Sulfate					PM_{10} Nitrate				
	Maximum 24-Hour ($\mu g/m^3$)	Geo-metric Average ($\mu g/m^3$)	Arith-metic Average ($\mu g/m^3$)	No. of Values ($\mu g/m^3$) ≥ 150	≥ 50	No. of Obser-vations	Maximum 24-Hour ($\mu g/m^3$)	Geo-metric Average ($\mu g/m^3$)	Arith-metic Average ($\mu g/m^3$)	No. of Values $\geq 10\ \mu g/m^3$	No. of Obser-vations	Maximum 24-Hour ($\mu g/m^3$)	Geo-metric Average ($\mu g/m^3$)	Arith-metic Average ($\mu g/m^3$)	No. of Values $\geq 20\ \mu g/m^3$	No of. Obser-vations
1987[a] (continued)																
Orange																
El Toro	107	36.6	40.4	0	15	60	16.4	3.54	4.79	5	60	15.7	1.76	2.53	0	60
Los Alamitos-Orange	163	43.1[b]	49.6[b]	1	21	56	18.0	4.39[b]	5.44[b]	6	56	13.5	1.80[b]	2.92[b]	0	56
Riverside																
Perris	137	31.8[b]	49.2[b]	0	5	15	16.4	1.86[b]	2.97[b]	1	15	29.1	2.81[b]	5.13[b]	1	15
Rubidoux	219	73.5	89.6	7	46	60	20.6	4.26	5.73	11	60	45.6	8.43	12.92	16	60
San Bernardino																
Fontana-Arrow Hwy	203	57.6	73.9	3	38	60	18.7	3.78	5.43	10	60	33.5	4.94	7.21	3	60
Ontario Airport	182	60.3	69.8	1	41	60	19.5	4.29	5.64	10	60	33.5	4.71	7.16	3	60
San Bernardino-Four	211	55.2	70.0	2	36	61	18.3	3.47	4.96	8	61	27.1	4.58	7.43	4	61
1988[c]																
Los Angeles																
Azusa[d]	92[d]	44.9[b]	50.8[b]	0	9	18	20.0	4.19	5.75	10	61	17.5	4.42	5.38	0	61
Azusa[e]	127[e]	61.2[b]	68.5[b]	0	32	43	NA	NA	NA	NA	NA	NA	NA	NA	NA	NA
Burbank[g]	100[d]	48.1[b]	54.4[b]	0	11	18	24.0	4.75[b]	6.36[b]	11	55	22.5	4.96[b]	6.60[b]	2	55
Burbank[h]	138[e]	61.6[b]	65.5[b]	0	29	41	NA	NA	NA	NA	NA	NA	NA	NA	NA	NA
L.A. North Main[i]	91[d]	48.5[b]	53.8[b]	0	10	21	26.2	5.06	6.59	11	58	20.5	4.53	6.24	1	58
L.A. North Main[j]	130[e]	56.2[b]	60.8[b]	0	23	37	NA	NA	NA	NA	NA	NA	NA	NA	NA	NA
North Long Beach[k]	120[d]	44.0[b]	48.2[b]	0	16	46	32.5	5.28	6.62	11	60	23.9	3.60	5.15	2	60
North Long Beach[l]	149[e]	58.7[b]	66.1[b]	0	8	14	NA	NA	NA	NA	NA	NA	NA	NA	NA	NA
Orange																
El Toro[m]	97[d]	33.5[b]	36.8[b]	0	6	41	20.1	3.71	4.64	2	61	28.4	2.95	4.15	2	61
El Toro[n]	88[e]	38.5[b]	41.7[b]	0	5	20	NA	NA	NA	NA	NA	NA	NA	NA	NA	NA
Los Alamitos[m]	132[d]	38.9[b]	43.7[b]	0	10	39	24.3	4.54[b]	5.42[b]	5	57	23.5	2.68[b]	4.23[b]	2	57
Los Alamitos[n]	126[e]	43.2[b]	49.8[b]	0	5	18	NA	NA	NA	NA	NA	NA	NA	NA	NA	NA

Table 2-3 (continued)

Annual Statistics for PM_{10} Concentrations in South Coast Air Basin, California

Basin/ County/Site	PM_{10} Mass						PM_{10} Sulfate					PM_{10} Nitrate				
	Maximum 24-Hour ($\mu g/m^3$)	Geo-metric Average ($\mu g/m^3$)	Arith-metic Average ($\mu g/m^3$)	No. of Values ($\mu g/m^3$) ≥ 150	≥ 50	No. of Obser-vations	Maximum 24-Hour ($\mu g/m^3$)	Geo-metric Average ($\mu g/m^3$)	Arith-metic Average ($\mu g/m^3$)	No. of Values $> 10\ \mu g/m^3$	No. of Obser-vations	Maximum 24-Hour ($\mu g/m^3$)	Geo-metric Average ($\mu g/m^3$)	Arith-metic Average ($\mu g/m^3$)	No. of Values $\geq 20\ \mu g/m^3$	No of. Obser-vations
1988[f] (continued)																
Riverside																
Perris[a]	48[d]	28.9[b]	31.4[b]	0	0	5	11.0	3.16[b]	4.17[b]	3	55	48.1	4.14[b]	6.20[b]	1	55
Perris[g]	164[e]	54.9[b]	62.7[b]	1	35	50	NA	NA	NA	NA	NA	NA	NA	NA	NA	NA
Rubidoux[a]	118[d]	60.5[b]	69.9[b]	0	13	17	23.1	4.43	5.78	10	61	95.1	11.54	16.98	22	61
Rubidoux[g]	252[e]	91.9[b]	104.6[b]	7	38	44	NA	NA	NA	NA	NA	NA	NA	NA	NA	NA
San Bernardino																
Fontana-Arrow Hwy[a]	148[d]	44.7[b]	56.6[b]	0	13	24	25.9	4.48[b]	6.07[b]	9	55	85.3	6.90[b]	10.01[b]	3	55
Fontana-Arrow Hwy[i]	287[e]	87.6[b]	97.3[b]	4	33	36	NA	NA	NA	NA	NA	NA	NA	NA	NA	NA
Ontario Airport[d]	106[d]	51.8[b]	58.9[b]	0	12	18	22.9	4.63	5.92	12	60	44.8	7.55	9.78	6	60
Ontario Airport[e]	192[e]	74.4[b]	81.6[b]	2	35	42	NA	NA	NA	NA	NA	NA	NA	NA	NA	NA
San Bernardino-Four[a]	289[d]	75.1[b]	87.7[b]	3	38	47	17.8	3.62	5.35	10	56	90.9	6.46	11.20	8	56
San Bernardino-Four[g]	75[e]	36.3[b]	40.9[b]	0	2	9	NA	NA	NA	NA	NA	NA	NA	NA	NA	NA

[a] California Air Resources Board (1987). This reference shows locations of all sampling sites. Sampling sites are grouped by County.
[b] Data are valid, but incomplete in that an insufficient number of valid data points were collected to meet EPA and/or ARB criteria for representativeness.
[c] California Air Resources Board (1988). This reference shows locations of all sampling sites. Sampling sites are grouped by County.
[d] Gravimetric, Sierra Andersen Model 321 through April 15.
[e] Gravimetric, Sierra Andersen Model 1200 commencing April 21.
[f] California Air Resources Board (1989). This reference shows locations of all sampling sites. Sampling sites are grouped by County.
[g] Gravimetric, Sierra Andersen Model 321 through April 27.
[h] Gravimetric, Sierra Andersen Model 1200 commencing May 3.
[i] Gravimetric, Sierra Andersen Model 321 through May 9.
[j] Gravimetric, Sierra Andersen Model 1200 commencing May 15.
[k] Gravimetric, Sierra Andersen Model 321 through September 30.
[l] Gravimetric, Sierra Andersen Model 1200 commencing October 6.
[m] Gravimetric, Sierra Andersen Model 321 through August 31.
[n] Gravimetric, Sierra Andersen Model 1200 commencing September 6.

Table 2-3 (continued)

Annual Statistics for PM_{10} Concentrations in South Coast Air Basin, California

- Gravimetric, Sierra Andersen Model 321 through January 28.
- Gravimetric, Sierra Andersen Model 1200 commencing February 3.
- Gravimetric, Sierra Andersen Model 321 through April 9.
- Gravimetric, Sierra Andersen Model 1200 commencing April 15.
- Gravimetric, Sierra Andersen Model 321 through May 21.
- Gravimetric, Sierra Andersen Model 1200 commencing May 27.
- Gravimetric, Sierra Andersen Model 321 through September 30.
- Gravimetric, Sierra Andersen Model 1200 commencing October 5.

Table 2-4
PM_{10} Mass, Sulfate, and Nitrate Concentrations on Federal 24-Hour PM_{10} Exceedance Days Between 1986 and 1988

Date	County	Site	PM_{10} ($\mu g/m^3$) Mass	Sulfate	Nitrate
1/2/86	Riverside	Rubidoux	160	13.3	55.2
1/21/86	San Bernardino	Ontario	221	20.3	79.5
1/22/86	San Bernardino	Fontana	236	19.5	90.6
2/25/86	San Bernardino	Ontario	162	8.8	48.4
7/31/86	Riverside	Rubidoux	154	12.9	25.2
9/5/86	San Bernardino	San Bernardino (4)	157	15.3	23.2
9/5/86	Riverside	Rubidoux	176	14.7	37.0
10/29/86	Los Angeles	Azusa	167	13.5	26.2
10/29/86	San Bernardino	Fontana	275	18.9	82.6
10/29/86	Riverside	Rubidoux	294	23.5	106.7
10/29/86	San Bernardino	Ontario	272	21.9	77.4
10/29/86	San Bernardino	San Bernardino	285	18.4	95.8
12/4/86	Los Angeles	Azusa	183	3.3	37.6
12/4/86	Los Angeles	Burbank	211	4.8	43.3
12/4/86	Los Angeles	L.A. Main	178	5.8	N/A[a]
12/4/86	Riverside	Rubidoux	165	3.1	26.2
12/4/86	San Bernardino	Fontana	181	3.2	38.1
12/4/86	San Bernardino	Ontario	207	4.2	44.4
2/2/87	Riverside	Rubidoux	158	5.1	45.6
6/26/87	Riverside	Rubidoux	160	13.1	30.2
9/6/87	Los Angeles	Azusa	188	14.2	18.6
9/18/87	Riverside	Rubidoux	184	13.1	33.2
9/18/87	San Bernardino	Fontana	167	12.6	8.9
9/30/87	Riverside	Rubidoux	182	7.8	36.8

Table 2-4 (continued)
PM_{10} Mass, Sulfate, and Nitrate Concentrations on Federal 24-Hour PM_{10} Exceedance Days Between 1986 and 1988

			PM_{10} ($\mu g/m^3$)		
Date	County	Site	Mass	Sulfate	Nitrate
10/6/87	Los Angeles	Azusa	151	11.4	3.4
10/6/87	Orange	Los Alamitos	163	7.9	1.9
10/6/87	Riverside	Rubidoux	210	10.3	26.1
10/6/87	San Bernardino	Fontana	203	9.1	18.9
10/6/87	Los Angeles	Ontario	150	10.5	9.6
10/6/87	San Bernardino	San Bernardino (4)	160	7.2	18.1
10/18/87	Riverside	Rubidoux	219	20.6	29.0
10/18/87	San Bernardino	Fontana	194	18.7	16.3
10/18/87	Los Angeles	Ontario	182	19.5	16.0
10/18/87	San Bernardino	San Bernardino (4)	211	18.3	20.3
11/23/87	Riverside	Rubidoux	155	6.7	35.8
12/11/87	Los Angeles	Los Angeles	158	7.1	38.3
6/14/88	Riverside	Rubidoux	158	12.6	26.8
8/13/88	Riverside	Rubidoux	153	9.6	31.2
8/19/88	Riverside	Rubidoux	153	10.1	34.7
8/31/88	San Bernardino	Fontana	155	12.5	13.7
9/7/88	San Bernardino	San Bernardino (4)	159	10.7	11.3
9/30/88	Riverside	Rubidoux	177	7.3	19.8
10/18/88	San Bernardino	San Bernardino (4)	171		
10/24/88	Riverside	Perris	164	11.0	48.1
10/24/88	Riverside	Rubidoux	252	23.1	95.1
10/24/88	San Bernardino	Fontana	287	25.9	85.3
10/24/88	Los Angeles	Ontario	192	22.9	44.8
10/24/88	San Bernardino	San Bernardino (4)	289	17.8	90.9
10/30/88	Riverside	Rubidoux	159	5.5	30.1

Table 2-4 (continued)
PM_{10} Mass, Sulfate, and Nitrate Concentrations on Federal 24-Hour PM_{10} Exceedance Days Between 1986 and 1988

Date	County	Site	PM_{10} ($\mu g/m^3$) Mass	Sulfate	Nitrate
11/5/88	Riverside	Rubidoux	166	8.2	33.0
11/5/88	San Bernardino	Fontana	151	11.0	33.2
11/29/88	San Bernardino	Fontana	171	0.8	0.8
11/29/88	Los Angeles	Ontario	172	0.8	0.9

[a] N/A - Information Not Available

PM_{10} exceedance days occurred during the fall and winter seasons. Region-wide PM_{10} exceedances are found on October 29 and December 4, 1986, and on October 6, 18, and 24, 1987, with elevated PM_{10} mass and nitrate concentrations at 4 to 5 sites in the eastern SoCAB. Excess nitrate concentrations ($> 20\ \mu g/m^3$) often accounted for 20% to 40% of the PM_{10} mass on these standard exceedance days. The Rubidoux site stands out as having the highest PM_{10}, the highest nitrate, and among the highest sulfate on days with PM_{10} exceedances.

Most of what is known about the concentrations, spatial distribution, particle size, and chemical composition of suspended particulate matter in the SoCAB has been derived from a few intensive measurement and modeling programs conducted over the past two decades.

Hidy and Friedlander (1970) report the first Chemical Mass Balance (CMB) source apportionment for the SoCAB, using very approximate estimates for the quantity of marker species in each source type. With rudimentary chemical composition measurements on source and receptor samples, Hidy and Friedlander (1970) estimated that 5% of suspended particles were of sea salt origin, 7 to 17% were from soil dust, 13% derived from primary motor vehicle exhaust, 4% were from residual oil combustion, 12% were from sulfates, and 12% were from nitrates. Sampling locations and methods were not well characterized nor were particle size fractions measured in this study. Miller *et al.* (1972) assembled particulate source profiles and ambient data from a variety of references, and estimated 3.5% from sea salt, 10% from soil dust, 8% from primary motor vehicle exhaust, less than 1% from residual oil combustion, 17% from noncarbonate carbon, and 5% from iron oxide (presumably from steel mills). Miller *et al.* (1972) did not provide estimates of sulfate or nitrate contributions. These source contribution estimates were more important for their development of methodology than for their accuracy. They were among the first to attempt source apportionment using ambient data rather than emissions inventories, and disagreements with the existing inventories were significant.

The California Aerosol Characterization Experiment (ACHEX) (Hidy *et al.*, 1975) provided the first comprehensive data base for understanding aerosol in the SoCAB during sampling periods in 1972 and 1973. The main focus during this study was on Total Suspended Particles (TSP, particles with aerodynamic diameter less than $\sim 40\ \mu m$) and $PM_{2.5}$. Friedlander (1973a) and Gartrell and Friedlander (1975) applied the CMB to samples from Pasadena, Riverside, and Pomona, CA. Typical source apportionments are those reported by Friedlander (1973b), which were 11.4% from soil dust, 8.2% from motor vehicle exhaust, $<1\%$ from residual oil combustion, and 1.7% from cement dust for a $100\ \mu g/m^3$ TSP concentration. Hammerle and Pierson (1975) attributed a two-week average TSP concentration of $31.4\ \mu g/m^3$ taken at Pasadena to 20% soil dust, 5.6% motor vehicle exhaust, 0.3% cement dust, and less than 0.3% oil fly ash.

Cass and McRae (1981; 1983) examined trace element data from nine TSP sampling sites in the SoCAB for the year 1976. They estimated that, for the basin as a whole, 20% of the average TSP was derived from motor vehicle exhaust, 1-2% came from residual oil combustion, 20 to 50% was from soil dust or road dust, and 15% was contributed by sulfates and nitrates.

Particulate source profiles, ambient measurement technology, and receptor model methodology improved substantially in the 1980s, and more accurate and precise source apportionments using receptor models have resulted. The most useful information was derived from the 1986 California Institute of Technology (CIT) aerosol monitoring program in the SoCAB (Solomon *et al.*, 1989). This study is especially significant since it was the first to obtain long-term (one year, every sixth day, 24-hour averages), chemically-speciated PM_{10} measurements at nine sites (San Nicolas Island, Long Beach, Anaheim, Hawthorne, Downtown Los Angeles, Burbank, Upland, Rubidoux, and Tanbark Flats). An associated source sampling program (Cooper *et al.*, 1987) acquired profiles which allowed CMB source contribution estimates to be made (Gray *et al.*, 1988) as a basis for the SCAQMD PM_{10} Air Quality Management Plan. Zeldin *et al.* (1990) re-performed CMB calculations on the same ambient concentrations using profiles reported by NEA (1990a; 1990b; 1990c).

Tables 2-5 and 2-6 summarize the source contributions to annual average and maximum 24-hour PM_{10} standard exceedances at the seven urban locations found by both CMB efforts. The federal annual average PM_{10} standard was exceeded at all sites except Lennox, CA. The major contributor to annual average PM_{10} during 1986 was geological material (paved road dust, soil dust, and freeway dust). One third to nearly half of the annual PM_{10} came from this source type. Secondary ammonium nitrate was the second largest contributor to the annual average, ranging from 18% to 26% of PM_{10} among the SoCAB sites. Ammonium sulfate was the third largest contributor at 7% to 15%, and secondary organic carbon was tied for third place with contributions of 7% to 17%. Gray *et al.* (1988) estimated that primary motor vehicle exhaust (leaded gasoline plus diesel) contributed 6% to 11% of annual average PM_{10}, marine aerosol contributed 1% to 4%, and residual oil combustion (the only major industrial source) contributed $< 1\%$ of the annual average of PM_{10}. Lime or gypsum, presumably from cement production or construction, was only detected at the Rubidoux site at $\sim 5\%$ of the annual average PM_{10}. As a result of the CMB analyses by Gray *et al.* (1988) and Chow *et al.* (1992), uninventoried cement plants northeast of the Rubidoux site were identified as potential fugitive dust sources. The low quantity of unexplained mass for the annual average source apportionments implies that other source types are not likely to have made significant contributions to PM_{10}.

The highest PM_{10} concentrations measured in this network during 1986 showed exceedances of the 24-hour federal standard only at Burbank, Downtown Los Angeles, Rubidoux, and Upland, consistent with those reported in Table 2-3. For the highest 24-hour PM_{10} concentrations in 1986, Gray *et al.* (1988) found that ammonium nitrate and geological material were the major contributors in every case, with the largest contributions from these sources found at the Rubidoux and Upland sites. The ammonium sulfate contributions to the highest PM_{10} at Long Beach, Rubidoux, and Upland were four to six times larger than the ammonium sulfate contributions to the highest PM_{10} contributions at the remaining sites. Primary motor vehicle exhaust contributed 4% to 17% of the highest PM_{10} concentrations. Secondary organic carbon was also estimated to be a significant contributor at 7% to 20% of the highest PM_{10} concentrations. Significant fractions of the highest PM_{10} concentrations were unexplained at Long Beach, Rubidoux, and Upland. Gray *et al.* (1988) speculate that the unexplained mass might be due to unmeasured liquid water associated with the large contributions from soluble ammonium nitrate and ammonium sulfate in these samples. Basin-

Table 2-5
Chemical Mass Balance PM_{10} Source Contribution Estimates in the South Coast Air Basin[a]

Source Type	Source Contribution Estimates at Each Site ($\mu g/m^3$)							
	Anaheim	Burbank	Long Beach	Lennox	Los Angeles	Los Angeles ($PM_{2.5}$)	Rubidoux	Upland
1986 Annual Average								
Motor Vehicle Diesel	3.6	5.2	4.4	3.9	5.6	5.8	5.1	3.6
Motor Vehicle Leaded Gas	0.5	0.9	0.7	0.7	0.8	0.7	0.5	0.5
Secondary Carbon	8.2	9.8	6.4	7.6	7.9	11.1	5.9	7.8
$(NH_4)_2SO_4$	7.0	7.2	8.0	7.6	7.6	7.3	6.4	6.4
NH_4NO_3	9.8	10.2	9.2	7.9	11.2	7.0	21.3	14.5
Paved Road Dust	10.2	16.7	19.7	9.4	23.8	3.2	41.0	25.4
Soil Dust	0	0	0	0	0	0	2.1	0
Freeway Dust	11.0	4.6	1.0	6.6	0	0	0	0
Lime (Gypsum)	0	0	0	0.1	0	0	4.0	0.4
Residual Oil	0.4	0.1	0.1	0.2	0	0.0	0.3	0.6
Marine	1.4	0.9	2.0	3.1	1.3	0.2	1.0	0.6
Unexplained	0.1	1.2	0.3	-0.4	2.0	1.4	-0.2	-1.8
Total Mass	52.1	56.6	51.9	46.9	60.2	36.8	87.4	58.0
Highest 24-Hour Average[b]								
Motor Vehicle Diesel	13.4	22.0	6.2	12.5	17.9	20.9	11.5	10.1
Motor Vehicle Leaded Gas	1.2	2.8	1.1	1.8	2.5	1.7	1.7	1.7
Secondary Carbon	21.3	27.8	17.9	21.2	15.9	26.6	22.0	21.1
$(NH_4)_2SO_4$	5.1	5.1	30.9	9.3	6.4	6.1	28.0	21.5
NH_4NO_3	48.0	69.7	20.0	63.3	66.6	65.8	123.6	86.8
Paved Road Dust	44.1	58.0	28.5	37.4	73.3	6.6	68.1	51.8
Lime (Gypsum)	0	0	0	0	0	0	3.7	0.0
Residual Oil	0	0	1.2	0	0	0.6	1.5	1.5
Marine	1.5	1.2	0	3.3	1.8	0.7	0.7	0.3
Unexplained	-4.9	0.7	25.6	-3.0	2.4	9.8	38.0	14.0
Total Mass	129.7	187.3	131.0	145.8	186.9	138.8	298.7	208.7

[a] From Gray *et al.*, 1988.

[b] Dates of Maximum 24-hour average PM_{10} in 1986: Anaheim: December 4; Burbank: December 4; Long Beach: March 27; Lennox: December 4; Los Angeles: December 4; Los Angeles ($PM_{2.5}$): December 4; Rubidoux: October 29; Upland: October 29.

Table 2-6
Revised Chemical Mass Balance PM_{10} Source Contribution Estimates in the South Coast Air Basin[a]

Source Type	Source Contribution Estimates at Each Site ($\mu g/m^3$)							
	Anaheim	Burbank	Long Beach	Lennox	Los Angeles	Los Angeles ($PM_{2.5}$)	Rubidoux	Upland
1986 Annual Average								
Motor Vehicle[b]	3.5	6.2	4.8	4.6	6.9	8.6	6.8	3.6
Secondary Carbon	5.4	8.0	5.5	5.5	7.8	9.4	6.2	5.2
$(NH_4)_2SO_4$	6.3	6.4	7.3	7.2	6.7	6.6	6.1	5.9
NH_4NO_3	9.9	10.2	8.3	7.8	11.2	6.3	22.7	14.4
Geological[c]	23.5	21.2	19.2	16.4	23.0	2.8	37.6	26.1
Lime (Gypsum)	0	0	0	0	0	0	7.0	0
Residual Oil	1.0	1.1	1.5	1.6	1.3	0.9	0.7	0.8
Marine	3.0	2.2	3.0	3.8	2.7	0.3	2.0	1.6
Unexplained	-0.5	1.3	2.3	0	0.6	0.5	-1.7	0.4
Total Mass	52.1	56.6	51.9	46.9	60.2	35.4	87.4	58.0
Highest 24-Hour Average[d]								
Motor Vehicle	14.0	30.8	7.4	19.6	21.1	32.5	18.2	1.5
Secondary Carbon	9.8	20.0	15.6	16.6	15.2	19.1	18.8	15.5
$(NH_4)_2SO_4$	3.4	2.1	28.9	7.9	3.8	3.9	26.0	20.0
NH_4NO_3	49.1	69.4	19.2	63.3	67.8	69.3	124.3	86.5
Geological	40.7	52.7	27.0	32.8	68.6	5.8	61.8	46.6
Lime (Gypsum)	0	0	0	0	0	0	9.2	0
Residual Oil	1.2	1.4	2.6	3.6	2.0	1.0	1.6	2.5
Marine	1.8	1.2	0.0	2.8	1.6	0.7	0.7	0.2
Unexplained	9.7	9.7	30.3	-0.8	6.8	6.5	38.1	35.9
Total Mass	129.7	187.3	131.0	145.8	186.9	138.8	298.7	208.7

[a] From Zeldin *et al.*, 1990.

[b] Include paved road dust, soil dust, and freeway dust listed in Table 2-5.

[c] Include motor vehicle diesel and motor vehicle leaded gas listed in Table 2-5.

[d] Dates of Maximum 24-hour average PM_{10} in 1986: Anaheim: December 4; Burbank: December 4; Long Beach: March 27; Lennox: December 4; Los Angeles: December 4; Los Angeles ($PM_{2.5}$): December 4; Rubidoux: October 29; Upland: October 29.

wide events are observable in corresponding highest PM_{10} concentrations at Anaheim, Burbank, Lennox and Downtown Los Angeles on December 4, 1986, and at Rubidoux and Upland on October 29, 1986. These correspond to the basin-wide episodes identified in Table 2-4.

The source contributions in Table 2-5 are reasonably accurate except for the secondary organic carbon contribution. Examination of the day-specific contributions documented by SCAQMD shows that these contributions are relatively constant, regardless of time of year or location. This is not consistent with the findings of Turpin and Huntzicker (1991) or with those of Gray *et al.* (1986). Several pieces of evidence support the contention that a portion of what is interpreted by Gray *et al.* (1988) as secondary organic carbon should be attributed to resuspended road dust and to primary motor vehicle exhaust.

While the average $PM_{2.5}$ total to elemental carbon ratios found by Gray *et al.* (1986) ranged from 2.4 to 3, Solomon *et al.* (1989) found PM_{10} ratios which ranged from 4 to 5. Solomon *et al.* (1989) attributed this difference to: 1) additional organic carbon in coarse particles from plant fragments and humic materials; and 2) a larger contribution from secondary organic carbon during 1986 than was observed during 1982. Solomon *et al.* (1989) do not note that another reason for the difference might be due to the difference between the carbon analysis methods used for the 1982 sample analyses (Johnson *et al.*, 1980; Huntzicker *et al.*, 1982) and the different method (Cary, 1990) applied to the 1986 samples. Differences between the organic and elemental carbon attributions of different analysis methods will be discussed in Section 3 of this report. These methods give different abundances for organic and elemental carbon and these differences are important. The source profiles used by Gray *et al.* (1988) applied carbon analysis methods more similar to those used in the 1982 study than to those used during the 1986 study.

The motor vehicle profiles used by Gray *et al.* (1988) did not represent emissions for the entire vehicle fleet. Their leaded gasoline profile did not include the organic carbon which is expected to be emitted by the significant unleaded vehicle fleet operating in the SoCAB during 1987, as will be discussed further in Section 5 of this report. Had unleaded vehicle exhaust been included in the profile, the proportion of lead would decrease and the portion of ambient organic carbon attributable to vehicle exhaust would increase at the expense of the secondary organic carbon contribution.

Finally, only a few of the geological samples used by Gray *et al.* (1988) were submitted to carbon analyses (Cooper *et al.*, 1987), and carbon accounted for up to 20% of the mass in these cases. Some geological profiles were used in the CMB modeling which did not contain this carbon component because it wasn't measured in them, even though it was probably a significant component. This missing carbon would be interpreted as secondary carbon in the model output. This carbon was added to the profiles reported by NEA (1990a; 1990b; 1990c).

NEA (1990a; 1990b; 1990c) re-analyzed some of the archived source samples taken by Cooper *et al.* (1987) for carbon and ions. These were used to obtain the source contributions in Table 2-6. The new estimates for secondary organic carbon contributions are generally less than those in Table 2-5. Zeldin *et al.* (1990) also compare source contributions using the NEA

profiles with CMB source profiles derived from a multivariate model (Kim *et al.*, 1992). Both results are generally in good agreement within an acceptable error range.

The Rubidoux site stands out as having the highest PM_{10} measured in the SoCAB and as having the highest ammonium nitrate contributions to PM_{10}. The importance of air mass transport from the coast to Rubidoux was verified by Russell and Cass (1984). Results from their August 30-31, 1982, field experiment showed that the water-soluble portion of particulate matter was primarily composed of nitrate, sulfate, and ammonium ions, with significant quantities of sodium, magnesium, chloride, potassium and calcium ions. Nitrate was shown to accumulate in air masses which stagnate overnight near the coast with transport inland by the morning sea-breeze. Most of the inorganic nitrate at Rubidoux was found as particulate ammonium nitrate, as opposed to gaseous nitric acid, which indicates an excess of ammonia gas to neutralize acidic species. As noted in Section 2.1, Russell and Cass (1986) identify a large group of dairies and animal husbandry operations in the Chino area, approximately 13 km west (and upwind) of the Rubidoux site.

Chow *et al.* (1992) conducted a year-long PM_{10} neighborhood-scale monitoring study at Rubidoux and two other sites within 5 km of Rubidoux during 1988 to determine whether or not Rubidoux PM_{10} concentrations should be used as design values for particulate control measures in the SoCAB. The annual average and maximum 24-hour PM_{10} concentrations, chemical compositions, and source contributions were remarkably similar to those found by Solomon *et al.* (1989) and Gray *et al.* (1988) at Rubidoux during 1986. The major difference was that much of the secondary organic carbon found by Gray *et al.* (1988) was attributed to primary motor vehicle exhaust. Chow *et al.* (1992) found that source contributions to the annual average and to the highest 24-hour PM_{10} were similar at the three sites for all source types except geological material and lime/gypsum (interpreted as "construction" contributions). For the three highest PM_{10} concentrations during the study period, all of which exceeded the 24-hour standard, the geological source contribution at Rubidoux was higher than that measured at the Riverside/Magnolia site 5 km to the south-southeast by 33 $\mu g/m^3$ on September 30, 1988, by 21 $\mu g/m^3$ on October 24, 1988, and by 52 $\mu g/m^3$ on May 11, 1988. A large fraction of this geological material at Rubidoux was directly attributable to a gypsum/lime source while gypsum/lime was found in negligible quantities at the other two sites in the neighborhood. Wang *et al.* (1992) performed a microinventory in the Rubidoux vicinity. This inventory found grading and leveling as well as quarrying activities within 5 km northwest of the sampling site. This microinventory found significantly higher silt loadings and traffic on unshouldered roads near the Rubidoux site than were apparent near the other two neighborhood-scale sites. Chow *et al.* (1992) concluded that the Rubidoux site receives primary geological and lime/gypsum contributions from sources within a few kilometers of the site as well as from the much larger urban-scale areas. Since secondary nitrate and sulfate contributions were similar at all sites, Chow *et al.* (1992) concluded that these did not originate on a neighborhood-scale and that reductions in upwind emissions would be required to reduce these contributions.

The high ammonium nitrate concentrations measured at Rubidoux and other sites demonstrate that ammonia and nitric acid have a major effect on ambient PM_{10}. Measurements for these species are reported by: 1) Russell and Cass (1984) with 2-hour resolution at ten sites

for August 30-31, 1982; 2) Solomon *et al.* (1992) with 24-hour resolution every sixth day at seven sites during 1986; 3) Wolff *et al.* (1991) with 12-hour resolution every day at the SCAQS Claremont site from June 15 to July 24 and from August 18 to September 3, 1987, and at the SCAQS Long Beach site from November 7 to 18 and from December 2 to 12, 1987; and 4) Watson *et al.* (1991a) with 12-hour resolution every sixth day at three sites from October 1988 to September 1989. Table 2-7 compares average concentrations of nitric acid, ammonia, and particulate nitrate of 12- and 24-hour samples reported in some of these references for the same or nearby sampling sites.

Direct comparisons in Table 2-7 are difficult since sampling methods, sampling times, sampling periods, and locations are not identical among the different studies. Year to year variations are apparent, however, for gaseous nitric acid, ammonia, and denuded $PM_{2.5}$ particulate nitrate measurements taken between 1986 and 1989. The annual average nitric acid concentrations at the Downtown Los Angeles site were 6 $\mu g/m^3$ for 24-hour samples in 1986 (Solomon *et al.*, 1992) and 5.7 $\mu g/m^3$ and 0.3 $\mu g/m^3$ for daytime (0600 to 1800 PST) and nighttime (1800 to next day 0600 PST) samples in 1988/1989 (Watson *et al.*, 1991a), respectively. Similar results of one-year average nitric acid concentrations were found at the Upland site with 5.5 $\mu g/m^3$ in 1986 and at the Azusa site with 3.0 $\mu g/m^3$ in 1988/1989. At the Long Beach site, Wolff *et al.* (1991) report 12-hour average daytime (0600 to 1800 PST) nitric acid concentration of 3.4 $\mu g/m^3$ and 1.4 $\mu g/m^3$ for the fall 1987 SCAQS intensive and non-intensive periods. These values are comparable to the 2.6 $\mu g/m^3$ annual average 12-hour daytime nitric acid concentration reported by Watson *et al.* (1991a) for the period of 1988/1989. Maximum nitric acid concentrations were 16.6 $\mu g/m^3$ for 24-hour samples in 1986 and 20.3 $\mu g/m^3$ for 12-hour samples in 1988/1989 at the Downtown Los Angeles site. Wolff *et al.* (1991) reported a maximum 12-hour nitric acid concentration of 8.1 $\mu g/m^3$ in 1987, which is lower than the 15.7 $\mu g/m^3$ measured in 1986 and 9.6 $\mu g/m^3$ measured in 1988/1989.

$PM_{2.5}$ nitrate concentrations exhibited a similar trend. The maximum nitrate concentrations were 42.7 $\mu g/m^3$ (24-hour) in 1986, 77.8 $\mu g/m^3$ (12-hour) in 1987, and 25.2 $\mu g/m^3$ (12-hour) in 1988/1989. Solomon *et al.* (1992) did not report any ammonia measurements. The daytime and nighttime ammonia concentrations were 3.6 $\mu g/m^3$ and 3.4 $\mu g/m^3$ in 1987 and 8.0 $\mu g/m^3$ and 4.7 $\mu g/m^3$ in 1988/1989 at the Long Beach site.

Other important aerosol measurement and data analysis studies have been reported for the SoCAB which have not been cited previously (e.g., Appel *et al.*, 1976, 1979; Cass, 1978a, 1978b, 1979; Cronn *et al.*, 1977; Ehrman *et al.*, 1992; Gordon and Bryan, 1973; Gordon, 1976; Grosjean, 1983, 1984; Hansen *et al.* 1982; Heisler et al, 1973; Miguel and Friedlander, 1978; Pitts *et al.*, 1985a, 1985b; Pratsinis *et al.*, 1984, 1988; Rosen *et al.*, 1982; Schuetzle *et al.*, 1975; Tuazon *et al.*, 1981), and their observations and conclusions are in general agreement with those of the references cited in this section.

Table 2-7
Comparison of Nitric Acid, Ammonia, and $PM_{2.5}$ Denuded Nitrate Among Previous Studies

	Burbank	Downtown Los Angeles	Hawthorne	Long Beach	Anaheim	Rubidoux	Azusa	Claremont
I. NITRIC ACID								
Solomon *et al.* (1992)								
-- 1986 Annual Average	6.7	6.0	3.1	3.4	3.2	1.7	6.9[a]	NA[b]
Wolff *et al.* (1991)								
-- 1987 Intensive[c]								
- Day (0600-1800 PST)	NA	NA	NA	3.4	NA	NA	NA	17.4
- Night (1800-0600 PST)	NA	NA	NA	0.5	NA	NA	NA	3.6
-- 1987 Nonintensive[d]	NA	NA	NA	1.4	NA	NA	NA	9.9
Watson *et al.* (1991a)								
-- 1988/1989 Annual Average								
- Day (0600-1800 PST)[e]	NA	5.7	NA	2.6	NA	NA	5.5	NA
- Night (1800-0600 PST)[e]	NA	0.3	NA	0.6	NA	NA	0.5	NA
Solomon *et al.* (1992)								
-- 1986 24-hour Maxima	17.4	16.6	13.0	15.7	13.5	6.7	21.0[a]	NA
Wolff *et al.* (1991)								
-- 1987 12-hour Maxima	NA	NA	NA	8.1	NA	NA	NA	45.5
Watson *et al.* (1991a)								
-- 1988/1989 12-hour Maxima								
- Day (0600-1800 PST)	NA	20.3	NA	9.6	NA	NA	32.3	NA
- Night (1800-0600 PST)	NA	4.0	NA	7.5	NA	NA	9.0	NA

Table 2-7 (continued)
Comparison of Nitric Acid, Ammonia, and $PM_{2.5}$ Denuded Nitrate Among Previous Studies

	Burbank	Downtown Los Angeles	Hawthorne	Long Beach	Anaheim	Rubidoux	Azusa	Claremont
II. $PM_{2.5}$ DENUDED NITRATE								
Solomon *et al.* (1992)								
-- 1986 Annual Average	9.5	9.7	6.2	7.6	8.6	18.2	13.3[a]	NA
Wolff *et al.* (1991)								
-- 1987 Intensive								
- Day (0600-1800 PST)	NA	NA	NA	18.7	NA	NA	NA	9.9
- Night (1800-0600 PST)	NA	NA	NA	10.8	NA	NA	NA	6.0
-- 1987 Nonintensive	NA	NA	NA	9.8	NA	NA	NA	7.1
Watson *et al.* (1991a)								
-- 1988/1989 Annual Average								
- Day (0600-1800 PST)	NA	11.0	NA	6.5	NA	NA	13.3	NA
- Night (1800-0600 PST)	NA	6.5	NA	4.0	NA	NA	7.1	NA
Solomon *et al.* (1992)								
-- 1986 24-hour Maxima	50.8	56.3	39.4	42.7	37.7	109.0	78.0[a]	NA
Wolff *et al.* (1991)								
-- 1987 12-hour Maxima	NA	NA	NA	23.6	NA	NA	NA	77.8
Watson *et al.* (1991a)								
-- 1988/1989 12-hour Maxima								
- Day (0600-1800 PST)	NA	36.7	NA	22.8	NA	NA	54.5	NA
- Night (1800-0600 PST)	NA	30.5	NA	25.2	NA	NA	7.3	NA

Table 2-7 (continued)
Comparison of Nitric Acid, Ammonia, and $PM_{2.5}$ Denuded Nitrate Among Previous Studies

	Burbank	Downtown Los Angeles	Hawthorne	Long Beach	Anaheim	Rubidoux	Azusa	Claremont
III. AMMONIA								
Solomon *et al.* (1992)								
-- 1986 Annual Average	NA	NA	NA	NA	NA	NA	NA	NA
Wolff *et al.* (1991)								
-- 1987 Intensive								
- Day (0600-1800 PST)	NA	NA	NA	3.6	NA	NA	NA	1.7
- Night (1800-0600 PST)	NA	NA	NA	3.4	NA	NA	NA	1.3
-- 1987 Nonintensive	NA	NA	NA	3.1	NA	NA	NA	1.3
Watson *et al.* (1991a)								
-- 1988/1989 Annual Average								
- Day (0600-1800 PST)	NA	10.4	NA	8.0	NA	NA	9.4	NA
- Night (1800-0600 PST)	NA	5.7	NA	4.7	NA	NA	5.3	NA
Solomon *et al.* (1992)								
-- 1986 24-hour Maxima	NA	NA	NA	NA	NA	NA	NA	NA
Wolff *et al.* (1991)								
-- 1987 12-hour Maxima	NA	NA	NA	8.5	NA	NA	NA	14.4
Watson *et al.* (1991a)								
-- 1988/1989 12-hour Maxima								
- Day (0600-1800 PST)	NA	24.3	NA	18.0	NA	NA	22.6	NA
- Night (1800-0600 PST)	NA	18.9	NA	11.8	NA	NA	14.0	NA

Table 2-7 (continued)
Comparison of Nitric Acid, Ammonia, and $PM_{2.5}$ Denuded Nitrate Among Previous Studies

[a] At the Upland site near Azusa.
[b] Data not available.
[c] See Table 3-2 for Intensive study period.
[d] Nonintensive periods are: 06/15/87 to 07/24/87 and 08/18/87 to 09/03/87 at the Claremont site and 11/07/87 to 11/18/87 and 12/03/87 to 12/12/87 at the Long Beach site except those stated in Table 3-2 as intensive period. Sampling periods are normally 0600 to 1800 and 1800 to next day 0600 PST, except those sampling between 06/15/87 and 06/22/87, which are 0900 to 2100 PST and 2100 to next day 0900 PST.
[e] Sampling periods are 0600 to 1800 and 1800 to next day 0600 PST.

2.6 Previous Organic Gas Studies

Since the initial efforts to develop ozone reduction strategies for the Los Angeles area in the early 1960s, there has been continued interest in determining the relative contributions of ROG emissions to ambient levels of VOCs. Prior to application of the CMB receptor model, source contributions were inferred by comparing ratios of individual VOCs or classes of VOCs observed in the ambient air with corresponding ratios in source samples. In the summer and fall of 1960, Neligan (1962) compared C_2 through C_7 hydrocarbons in ambient air from central Los Angeles with the distribution of these groupings in motor vehicle exhaust, and reported a greater proportion of the lower molecular weight paraffinic hydrocarbons in ambient samples than in exhaust emissions; they attributed this discrepancy to contributions from natural gas. These results were reaffirmed by Altshuller and Bellar (1963). Stephens and Burleson (1967) agreed with these earlier results when they examined VOC measurements collected in Riverside, CA, but they discovered that natural gas contributions alone could not explain the propane/ethane ratios in ambient samples. Stephens and Burleson (1967) suggested a combination of gasoline evaporation losses, emissions from oil fields, and natural gas losses to account for ambient concentrations. Stephens and Burleson (1967) later indicated that evaporated gasoline could not account for the excess propane in ambient air. Samples of air trajectories which travelled over oil fields showed that a part of the excess propane could be attributed to oil field vapors. From the ratio of total paraffins (less methane) to carbon monoxide (CO) in motor vehicle exhaust and the average CO concentration in the ambient samples, Kopczynski *et al.* (1972) estimated that one third of the hydrocarbon concentration (as C) measured in 1968 at Downtown Los Angeles could be attributed to natural gas and gasoline vapors.

Source apportionment of atmospheric hydrocarbons in the SoCAB was first performed by Mayrsohn and Crabtree (1976). Multivariate regression analysis was used to determine the optimum combination of source contributions to VOCs measured during the summer of 1973 at the Downtown Los Angeles, Azusa, and Redland sites. On average, motor vehicle exhaust contributed less than 50% to the ambient nonmethane hydrocarbon (NMHC) at three sites. Gasoline and gasoline vapor together accounted for the second largest contributor to NMHC, totaling 30% to 35% by weight. The remaining NMHC consisted of commercial and geogenic natural gas, totaling about 20% by weight. These results were regarded as upper limits because profiles for other VOC sources were not included in the analysis.

A second source reconciliation study was conducted in 1974 by Mayrsohn *et al.* (1977). The sampling network was expanded to eight sites, and 900 ambient samples were analyzed for C_2 through C_{10} hydrocarbons. The average source contributions in this study were: 53% from motor vehicle exhaust; 12% from liquid gasoline; 10% from gasoline vapor; 5% from commercial natural gas; 19% from geogenic natural gas; and 1% from liquefied propane gas.

Feigley and Jeffries (1979) apportioned ambient hydrocarbons measured during the Los Angeles Reactive Pollutant Program (LARPP) using the source profiles developed by Mayrsohn *et al.* (1977). Vehicle-related emissions were estimated to account for 93% of NMHC. The remaining source contribution estimates to NMHC were 4% from commercial natural gas and 3% from liquefied petroleum gas. The combined source contribution estimates of commercial

natural gas, geogenic natural gas, and liquefied petroleum gas from this study (7%) is considerably less than those reported by Mayrsohn *et al.* (1977) (25%) due to the use of the additional fitting species: methane above background and hexane.

As part of an effort to verify and improve the SCAQS speciated organic emissions inventory for use in photochemical modeling, Harley *et al.* (1992a) performed a CMB analysis of the SCAQS VOC data base using several profiles with updated speciation. The average source contributions at the eight summer SCAQS sites ranged from 30% to 40% for vehicle exhaust, 30% to 40% for whole (liquid) gasoline, 10% to 15% for gasoline vapors, 5% to 10% for waste and natural gas, and 5% to 10% for degreasing solvents. The average combined vehicle-related contributions among the eight sites ranged from 75% to 85% of total NMHC. The relative contributions of liquid gasoline were about three times higher than those estimated by Mayrsohn *et al.* (1977) and comparable to those estimated by Feigley and Jeffries (1979).

The variability of these results indicates that substantial collinearity may exist among the source profiles for vehicle exhaust, liquid gasoline, gasoline vapor, and other petroleum-related sources, and that source contribution estimates are dependent upon the selection of the particular set of source profiles and fitting species in each individual CMB calculation. Sensitivity tests are needed to examine the effects of using alternative profiles within the same source type and different sets of fitting species on the CMB source contribution estimates.

Several other VOC measurement field studies have been conducted in the SoCAB (e.g., Lonneman *et al.*, 1974; Grosjean and Fung, 1984). The ambient VOC and other air quality data from the SCAQS program are more extensive than those from any of the previous studies in the SoCAB. These are some of the most comprehensive data available for any urban area in the United States. Validation and exploratory analysis of the SCAQS VOC data base were performed by Lurmann and Main (1992). The spatial and temporal patterns of VOC concentrations and composition are described in detail in their report.

3.0 MEASUREMENTS

The SCAQS program plan (Blumenthal *et al.*, 1987) and Section 2 provide justification for the observables, sample durations, sampling frequency, and monitoring periods for the SCAQS measurements. This section describes the SCAQS particulate and volatile organic compounds (VOC) networks, documents the measurement methods, and evaluates the measurements themselves.

3.1 Sampling Locations

The ambient particulate and VOC monitoring network for the SCAQS consists of nine Type B sites as shown in Figure 3-1. Six sampling sites (Burbank, Downtown Los Angeles, Hawthorne, Long Beach, Anaheim, and Riverside) operated during both the summer and fall, with an additional three sampling sites (San Nicolas Island, Azusa, and Claremont) operated only during the summer.

A brief description of sampling site locations, coordinates, elevations, and the adjacent environment and terrain is presented in Table 3-1. These sampling sites were selected to represent different industrial, commercial, residential, and agricultural land-uses in urban, suburban, and background areas, and to characterize source emissions and transport within the SoCAB. Claremont and Long Beach were Type A research sites at which several particulate sampling systems were collocated with additional meteorological, gaseous, acidity, and visibility measurements (Lawson, 1990).

The summer period emphasized elevated ozone concentrations and west-to-east transport, and included five episodes on eleven sampling days: 1) June 19, 1987; 2) June 24 and 25, 1987; 3) July 13 to 15, 1987; 4) August 27 to 29, 1987; and 5) September 2 and 3, 1987. The fall study was designed to investigate air quality during stagnant conditions and consisted of three episodes on six sampling days: 1) November 11 to 13, 1987; 2) December 3, 1987; and 3) December 10 and 11, 1987.

Diurnal sampling using four- to seven-hour filter-based gas/aerosol samples was conducted during summer (0000 to 0500, 0500 to 0900, 0900 to 1300, 1300 to 1700, 1700 to 2400 PST) and fall (0000 to 0600, 0600 to 1000, 1000 to 1400, 1400 to 1800, 1800 to 2400 PST). Five sample sets were acquired for each episode day. Hourly VOC samples were collected with electropolished stainless steel canisters three to six times per day during summer (beginning at 0400, 0600, 0800, 1100, 1300, 1500 PST) and fall (beginning 0500, 0700, 0900, 1200, 1400, 1600 PST). Table 3-2 summarizes the SCAQS filter-based gaseous and aerosol measurements, averaging times, sampling frequency/periods, and measurement methods. Information for the VOC measurements is given in Table 3-3.

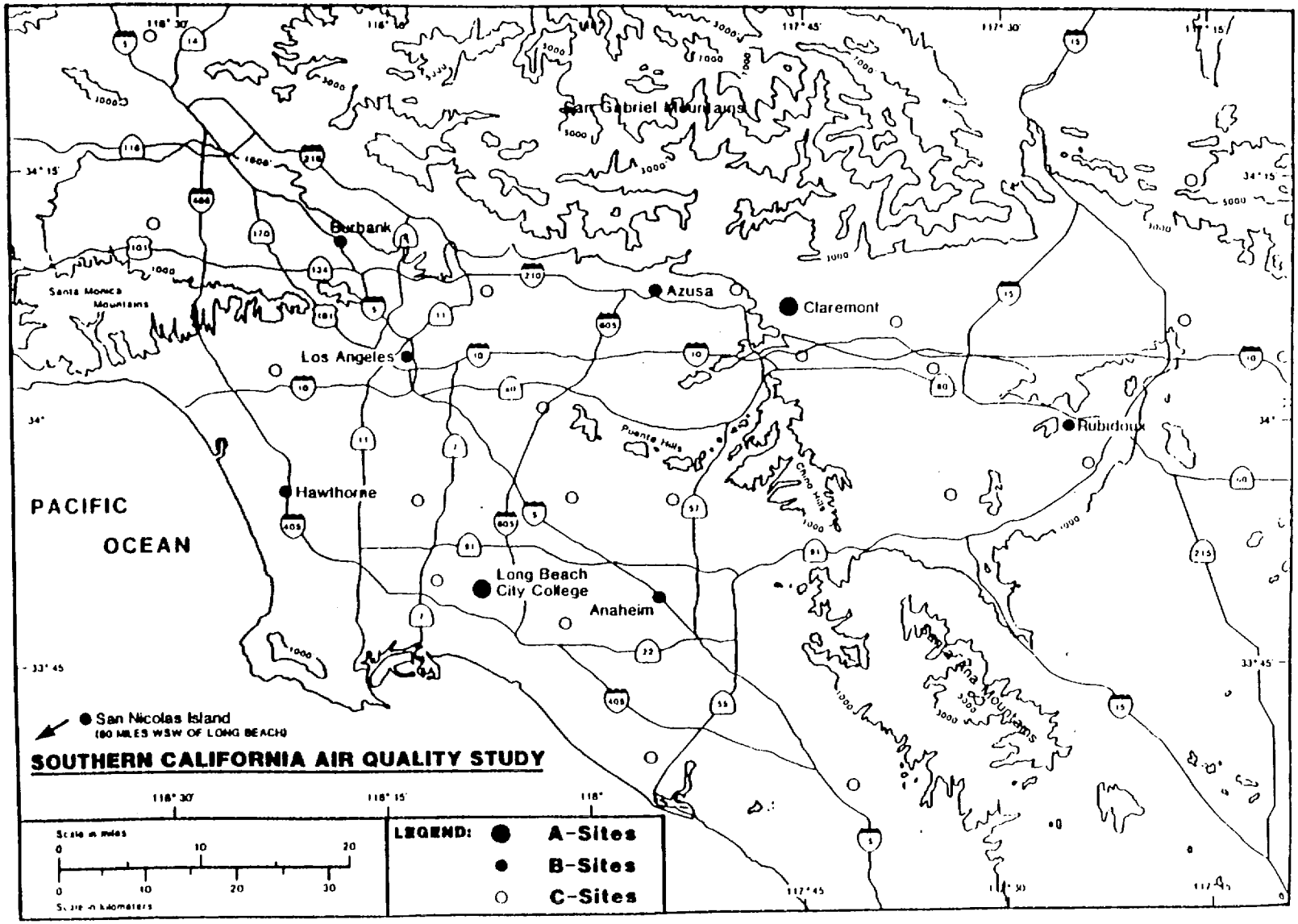

Figure 3-1. Locations of the Southern California Air Quality Study Monitoring Sites

Table 3-1
SCAQS Aerosol and Volatile Organic Compounds Sampling Site Descriptions[a]

Site Locations (code)	Coordinates		Elevation (m)	Site Descriptions
1. Summer and Fall Sampling Sites				
Burbank (BURK) 228 W. Palm Ave. Burbank, CA 91502	Latitute (deg/min/sec): Longitude (deg/min/sec): UTM North (km): UTM East (km):	34°10'58" N 118°18'27" W 3,783,000 379,500	Above Ground: 4.0 Above MSL[b]: 168.2	An urban industrial/commercial/residential site, located northeast of Victory Blvd. with light traffic. Freeway I-5 is ~0.5 kilometers (km) to the northeast and a parking lot is located ~0.15 km to the north. The Burbank power plant, fired by natural gas with fuel oil standby, is located one block to the northeast. The site is located in the San Fernando Valley on relatively flat terrain with hills on the north and south.
Downtown Los Angeles (CELA) 1630 N. Main St. Los Angeles, CA 90012	Latitute (deg/min/sec): Longitude (deg/min/sec): UTM North (km): UTM East (km):	34°04'02" N 118°13'31" W 3,770,100 386,900	Above Ground: 5.0 Above MSL: 87.0	An urban industrial/commercial site, located on the roof of the Los Angeles County Department of Water and Power (DWP). There are railroad tracks less than 0.2 km to the east with moderate use. The site is close to the high-rise buildings of downtown and ~2.5 km northeast of the Los Angeles Civic Center. Elysian Park (Dodger Stadium) is on a hill less than 1.6 km to the northwest. Freeway 110 is ~1.2 km to the west, Freeway I-5 is ~1 km to the east, and the junctions of the Freeways 101, I-5, and I-10 are ~1.5 km to the south. Moderate commercial truck, train, and automobile traffic around the site. The terrain immediately around the site is relatively flat, but there are high hills starting ~1.5 km to the north.

Table 3-1 (continued)
SCAQS Aerosol and Volatile Organic Compounds Sampling Site Descriptions[a]

Site Locations (code)	Coordinates		Elevation (m)	Site Descriptions
I. Summer and Fall Sampling Sites (continued)				
Hawthorne (HAWT) 5234 W. 120th St. Lennox, CA 90250	Latitute (deg/min/sec): Longitude (deg/min/sec): UTM North (km): UTM East (km):	33°55'23" N 118°22'09" W 3,754,300 373,400	Above Ground: 3.0 Above MSL: 21.3	A suburban commercial/residential site, located on top of a 3 × 7 trailer inside of the Anza Elemental School playground, adjacent to the cities of Hawthorne, Westchester, and El Segundo. The site is west of Freeway 405 and 0.8 km south of the new Freeway 105, with heavy commuter and arterial traffic. The Los Angeles International Airport property begins to the northwest with the nearest runway ~2 km away. The ocean is less than 6 km away. During the study, construction on a Freeway 105 interchange resulted in a large amount of earth moving on Freeway 405. The surrounding terrain is relatively flat and the site has good exposure to air flow.
Long Beach (LBCC) 4901 E. Carson St. Long Beach, CA 90807	Latitute (deg/min/sec): Longitude (deg/min/sec): UTM North (km): UTM East (km):	33°49'49" N 118°08'18" W 3,743,700 394,700	Above Ground: 1.5 Above MSL: 17.0	An urban industrial/commercial/residential site, located on the Long Beach City College campus, south of the track field, with the baseball diamond to the west, and McDonnell-Douglas Aircrafts hangers to the south. Freeway 405 is ~2.5 km to the south, with Long Beach Municipal Airport ~0.8 km to the southwest and Foothill ~1 km to the north. Traffic is moderate but increases significantly when college is in session and industrial shift changes. Local sources of primary oil refinery emissions surrounded this site. The terrain surrounding the site is relatively flat except for Signal Hill (~6 km to the west).

Table 3-1 (continued)
SCAQS Aerosol and Volatile Organic Compounds Sampling Site Descriptions*

Site Locations (code)	Coordinates		Elevation (m)	Site Descriptions
I. Summer and Fall Sampling Sites (continued)				
Anaheim (ANAH) 1010 S. Harbor Blvd. Anaheim, CA 92805	Latitute (deg/min/sec): Longitude (deg/min/sec): UTM North (km): UTM East (km):	33°49'19" N 117°55'07" W 3,742,500 415,000	Above Ground: 1.0 Above MSL: 41.0	An urban commercial/residential site, located behind the Orange County Agriculture Facility, ~0.5 km east of Freeway I-5 and 1.2 km northeast of Disneyland with moderate to heavy traffic. Citron Park is located to the west and southwest (across Harbor Blvd.) and a residential trailer park is located to the southeast. Smooth terrain with no significant topographical features in the close vicinity of the site, and air flow to the site is nearly unrestricted.
Riverside/Rubidoux (RIVR) 5888 Mission Blvd. Rubidoux, CA 92509	Latitute (deg/min/sec): Longitude (deg/min/sec): UTM North (km): UTM East (km):	33°59'59" N 117°25'01" W 3,762,000 461,500	Above Ground: 1.0 Above MSL: 214.0	A suburban commercial/residential/agricultural site, located on a platform in the parking lot behind the Riverside Health Facility. Freeway 60 is ~1 km to the north, and Flabob airport (a small airstrip) is ~1.5 km to the south with moderate traffic. There is a relatively large amount of vacant and agricultural land in the vicinity. The topography within a 3 km radius is characterized as rolling, with Rattlesnake Mountain (~60 m) ~1.5 km to the north. The exposure of the site to air flow is fair.

Table 3-1 (continued)
SCAQS Aerosol and Volatile Organic Compounds Sampling Site Descriptions*

Site Locations (code)	Coordinates		Elevation (m)	Site Descriptions
II. Additional Summer Sampling Sites				
San Nicolas Island (SNIC) U.S Navy Pacific Missile Test Center San Nicolas Island, CA	Latitute (deg/min/sec): Longitude (deg/min/sec): UTM North (km): UTM East (km):	33°15'24" N 119°29'09" W 3,682,300 268,400	Above Ground: 3.5 Above MSL: 122.0	A rural background site, located ~1 km from the shore on the northeast side of the island and ~104 km off the Southern California coast. Except for some military offices, residences, a small power station with five generators (~8 km from the site), and an airport (~2.5 km from the site), the land is primarily undeveloped. The terrain of the island is low rolling hills to a maximum height of just over 300 m, with good air flow exposure.
Azusa (AZUS) 803 N. Loren Ave Azusa, CA 91702	Latitute (deg/min/sec): Longitude (deg/min/sec): UTM North (km) UTM East (km):	34°08'09" N 117°55'23" W 3,777,400 414,900	Above Ground: 4.0 Above MSL: 90.0	An urban commercial/residential site, located in an industrial park ~05 km north of Foothill Blvd. and ~1 km north Freeway 210. There is a residential area in the west, a residential trailer park to the east, and a vacant area behind the trailer park followed by some commercial buildings. Rock quarries are operating ~1 km to the west and in the foothills to the north. Railroad tracks are located to the north on vacant land less than 0.5 km away, before 10th street, and also ~0.8 km to the south.

Table 3-1 (continued)
SCAQS Aerosol and Volatile Organic Compounds Sampling Site Descriptions[a]

Site Locations (code)	Coordinates		Elevation (m)	Site Descriptions
II. Additional Summer Sampling Sites (continued)				
Claremont (CLAR) Pomona College Foothill Blvd. Claremont, CA 91711	Latitute (deg/min/sec): Longitude (deg/min/sec): UTM North (km): UTM East (km):	34°06'07" N 117°42'14" W 3,773,500 435,100	Above Ground: 1.5 Above MSL: 364.0	A suburban residential site, located on a platform south of Bower Center in a large parking lot of the Claremont McKenna College campus, ~0.5 km from San Bernardino County. Freeway I-10 is ~1.5 km south of the site. The small Cable Airport is ~1.5 km to the northwest in Upland. Nearby traffic is light to moderate but increases when classes are in session. The land 0.2 km east of the site is predominantly undeveloped. The land in other directions is used primarily for campus and residential buildings. The terrain at the site is relatively flat, with foothills and mountains in the distance.

[a] Chan and Durkee (1989).
[b] Mean Sea Level.

Table 3-2
SCAQS Filter-Based Gaseous and Aerosol Measurements[a]

Measurement	Sampling Sites[b]	Averaging Time	Sample Frequency and Period[c,d]	Measurement Method Instrument
$PM_{2.5}$ Particles (0 to 2.5 μm)	Nine sites in summer: BURK, CELA, HAWT, LONG, ANAH, RIVR, SNIC, AZUS, and CLAR.	0000 to 0500 PST 0500 to 0900 PST 0900 to 1300 PST 1300 to 1700 PST 1700 to 2400 PST	5 times/day for 11 episodic days from 6/19/87 through 9/03/87	SCAQS sampler with Bendix Model 240 Cyclone Inlet
	Six sites in the fall: BURK, CELA, HAWT, LONG, ANAH, and RIVR.	0000 to 0600 PST 0600 to 1000 PST 1000 to 1400 PST 1400 to 1800 PST 1800 to 2400 PST	5 times/day for 6 episodic days from 11/11/87 through 12/11/87	SCAQS sampler with Bendix Model 240 Cyclone Inlet
PM_{10} Particles (0 to 10 μm)	Nine sites in summer: BURK, CELA, HAWT, LONG, ANAH, RIVR, SNIC, AZUS, and CLAR.	0000 to 0500 PST 0500 to 0900 PST 0900 to 1300 PST 1300 to 1700 PST 1700 to 2400 PST	5 times/day for 11 episodic days from 6/19/87 through 9/03/87	SCAQS sampler with Sierra-Andersen Model 254-I 10 μm Inlet
	Six sites in the fall: BURK, CELA, HAWT, LONG, ANAH, RIVR.	0000 to 0600 PST 0600 to 1000 PST 1000 to 1400 PST 1400 to 1800 PST 1800 to 2400 PST	5 times/day for 6 episodic days from 11/11/87 through 12/11/87	SCAQS sampler with Sierra-Andersen Model 254-I 10 μm Inlet
Nitric Acid (HNO_3), Ammonia (NH_3), and Sulfur Dioxide (SO_2)	Nine sites in summer: BURK, CELA, HAWT, LONG, ANAH, RIVR, SNIC,[e] AZUS, and CLAR.	0000 to 0500 PST 0500 to 0900 PST 0900 to 1300 PST 1300 to 1700 PST 1700 to 2400 PST	5 times/day for 11 episodic days from 6/19/87 through 9/03/87	SCAQS Sampler with PFA Teflon-coated AIHL Cyclone Inlet and Plenum Using the Denuder Difference Method and Impregnated Filters
	Six sites in the fall: BURK, CELA, HAWT, LONG, ANAH, RIVR.	0000 to 0600 PST 0600 to 1000 PST 1000 to 1400 PST 1400 to 1800 PST 1800 to 2400 PST	5 times/day for 6 episodic days from 11/11/87 through 12/11/87	SCAQS Sampler with PFA teflon-coated Bendix 240 Cyclone Inlet and Plenum Using the Denuder Difference Method and Impregnated Filters

Table 3-2 (continued)
SCAQS Filter-Based Gaseous and Aerosol Measurements[a]

Measurement	Sampling Sites[b]	Averaging Time	Sample Frequency and Period[c,d]	Measurement Method Instrument
$PM_{2.5}$ and PM_{10} Particle Mass	Nine sites in summer: BURK, CELA, HAWT, LONG, ANAH, RIVR, SNIC, AZUS, and CLAR.	0000 to 0500 PST 0500 to 0900 PST 0900 to 1300 PST 1300 to 1700 PST 1700 to 2400 PST	5 times/day for 11 episodic days from 6/19/87 through 9/03/87	Gravimetric Analysis on Teflon Filters (Mettler Electro-micro balance)
	Six sites in the fall: BURK, CELA, HAWT, LONG, ANAH, RIVR.	0000 to 0600 PST 0600 to 1000 PST 1000 to 1400 PST 1400 to 1800 PST 1800 to 2400 PST	5 times/day for 6 episodic days from 11/11/87 through 12/11/87	Gravimetric Analysis on Teflon Filters (Mettler Electro-microbalance)
$PM_{2.5}$ Particle b_{abs}	Nine sites in summer: BURK, CELA, HAWT, LONG, ANAH, RIVR, SNIC, AZUS, and CLAR.	0000 to 0500 PST 0500 to 0900 PST 0900 to 1300 PST 1300 to 1700 PST 1700 to 2400 PST	5 times/day for 11 episodic days from 6/19/87 through 9/03/87	Integrating Plate Analysis on Nuclepore Polycarbonate Filters (U.C. Davis and Radiance Research Instruments)
	Six sites in the fall: BURK, CELA, HAWT, LONG, ANAH, RIVR.	0000 to 0600 PST 0600 to 1000 PST 1000 to 1400 PST 1400 to 1800 PST 1800 to 2400 PST	5 times/day for 6 episodic days from 11/11/87 through 12/11/87	Integrating Plate Analysis on Nuclepore Polycarbonate Filters (U.C. Davis and Radiance Research Instruments)
$PM_{2.5}$ and PM_{10} Particle Elements	Nine sites in summer: BURK, CELA, HAWT, LONG, ANAH, RIVR, SNIC, AZUS, and CLAR.	0000 to 0500 PST 0500 to 0900 PST 0900 to 1300 PST 1300 to 1700 PST 1700 to 2400 PST	5 times/day for 11 episodic days from 6/19/87 through 9/03/87	X-ray Fluorescence Analysis on Teflon Filters (Siemens MRS-3 Wavelength Dispersive XRF Analyzer)

Table 3-2 (continued)
SCAQS Filter-Based Gaseous and Aerosol Measurements[a]

Measurement	Sampling Sites[b]	Averaging Time	Sample Frequency and Period[c,d]	Measurement Method Instrument
$PM_{2.5}$ and PM_{10} Particle Elements (continued)	Six sites in the fall: BURK, CELA, HAWT, LONG, ANAH, RIVR.	0000 to 0600 PST 0600 to 1000 PST 1000 to 1400 PST 1400 to 1800 PST 1800 to 2400 PST	5 times/day for 6 episodic days from 11/11/87 through 12/11/87	X-ray Fluorescence Analysis on Teflon Filters (Siemens MRS-3 Wavelength Dispersive XRF Analyzer)
$PM_{2.5}$ and PM_{10} Particle Chloride (Cl^-), Nitrate (NO_3^-), and Sulfate ($SO_4^=$)	Nine sites in summer: BURK, CELA, HAWT, LONG, ANAH, RIVR, SNIC, AZUS, and CLAR.	0000 to 0500 PST 0500 to 0900 PST 0900 to 1300 PST 1300 to 1700 PST 1700 to 2400 PST	5 times/day for 11 episodic days from 6/19/87 through 9/03/87	Ion Chromatographic Analysis on Teflon Filter Extracts and Nylon Backup Filter Extracts (Dionex Model 10)
	Six sites in the fall: BURK, CELA, HAWT, LONG, ANAH, RIVR.	0000 to 0600 PST 0600 to 1000 PST 1000 to 1400 PST 1400 to 1800 PST 1800 to 2400 PST	5 times/day for 6 episodic days from 11/11/87 through 12/11/87	Ion Chromatographic Analysis on Teflon Filter Extracts and Nylon Backup Filter Extracts (Dionex Model 10)
Water Soluble $PM_{2.5}$ and PM_{10} Particle Sodium (Na^+) and Potassium (K^+) Ions	Nine sites in summer: BURK, CELA, HAWT, LONG, ANAH, RIVR, SNIC, AZUS, and CLAR.	0000 to 0500 PST 0500 to 0900 PST 0900 to 1300 PST 1300 to 1700 PST 1700 to 2400 PST	5 times/day for 11 episodic days from 6/19/87 through 9/03/87	Atomic Absorption Spectrophotometry on Teflon Filter Extracts (Instrumentation Laboratories Model 951)

Table 3-2 (continued)
SCAQS Filter-Based Gaseous and Aerosol Measurements[a]

Measurement	Sampling Sites[b]	Averaging Time	Sample Frequency and Period[c,d]	Measurement Method Instrument
Soluble $PM_{2.5}$ and PM_{10} Particle Sodium (Na^+) and Potassium (K^+) Ions (continued)	Six sites in the fall: BURK, CELA, HAWT, LONG, ANAH, RIVR.	0000 to 0600 PST 0600 to 1000 PST 1000 to 1400 PST 1400 to 1800 PST 1800 to 2400 PST	5 times/day for 6 episodic days from 11/11/87 through 12/11/87	Atomic Absorption Spectrophotometry on Teflon Filter Extracts (Instrumentation Laboratories Model 951)
$PM_{2.5}$ and PM_{10} Particle Ammonium (NH_4^+)	Nine sites in summer: BURK, CELA, HAWT, LONG, ANAH, RIVR, SNIC, AZUS, and CLAR.	0000 to 0500 PST 0500 to 0900 PST 0900 to 1300 PST 1300 to 1700 PST 1700 to 2400 PST	5 times/day for 11 episodic days from 6/19/87 through 9/03/87	Technicon Automatic Colorimetry on Teflon Filter Extracts (Technicon Model IV)
	Six sites in the fall: BURK, CELA, HAWT, LONG, ANAH, RIVR.	0000 to 0600 PST 0600 to 1000 PST 1000 to 1400 PST 1400 to 1800 PST 1800 to 2400 PST	5 times/day for 6 episodic days from 11/11/87 through 12/11/87	Technicon Automatic Colorimetry on Teflon Filter Extracts (Technicon Model IV)
$PM_{2.5}$ and PM_{10} Particle Organic and Elemental Carbon	Nine sites in summer: BURK, CELA, HAWT, LONG, ANAH, RIVR, SNIC, AZUS, and CLAR.	0000 to 0500 PST 0500 to 0900 PST 0900 to 1300 PST 1300 to 1700 PST 1700 to 2400 PST	5 times/day for 11 episodic days from 6/19/87 through 9/03/87	Thermal Manganese Oxidation Carbon Analysis on Pre-fired Quartz Filters (Modified Dohrmann Model 50 Carbon Analyzer)

Table 3-2 (continued)
SCAQS Filter-Based Gaseous and Aerosol Measurements[a]

Measurement	Sampling Sites[b]	Averaging Time	Sample Frequency and Period[c,d]	Measurement Method Instrument
$PM_{2.5}$ and PM_{10} Particle Organic and Elemental Carbon (continued)	Six sites in the fall: BURK, CELA, HAWT, LONG, ANAH, RIVR.	0000 to 0600 PST 0600 to 1000 PST 1000 to 1400 PST 1400 to 1800 PST 1800 to 2400 PST	5 times/day for 6 episodic days from 11/11/87 through 12/11/87	Thermal Manganese Oxidation Carbon Analysis on Pre-fired Quartz Filters (Modified Dohrmann Model 50 Carbon Analyzer)
$PM_{2.5}$ Particle Organic and Elemental Carbon	Nine sites in summer: BURK, CELA, HAWT, LONG, ANAH, RIVR, SNIC, AZUS, and CLAR.	0000 to 0500 PST 0500 to 0900 PST 0900 to 1300 PST 1300 to 1700 PST 1700 to 2400 PST	5 times/day for 11 episodic days from 6/19/87 through 9/03/87	Thermal Manganese Oxidation Carbon Analysis on Pre-fired Quartz Backup Filters (Modified Dohrmann Model 50 Carbon Analyzer)
	Six sites in the fall: BURK, CELA, HAWT, LONG, ANAH, RIVR.	0000 to 0600 PST 0600 to 1000 PST 1000 to 1400 PST 1400 to 1800 PST 1800 to 2400 PST	5 times/day for 6 episodic days from 11/11/87 through 12/11/87	Thermal Manganese Oxidation Carbon Analysis on Pre-fired Quartz Backup Filters (Modified Dohrmann Model 50 Carbon Analyzer)
Sulfur Dioxide (SO_2)	Nine sites in summer: BURK, CELA, HAWT, LONG, ANAH, RIVR, SNIC, AZUS, and CLAR.	0000 to 0500 PST 0500 to 0900 PST 0900 to 1300 PST 1300 to 1700 PST 1700 to 2400 PST	5 times/day for 11 episodic days from 6/19/87 through 9/03/87	Ion Chromatographic Analysis on Potassium Carbonate (K_2CO_3) Impregnated Whatman 41 Cellulose-fiber Filter Extracts (Dionex Model 10 Chromatograph)

Table 3-2 (continued)
SCAQS Filter-Based Gaseous and Aerosol Measurements[a]

Measurement	Sampling Sites[b]	Averaging Time	Sample Frequency and Period[c,d]	Measurement Method Instrument
Sulfur Dioxide (SO_2) (continued)	Six sites in the fall: BURK, CELA, HAWT, LONG, ANAH, RIVR.	0000 to 0600 PST 0600 to 1000 PST 1000 to 1400 PST 1400 to 1800 PST 1800 to 2400 PST	5 times/day for 6 episodic days from 11/11/87 through 12/11/87	Ion Chromatographic Analysis on Potassium Carbonate (K_2CO_3) Impregnated Whatman 41 Cellulose-fiber Filter Extracts (Dionex Model 10 Chromatograph)
Ammonia (NH_3)	Nine sites in summer: BURK, CELA, HAWT, LONG, ANAH, RIVR, SNIC,[e] AZUS, and CLAR.	0000 to 0500 PST 0500 to 0900 PST 0900 to 1300 PST 1300 to 1700 PST 1700 to 2400 PST	5 times/day for 11 episodic days from 6/19/87 through 9/03/87	Automated Colorimetric Analysis on Oxalic Acid Impregnated Quartz-fiber Filter Extracts (Technicon Model IV)
	Six sites in the fall: BURK, CELA, HAWT, LONG, ANAH, RIVR.	0000 to 0600 PST 0600 to 1000 PST 1000 to 1400 PST 1400 to 1800 PST 1800 to 2400 PST	5 times/day for 6 episodic days from 11/11/87 through 12/11/87	Automated Colorimetric Analysis on Oxalic Acid Impregnated Quartz-fiber Filter Extracts (Technicon Model IV)
Denuder Difference Nitric Acid (HNO_3)	Nine sites in summer: BURK, CELA, HAWT, LONG, ANAH, RIVR, SNIC, AZUS, and CLAR.	0000 to 0500 PST 0500 to 0900 PST 0900 to 1300 PST 1300 to 1700 PST 1700 to 2400 PST	5 times/day for 11 episodic days from 6/19/87 through 9/03/87	Ion Chromatographic Analysis on Teflon and Nylon Back-up Filter Extracts (Dionex Model 10)
	Six sites in the fall: BURK, CELA, HAWT, LONG, ANAH, RIVR.	0000 to 0600 PST 0600 to 1000 PST 1000 to 1400 PST 1400 to 1800 PST 1800 to 2400 PST	5 times/day for 6 episodic days from 11/11/87 through 12/11/87	Ion Chromatographic Analysis on Teflon and Nylon Back-up Filter Extracts (Dionex Model 10)

Table 3-2 (continued)
SCAQS Filter-Based Gaseous and Aerosol Measurements[a]

[a] Countess (1989).

[b] Site names are: Burbank (BURK), Downtown Los Angeles (CELA), Hawthorne (HAWT), Long Beach (LONG), Anaheim (ANAH), Riverside/Rubidoux (RIVR), San Nicolas Island (SNIC), Azusa (AZUS), and Claremont (CLAR).

[c] The eleven Summer sampling days are: 06/19/87, 06/24/87, 06/25/87, 07/13/87, 07/14/87, 07/15/87, 08/27/87, 08/28/87, 08/29/87, 09/02/87, and 09/03/87.

[d] The six fall sampling days are: 11/11/87, 11/12/87, 11/13/87, 12/03/87, 12/10/87, and 12/11/87.

[e] Sampling schedule at San Nicolas Island for ammonia (NH_3) is as follows:

Sampling Date	Averaging Time	Sampling Date	Averaging Time
08/27/87	0101 to 0900 PST	09/02/87	1201 to 0900 PST
	0901 to 1700 PST		0901 to 1700 PST
	1701 to 0500 PST		1701 to 0500 PST
08/28/87	0501 to 1300 PST	09/03/87	0501 to 1300 PST
	1301 to 1700 PST		1301 to 1200 PST
	1701 to 1200 PST		
08/29/87	1201 to 0500 PST		
	0501 to 1300 PST		
	1301 to 1700 PST		
	1701 to 1200 PST		

Table 3-3
SCAQS Volatile Organic Compounds[a] Measurements

	Summer Hourly Sampling Start Time (PST)						Fall Hourly Sampling Start Time (PST)					
	0400	0600	0800	1100	1300	1500	0500	0700	0900	1200	1400	1600
Burbank (BURK)	NA[b]	X	NA	X	NA	X	NA	X	NA	X	NA	X
Downtown LA (CELA)	NA	X	NA	X	NA	X	X	X	X	X	X	X
Hawthorne (HAWT)	NA	X	NA	X	NA	X	NA	X	NA	X	NA	X
Long Beach (LONG)	X	X	X	X	X	X	X	X	X	X	X	X
Anaheim (ANAH)	NA	X	NA	X	NA	X	NA	X	NA	X	NA	X
Riverside/ Rubidoux (RIVR)	NA	X	NA	X	NA	X	NA	X	NA	X	NA	X
San Nicolas Island (SNIC)	NA	X	NA	X	NA	X	NA	NA	NA	NA	NA	NA
Azusa (ASUS)	NA	X	NA	X	NA	X	NA	NA	NA	NA	NA	NA
Claremont (CLAR)	X	X	X	X	X	X	NA	NA	NA	NA	NA	NA

[a] See Lurmann and Main (1992) for Volatile Organic Compounds (VOC) species identified in SCAQS.
[b] No sample was collected.

3.2 Ambient Particulate Measurements

The SCAQS gaseous/aerosol samplers were located at each of the nine sampling sites. Each sampler included $PM_{2.5}$, PM_{10}, and TSP inlets for concurrent gas and aerosol sampling through 12 channels. Figure 3-2 diagrams the SCAQS sampling system and shows the species measured by each leg of the system (Fitz and Zwicker, 1988). This version of the SCAQS sampler differs slightly from the version described by Wolff *et al.* (1991). Three major components are included in the SCAQS sampling system:

- Component one collected gaseous nitric acid (HNO_3) by the denuder difference method, and gaseous ammonia (NH_3) and gaseous sulfur dioxide (SO_2) on absorbent filter material. Channels 1 and 2 of this sampling system consisted of a raincap followed by open-faced Teflon filter holders to collect total nitrate (particulate nitrate plus nitric acid) on Teflon/nylon filter packs and SO_2 on sodium carbonate impregnated filters at flow rates of 11 and 22 ℓ/min, respectively. Channels 3 to 5 were preceded by a PFA Teflon-coated Air Industrial Hygiene Laboratory (AIHL) cyclone (John and Reischl, 1980)(manufactured by Cal Tech., Pasadena, CA), which removed particles greater than 2.2 μm in aerodynamic diameters at a flow rate of 22 ℓ/min. Channel 3 contained a magnesium-oxide coated multi-tube nitric acid denuder followed by a Teflon/nylon filter pack to collect $PM_{2.5}$ particulate nitrate. Channel 4 collected both gaseous nitric acid and $PM_{2.5}$ particulate nitrate. Nitric acid is determined by the difference in nitrate between Channels 4 and 3 (Shaw *et al.*, 1982). Channel 5 was preceded by an oxalic-acid coated denuder tube to collect NH_3 (which was removed by washing the tube) and followed by an oxalic-acid impregnated quartz-fiber filter to collect volatilized $PM_{2.5}$ ammonium (NH_4^+) (Ferm, 1979).

- Component two determined $PM_{2.5}$ particle mass and chemical composition. It was preceded by an uncoated Bendix/Sensidyne Model 240 cyclone preseparator (Clearwater, FL) which removed particles greater than 2.5 μm in aerodynamic diameter at a flow rate of 113 ℓ/min (Chan and Lippmann, 1977; Mueller *et al.*, 1983). In-line stainless steel Gelman filter holders contained a variety of filter stacks. The air stream following the cyclone was divided into the following four channels: Channel 6 was equipped with a polycarbonate Nuclepore filter for light absorption (b_{abs}) measurements at a flow rate of 5 ℓ/min. Channels 7 to 9 each extracted a flow of 35 ℓ/min. Channel 7 used a quartz-fiber filter for organic and elemental carbon analysis; Channel 8 contained a Teflon-membrane filter for mass and trace elemental analyses; and Channel 9 used a Teflon-membrane filter for chloride, nitrate, sulfate, ammonium, and soluble sodium analyses. A quartz-fiber backup filter followed the Teflon-membrane filter to assess the magnitude of organic artifacts.

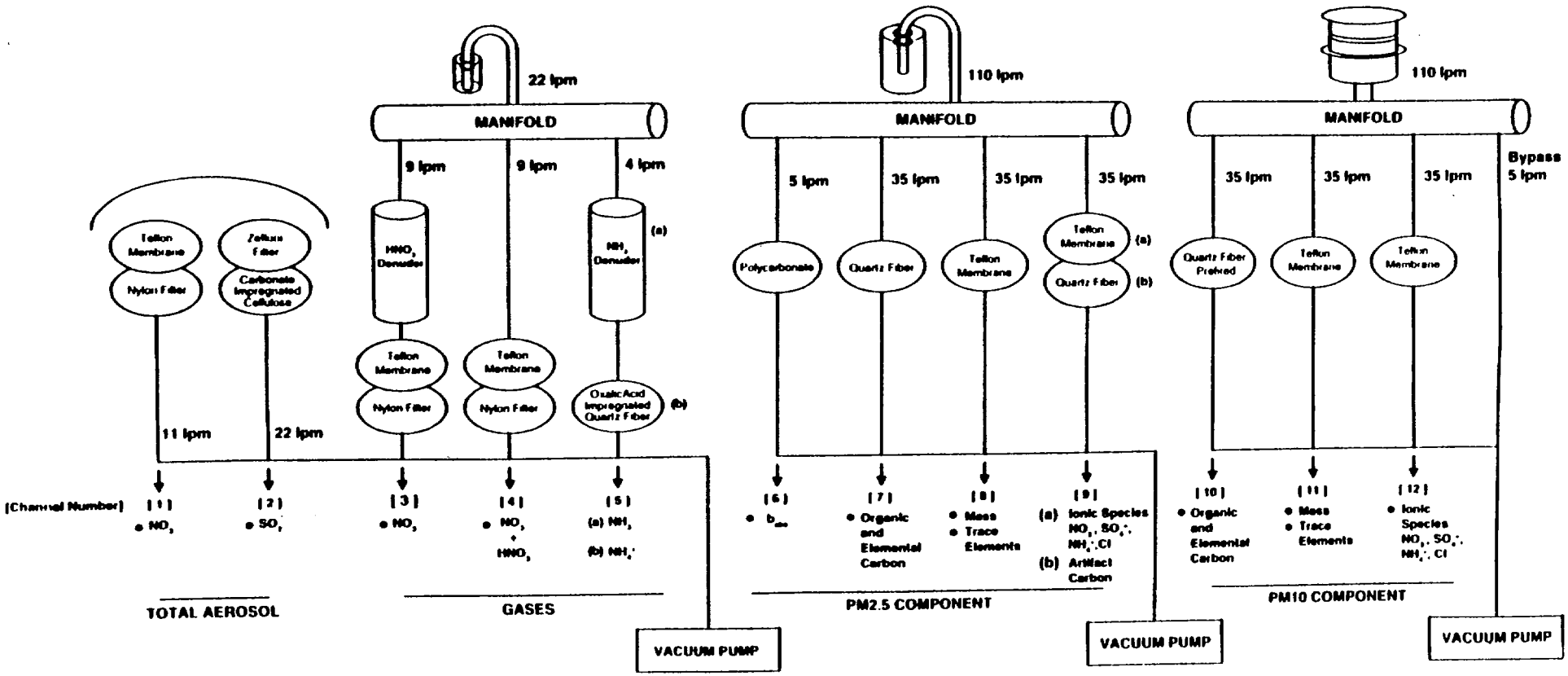

Figure 3-2. Flow Diagram of the SCAQS Sampler (Fitz and Zwicker, 1988)

- Component three determined PM_{10} particle mass and chemical composition. It was equipped with a Sierra Andersen (Atlanta, GA) Model SA-254I medium-volume PM_{10} inlet which removed particles greater than 10 μm in aerodynamic diameter at a flow rate of 113 ℓ/min (Olin and Bohn, 1983). In-line stainless steel filter holders were also used in this component. The sampling approach for Channels 10 to 12 was similar to that of Component two for $PM_{2.5}$ except that no light absorption or carbon artifacts were measured.

A total of 675 sample-sets collected during the summer and fall were submitted for chemical speciation. Samples were analyzed for light absorption by the Integrating Plate method at the University of California Davis (Sacramento, CA) and Radiance Research (Seattle, WA); for elements (aluminum to lead) by x-ray fluorescence at NSI Service Technology Corporation (Research Triangle Park, NC); for water soluble chloride, nitrate, and sulfate by ion chromatography at C-E Environmental, Inc. (Camarillo, CA); for water soluble ammonium by automated colorimetry at C-E Environmental, Inc. (Camarillo, CA); for water soluble sodium by atomic absorption spectrophotometry at C-E Environmental, Inc. (Camarillo, CA); and for organic and elemental carbon by thermal manganese oxidation (TMO) at ENSR Consulting and Engineering (Camarillo, CA). Sampling and analysis methods are described in detail by Fitz and Zwicker (1988) and Countess (1989).

The use of in-line metal filter holders in the SCAQS aerosol sampler resulted in a spot, and sometimes a hole, in the center of the filter. The size of this spot varied from sample to sample. X-ray fluorescence and carbon analyses involved pieces ($\sim$0.2 to 2.0 cm^2) of each filter rather than the entire filter, and since the deposit is not homogeneous, these measurements are biased. To investigate the degree of non-uniformity, 80 of the Teflon-membrane filter samples were scanned edge-to-edge by proton induced x-ray emissions spectroscopy (PIXE) at the University of California, Davis, to establish element-specific gradients (Matsumura and Cahill, 1991). Fujita and Collins (1989) reported that measurements made from sections of the filter near its edge were several times lower than those made at its center. Table 3-4 reports the adjustment factors derived from the PIXE scanning. The elemental concentrations resulting from the x-ray fluorescence (XRF) analysis were divided by these factors before any further data analysis. These factors are probably not the same for every filter, and biases in the elemental data are expected. Carbon punches were taken from the center edge, and half radius of each filter in an attempt to compensate for the inhomogeneous deposit, since the inhomogeneities differ from filter to filter. Metal shavings, presumably from the metal filter holder fittings, were also observed on some of the filters (Cahill, 1989), and these might bias some of the mass measurements as well as some of the trace metal values. Chow *et al.* (1992) observed similar biases when the SCAQS samplers were used in the San Joaquin Valley, though the inhomogeneities were partially eliminated with flow diffusers between the filter holder cap and the support grid.

Table 3-4
Correction Factors Derived from PIXE Scanning of SCAQS Samples[a]

	XRF Correction Factor[b]
XRF/PIXE Standards	1.038
PM_{10} Soils, (Na, Mg, Al, Si)	1.21 ± 0.10
PM_{10} Soils, (K, Ca, Ti, Fe, Sr, Zn)	2.06 ± 0.28
PM_{10} Sulfur	1.25 ± 0.04
PM_{10} Combustion-derived aerosols (Mn, Cu, Zn, Br, Pb, V, Ni)	1.39 ± 0.31
$PM_{2.5}$ soils, (Na, Mg, Al, Si)	1.30* ± 0.44
$PM_{2.5}$ soils, (K, Ca, Ti, Fe, Sr, Zr)	1.30* ± 0.44
$PM_{2.5}$ Sulfur	1.22 ± 0.07
$PM_{2.5}$ Combustion-derived aerosols (Mn, Cu, Zn, Br, Pb, V, Ni)	1.63 ± 0.33

[a] Matsumura and Cahill (1991).

[b] The elemental concentrations derived from XRF analysis were divided by these factors.

3.3 Ambient Volatile Organic Compound (VOC) Measurements

One-hour integrated VOC samples were collected for C_2 through C_{12} hydrocarbons and C_1 through C_7 carbonyl compounds at the nine SCAQS sampling sites during the summer and fall as shown in Table 3-3. Hydrocarbon samples were collected in 6 liter (L) electropolished stainless steel canisters, and carbonyl compounds were collected with acidified 2,4-dinitrophenylhydrazine (DNPH)-impregnated C18 cartridges. A total of 473 sets of samples were collected from the nine sampling sites during the study.

These canister samples were analyzed at U.S. EPA's Atmospheric Research and Exposure Assessment Laboratory (AREAL) by the Heterogeneous Chemistry and Aerosol Research Branch (Research Triangle Park, NC) with a Varian 3700 gas chromatograph (GC) using a 60 m by 0.315 mm ID DB1 capillary gas chromatographic column and a flame ionization detector. The data were collected and processed using hardware and software from Dynamic Solutions Company. Identification and concentrations were provided for up to 100 compounds ranging from C_2 to C_{12} hydrocarbons. Additional details describing the method are given by Stockburger *et al.* (1989). Due to a tradeoff made in operating conditions to reduce the analysis time, U.S. EPA was unable to resolve C_2 compounds. The VOC samples were reanalyzed for C_2 to C_4 hydrocarbons at the Oregon Graduate Institute (OGI, Beaverton, OR) using a Hewlett Packard (HP) 5890-A gas chromatograph equipped with a pair of HP 3390 integrators. A matched pair of 4.6 m by 3.2 mm phenyl isocyanate/Durapak columns was used. Methane was also analyzed using a Carle 211M-S gas chromatograph with an HP 3388 data processor. Additional details are given in Rasmussen (1990).

A laboratory comparison study for speciated hydrocarbons was conducted as part of the quality assurance program for the SCAQS. This comparison included U.S. EPA and OGI as well as two other laboratories. Results showed that the values reported by U.S. EPA were within $\pm 8\%$ of the average values reported by all laboratories and the coefficients of variation (CV) among the four laboratories were generally within $\pm 10\%$ for concentrations above 5 ppb (Fujita and Collins, 1989). The reported minimum detection limit (MDL) is 0.2 ppbC for both U.S. EPA and OGI analyses.

The individual hydrazones formed by the reaction of carbonyl compounds with DNPH were analyzed by ENSR Consulting and Engineering (Camarillo, CA) using high pressure liquid chromatography (HPLC). Concentrations of C_1 through C_7 carbonyl compounds were obtained with minimum detection limits of 1-2 ppb. Additional details of the analytical method are given by Fung (1989). The DNPH values for formaldehyde (HCHO) were generally in good agreement with spectroscopic HCHO measurements taken at the Claremont and Long Beach sites during the summer by the University of California, Riverside (Fujita and Croes, 1990). However, a poor correlation with spectroscopic measurements and an atypical diurnal pattern indicated a problem with the DNPH measurements at the Long Beach site during the fall campaign. This problem was traced to the sampler timer, which was incorrectly programmed following a power outage at the site.

The hydrocarbon and carbonyl compound data base used in this study was compiled and validated by Sonoma Technology, Inc. (STI, Lurmann and Main, 1992). Lurmann and Main (1992) used the relative retention times calculated by the ARB for the hydrocarbons that were uniquely identified by Lonneman (Collins and Fujita, 1989) of U.S. EPA during the interlaboratory comparison to extend Stockburger's identification (Stockburger *et al.*, 1989). Lurmann and Main (1992) performed several validation tests involving ratios of individual compounds and compound types. They also reviewed field and laboratory notes to identify suspect samples and analyses. The validated data base includes OGI's C_2 and C_3 hydrocarbons, U.S. EPA's C_4 through C_{12} hydrocarbons and ENSR's C_1 through C_7 carbonyl compounds. U.S. EPA's C_2 and C_3 data were used only for the cases where the OGI C_2 and C_3 data were missing (71 out of 399 valid surface samples). Because of the uncertainty in U.S. EPA's C_2 data, only the total C_2s were included in the data base. Because ethylene (C_2) and acetylene (C_2) are key species in motor vehicle exhaust, the 71 samples with unresolved C_2 data are not included in the data analyses reported here. Additionally, since the first day of the study was considered a "shake down" day, data for June 19, 1987, are not included in the data analysis.

For this study, an uncertainty was calculated for each concentration value from root mean square errors (RMSE, the square root of the sum of the squares of two times the MDL and the square of the product of coefficient of variation and concentration).

3.4 Particulate Measurement Method Evaluations

Every measurement consists of four attributes: 1) a value; 2) a precision; 3) an accuracy; and 4) a validity (Hidy, 1985; Watson *et al.*, 1989). Countess (1989) describes the estimation of these attributes for the ion measurements. Performance testing via regular submission of standards, blank analysis, and replicate analysis were used to estimate precision. X-ray fluorescence precisions resulted from counting statistics. These precisions are reported within the SCAQS data bases so that they can be propagated through air quality models and used to evaluate how well different values compare with one another. The submission and evaluation of independent standards through quality audits were used to estimate accuracy (Collins and Fujita, 1989). Validity applies both to the measurement method and to each measurement taken with that method. The validity of each measurement is indicated by appropriate flagging within the data base, while the validity of the methods has been evaluated in this study by a number of tests.

The precision, accuracy, and validity of the SCAQS ambient aerosol measurements are defined as follows:

- Measurement is an observation at a specific time and place which possesses four attributes: 1) value--the center of the measurement interval; 2) precision--the width of the measurement interval; 3) accuracy--the difference between measured and reference values; and 4) validity--the compliance with assumptions made in the measurement method.

- Measurement method is the combination of equipment, reagents, and procedures which provide the value of a measurement. The full description of the measurement method requires substantial documentation. Two methods may use the same sampling systems and the same analysis systems but yield different results. For example, two samples for nitric acid on nylon filters are not identical methods if one performs acceptance testing on filter media and the other does not. Blank nylon filters possibly absorb HNO_3 when exposed to air, and they need to be washed and verified before sampling. Seemingly minor differences between methods can result in major differences between measurement values.

- Measurement method validity is the identification of measurement method assumptions, the quantification of effects of deviations from those assumptions, the ascertainment that deviations are within reasonable tolerances for the specific application, and the creation of procedures to quantify and minimize those deviations during a specific application. A substantial effort was expended in SCAQS to establish the validity of measurement methods as reported by Collins and Fujita (1989).

- Sample validation is accomplished by procedures which identify deviations from measurement assumptions and the assignment of flags to individual measurements for potential deviations from assumptions. Additional validation is accomplished by comparing values with known physical relationships. For example, $PM_{2.5}$ concentrations must never exceed corresponding PM_{10} concentrations. When they do, beyond a few precision intervals, either the PM_{10} or $PM_{2.5}$ sample is invalid.

- The comparability and equivalence of sampling and analysis methods are established by the comparison of values and precisions for the same measurement obtained by different measurement methods. Collocated sampling, interlaboratory, and intralaboratory comparisons are usually made to establish this comparability. Simultaneous measurements of the same observable are considered equivalent when more than 90% of the values differ by no more than the sum of two one-sigma precision intervals for each measurement.

- Completeness measures how many environmental measurements with specified values, precisions, accuracies, and validities were obtained out of the total number attainable. It measures the practicality of applying the selected measurement processes throughout the measurement period. Data bases which have excellent precision, accuracy, and validity may be of little utility if they contain so many missing values that data interpretation is impossible.

A data base with numerous data points such as SCAQS requires detailed documentation of precision, accuracy, and validity of the measurements. Collins and Fujita (1989) provide detailed documentation for the SCAQS quality assurance program. This information, plus that

drawn from other SCAQS measurement reports, is summarized here for the SCAQS aerosol data base. In addition, several additional sample validity and method validity tests are applied.

Approximately 8 to 15 dynamic field blanks for the aerosol samples were acquired at each of the sampling sites and reported by Countess (1989). No systematic temporal variations were observed for any of the measured species on these blanks. However, a site dependence was observed for many of the species measured on dynamic blanks from the background site located at the San Nicolas Island site (Countess, 1989). Lower NH_4^+ blank levels were found at the Azusa site with elevated NH_4^+ blank concentrations reported at the Rubidoux site.

3.4.1 Analytical Specifications

Tables 3-5 to 3-8 summarize the analytical specifications for the diurnal $PM_{2.5}$ and PM_{10} measurements during the summer and fall campaigns. The lower quantifiable limit (LQL) in these tables is defined as the average of the precisions for which the concentrations of the individual measurements are less than their corresponding precisions. These LQLs are, in general, much higher than the analytical MDLs because they include the standard deviation of the field blank and flow rate precisions. Tables 3-5 to 3-8 also report the total number of samples that are greater than LQLs for each chemical species.

$PM_{2.5}$ and PM_{10} mass, ions (i.e., nitrate, sulfate, ammonium), organic carbon, and elemental carbon were detected in over 90% of the samples. PM_{10} trace metals for aluminum, silicon, sulfur, potassium, calcium, manganese, iron, and zinc were also detected in over 80% of the cases and most of them are abundant in resuspended dust. Many of the XRF elements such as cobalt, arsenic, selenium, strontium, molybdenum, tin, antimony, cesium, platinum, and mercury were not detected very frequently, even though the LQLs are only a few nanograms per cubic meter. Since there are no known significant emitters of these species in the vicinity of the sampling sites, these species would not have an significant impact on the $PM_{2.5}$ or PM_{10} source apportionment. Sulfur dioxide and ammonia were generally detectable. Nitric acid was mostly below the LQLs during the early morning period (i.e., before 0900 or 1000 PST) especially in the fall.

3.4.2 Data Validation

Level I data validation consists of verifying field sampling parameters and ensuring that all samples collected were subjected to the specified chemical analyses. Level II data validation evaluates the chemical data for internal consistency and for consistency with expected environmental behavior. Various comparisons were made for: 1) $PM_{2.5}/PM_{10}$ ratios for mass and major chemical species; 2) sum of chemical species versus measured mass; 3) sulfate versus sulfur ratios; 4) $PM_{2.5}$ particulate nitrate versus nitric acid denuded nitrate; and 5) anion/cation balances.

Table 3-5

Analytical Specifications of Diurnal $PM_{2.5}$ Measurements Between 6/19/87 and 9/3/87 at Nine SCAQS Sites

Species	Analysis Method[a]	MDL ($\mu g/m^3$)[b]	LOL[c] ($\mu g/m^3$) 0000-0500 PST	0500-0900 PST	0900-1300 PST	1300-1700 PST	1700-2400 PST	Total Number of Valid Samples
Mass	Gravimetric	0.6[d]	3.287 (95/99)[e]	4.115 (92/98)	4.155 (96/99)	4.055 (96/98)	2.243 (99/99)	493
HNO_3	IC	0.04[d]	1.067 (46/95)	1.347 (60/89)	1.06 (84/92)	1.107 (82/94)	0.651 (79/93)	463
NH_3	AC	0.12[d]	0.326 (61/91)	0.413 (58/87)	0.404 (71/91)	0.438 (77/87)	0.228 (75/95)	451
SO_2	IC	0.06[d]	0.043 (88/98)	0.056 (90/99)	0.050 (90/99)	0.050 (92/99)	0.030 (89/99)	494
Chloride (Cl^-)	IC	0.04[d]	0.093 (63/99)	0.119 (44/99)	0.119 (9/99)	0.120 (9/99)	0.068 (62/99)	495
Nitrate (NO_3^-)	IC	0.04[d]	0.310 (86/99)	0.388 (85/99)	0.492 (79/99)	0.484 (71/99)	0.188 (93/99)	495
Sulfate ($SO_4^=$)	IC	0.04[d]	0.186 (98/99)	0.236 (97/99)	0.243 (98/99)	0.243 (99/99)	0.137 (99/99)	495
Ammonium (NH_4^+)	AC	0.03[d]	0.111 (96/97)	0.170 (95/98)	0.149 (95/96)	0.142 (98/98)	0.081 (97/97)	486
Organic Carbon (OC)	TMO	0.2[e]	0.650 (92/96)	0.764 (92/99)	0.764 (92/98)	0.778 (93/97)	0.427 (94/97)	487
Elemental Carbon (EC)	TMO	0.2[e]	0.040 (90/93)	0.213 (85/92)	0.182 (87/93)	0.060 (93/94)	0.088 (92/95)	467
Sodium (Na)	XRF	0.024[f]	0.106 (44/99)	0.137 (42/99)	0.145 (45/99)	0.137 (50/99)	0.075 (64/99)	495
Magnesium (Mg)	XRF	0.003[f]	0.014 (50/99)	0.018 (63/99)	0.018 (63/99)	0.018 (54/99)	0.010 (66/99)	495
Aluminum (Al)	XRF	0.024[f]	0.040 (25/99)	0.051 (45/99)	0.051 (41/99)	0.051 (35/99)	0.029 (49/99)	495
Silicon (Si)	XRF	0.009[f]	0.080 (27/99)	0.102 (51/99)	0.104 (41/99)	0.103 (37/99)	0.058 (30/99)	495
Phosphorus (P)	XRF	0.003[f]	0.007 (50/99)	0.010 (71/99)	0.010 (67/99)	0.010 (56/99)	0.005 (61/99)	495
Sulfur (S)	XRF	0.021[f]	0.067 (98/99)	0.084 (96/99)	0.084 (97/99)	0.091 (99/99)	0.048 (99/99)	495
Chlorine (Cl)	XRF	0.007[f]	0.188 (18/99)	0.241 (15/99)	0.242 (4/99)	0.240 (3/99)	0.134 (14/99)	495
Potassium (K)	XRF	0.006[f]	0.026 (50/99)	0.033 (57/99)	0.033 (53/99)	0.033 (44/99)	0.019 (67/99)	495
Calcium (Ca)	XRF	0.002[f]	0.051 (25/99)	0.065 (45/99)	0.069 (32/99)	0.066 (23/99)	0.036 (20/99)	495
Titanium (Ti)	XRF	0.002[f]	0.007 (23/99)	0.009 (43/99)	0.009 (39/99)	0.009 (27/99)	0.005 (26/99)	495
Vanadium (V)	XRF	0.005[f]	0.004 (47/99)	0.005 (48/99)	0.005 (62/99)	0.006 (31/99)	0.004 (68/99)	495
Chromium (Cr)	XRF	0.018[f]	0.032 (9/99)	0.040 (4/99)	0.040 (3/99)	0.041 (3/99)	0.022 (11/99)	495
Manganese (Mn)	XRF	0.013[f]	0.010 (57/99)	0.013 (58/99)	0.014 (65/99)	0.015 (59/99)	0.011 (53/99)	495
Iron (Fe)	XRF	0.006[f]	0.055 (32/99)	0.071 (55/99)	0.072 (53/99)	0.071 (38/99)	0.040 (33/99)	495
Cobalt (Co)	XRF	0.005[f]	0.004 (50/99)	0.005 (62/99)	0.006 (43/99)	0.006 (42/99)	0.004 (49/99)	495
Nickel (Ni)	XRF	0.005[f]	0.019 (3/99)	0.025 (1/99)	0.029 (1/99)	0.025 (1/99)	0.014 (2/99)	495
Copper (Cu)	XRF	0.005[f]	0.121 (7/99)	0.155 (11/99)	0.156 (11/99)	0.157 (8/99)	0.087 (14/99)	495
Zinc (Zn)	XRF	0.006[f]	0.079 (13/99)	0.101 (26/99)	0.107 (23/99)	0.102 (9/99)	0.056 (16/99)	495

Table 3-5 (continued)

Analytical Specifications of Diurnal $PM_{2.5}$ Measurements Between 6/19/87 and 9/3/87 at Nine SCAQS Sites

Species	Analysis Method[a]	MDL (μg/m³)[b]	LQL[c] (μg/m³) 0000-0500 PST	0500-0900 PST	0900-1300 PST	1300-1700 PST	1700-2400 PST	Total Number of Valid Samples
Arsenic (As)	XRF	0.008[f]	0.014 (48/99)	0.018 (42/99)	0.066 (1/99)	0.018 (40/99)	0.008 (59/99)	495
Selenium (Se)	XRF	0.009[f]	0.009 (30/99)	0.018 (16/99)	0.012 (22/99)	0.012 (19/99)	0.008 (53/99)	495
Bromine (Br)	XRF	0.010[f]	0.016 (12/99)	0.020 (13/99)	0.020 (10/99)	0.020 (9/99)	0.011 (40/99)	495
Strontium (Sr)	XRF	0.019[f]	0.025 (5/99)	0.030 (4/99)	0.033 (2/99)	0.032 (6/99)	0.018 (52/99)	495
Molybdenum (Mo)	XRF	0.045[f]	0.068 (12/99)	0.081 (8/99)	0.053 (26/99)	0.093 (9/99)	0.041 (54/99)	495
Cadmium (Cd)	XRF	0.002[f]	0.002 (28/99)	0.002 (29/99)	0.002 (25/99)	0.002 (13/99)	0.001 (38/99)	495
Tin (Sn)	XRF	0.007[f]	0.006 (55/99)	0.007 (54/99)	0.009 (41/99)	0.009 (31/99)	0.006 (61/99)	495
Antimony (Sb)	XRF	0.003[f]	0.003 (53/99)	0.005 (18/99)	0.018 (1/99)	0.004 (19/99)	0.003 (59/99)	495
Cacsium (Cs)	XRF	0.004[f]	0.003 (49/99)	0.004 (47/99)	0.005 (29/99)	0.005 (35/99)	0.004 (48/99)	495
Barium (Ba)	XRF	0.004[f]	0.004 (61/99)	0.005 (63/99)	0.006 (59/99)	0.005 (47/99)	0.004 (80/99)	495
Platinum (Pt)	XRF	0.019[f]	0.015 (55/99)	0.019 (55/99)	0.022 (53/99)	0.023 (35/99)	0.017 (49/99)	495
Mercury (Hg)	XRF	0.020[f]	0.015 (55/99)	0.020 (60/99)	0.023 (57/99)	0.024 (34/99)	0.018 (51/99)	495
Lead (Pb)	XRF	0.032[f]	0.045 (13/99)	0.057 (16/99)	0.058 (14/99)	0.058 (10/99)	0.032 (61/99)	495

[a] IC: Ion Chromatography.
AC: Automated Colorimetry.
TMO: Thermal Manganese Oxidation.
XRF: X-Ray Fluorescence.

[b] Minimum Detectable Limits (MDL) is the concentration at which instrument response equals three times the standard deviation of the response to a known concentration of zero. Sample volume varies from channel to channel for different sampling periods. Typical sample volumes are 8.4 m³ for a sampling period of four hours.

[c] Lower Quantifiable Limit (LQL) is defined as the average of the precisions ($\overline{\sigma_{C_i}}$) for which the concentration of the measurement (C_i) is less than its corresponding uncertainty (σ_{C_i}) where:

$$\overline{\sigma_{C_i}} = \frac{1}{n}\sum_{i=1}^{n} \sigma_{C_i} \text{ for } C_i < \sigma_{C_i}$$

C_i = concentration of species i

σ_{C_i} = uncertainty of C_i

[d] Countess (1989).

[e] Collins and Fujita (1989).

[f] Kellogg (1989).

[g] Number of samples is greater than LQL versus total number of valid samples.

Table 3-6
Analytical Specifications of Diurnal PM_{10} Measurements Between 6/19/87 and 9/3/87 at Nine SCAQS Sites

Species	Analysis Method[a]	MDL ($\mu g/m^3$)[b]	LQL[c] ($\mu g/m^3$) 0000-0500 PST	0500-0900 PST	0900-1300 PST	1300-1700 PST	1700-2400 PST	Total Number of Valid Samples
Mass	Gravimetric	0.6[d]	3.110 (98/99)[e]	3.980 (95/99)	4.115 (98/98)	4.029 (98/99)	2.244 (98/99)	494
Chloride (Cl^-)	IC	0.04[d]	0.090 (93/99)	0.110 (92/99)	0.113 (47/99)	0.113 (50/99)	0.060 (93/99)	495
Nitrate (NO_3^-)	IC	0.04[d]	0.352 (97/99)	0.441 (95/99)	0.387 (97/99)	0.477 (93/99)	0.255 (97/99)	495
Sulfate ($SO_4^=$)	IC	0.04[d]	0.120 (98/99)	0.150 (96/99)	0.163 (99/99)	0.155 (98/99)	0.090 (98/99)	495
Ammonium (NH_4^+)	AC	0.03[d]	0.153 (96/97)	0.190 (92/97)	0.200 (92/95)	0.200 (94/96)	0.111 (94/95)	480
Organic Carbon (OC)	TMO	0.2[e]	0.988 (94/96)	0.760 (94/98)	0.760 (97/98)	1.463 (94/97)	0.818 (95/97)	486
Elemental Carbon (EC)	TMO	0.2[e]	0.142 (91/97)	0.276 (86/96)	0.248 (92/97)	0.187 (92/96)	0.120 (93/96)	482
Sodium (Na)	XRF	0.025[f]	0.106 (97/99)	0.131 (94/99)	0.139 (95/99)	0.138 (96/99)	0.073 (97/99)	495
Magnesium (Mg)	XRF	0.003[f]	0.014 (96/99)	0.018 (94/99)	0.020 (97/99)	0.018 (96/99)	0.010 (98/99)	495
Aluminum (Al)	XRF	0.030[f]	0.039 (93/99)	0.050 (90/99)	0.057 (96/99)	0.050 (94/99)	0.028 (94/99)	495
Silicon (Si)	XRF	0.013[f]	0.078 (94/99)	0.101 (92/99)	0.101 (96/99)	0.100 (95/99)	0.056 (94/99)	495
Phosphorus (P)	XRF	0.003[f]	0.006 (80/99)	0.008 (82/99)	0.009 (85/99)	0.008 (76/99)	0.005 (82/99)	495
Sulfur (S)	XRF	0.021[f]	0.067 (98/99)	0.087 (96/99)	0.096 (99/99)	0.089 (98/99)	0.048 (98/99)	495
Chlorine (Cl)	XRF	0.003[f]	0.191 (78/99)	0.241 (72/99)	0.257 (37/99)	0.243 (36/99)	0.137 (83/99)	495
Potassium (K)	XRF	0.008[f]	0.026 (94/99)	0.033 (89/99)	0.032 (95/99)	0.033 (91/99)	0.018 (95/99)	495
Calcium (Ca)	XRF	0.001[f]	0.049 (91/99)	0.064 (88/99)	0.063 (94/99)	0.063 (90/99)	0.036 (94/99)	495
Titanium (Ti)	XRF	0.001[f]	0.007 (84/99)	0.009 (85/99)	0.009 (88/99)	0.009 (85/99)	0.005 (90/99)	495
Vanadium (V)	XRF	0.005[f]	0.004 (48/99)	0.005 (67/99)	0.006 (31/99)	0.005 (59/99)	0.003 (36/99)	495
Chromium (Cr)	XRF	0.019[f]	0.032 (4/99)	0.040 (4/99)	0.041 (6/99)	0.041 (6/99)	0.023 (10/99)	495
Manganese (Mn)	XRF	0.013[f]	0.011 (80/99)	0.013 (91/99)	0.013 (93/99)	0.014 (86/99)	0.008 (94/99)	495
Iron (Fe)	XRF	0.006[f]	0.054 (89/99)	0.070 (87/99)	0.069 (93/99)	0.070 (90/99)	0.039 (90/99)	495
Cobalt (Co)	XRF	0.005[f]	0.004 (75/99)	0.006 (60/99)	0.006 (32/99)	0.006 (54/99)	0.003 (62/99)	495
Nickel (Ni)	XRF	0.005[f]	0.004 (65/99)	0.005 (42/99)	0.006 (48/99)	0.006 (38/99)	0.003 (45/99)	495
Copper (Cu)	XRF	0.005[f]	0.121 (3/99)	0.157 (3/99)	0.158 (3/99)	0.155 (3/99)	0.088 (2/99)	495
Zinc (Zn)	XRF	0.006[f]	0.080 (14/99)	0.101 (32/99)	0.125 (33/99)	0.103 (14/99)	0.057 (14/99)	495
Arsenic (As)	XRF	0.008[f]	0.007 (35/99)	0.009 (72/99)	0.009 (46/99)	0.009 (42/99)	0.005 (63/99)	495
Selenium (Se)	XRF	0.009[f]	0.008 (47/99)	0.010 (51/99)	0.011 (36/99)	0.010 (51/99)	0.006 (52/99)	495
Bromine (Br)	XRF	0.010[f]	0.009 (50/99)	0.011 (47/99)	0.012 (34/99)	0.011 (58/99)	0.006 (56/99)	495
Strontium (Sr)	XRF	0.019	0.017 (43/99)	0.022 (45/99)	0.023 (44/99)	0.022 (44/99)	0.013 (46/99)	495
Molybdenum (Mo)	XRF	0.045	0.067 (11/99)	0.085 (20/99)	0.086 (16/99)	0.089 (9/99)	0.048 (14/99)	495
Cadmium (Cd)	XRF	0.002	0.002 (48/99)	0.002 (53/99)	0.003 (38/99)	0.002 (37/99)	0.001 (39/99)	495

Table 3-6 (continued)
Analytical Specifications of Diurnal PM_{10} Measurements Between 6/19/87 and 9/3/87 at Nine SCAQS Sites

Species	Analysis Method[a]	MDL ($\mu g/m^3$)[b]	LQL[c] ($\mu g/m^3$) 0000-0500 PST	0500-0900 PST	0900-1300 PST	1300-1700 PST	1700-2400 PST	Total Number of Valid Samples
Tin (Sn)	XRF	0.007	0.007 (41/99)	0.008 (54/99)	0.009 (45/99)	0.008 (55/99)	0.005 (47/99)	495
Antimony (Sb)	XRF	0.004	0.003 (39/99)	0.004 (43/99)	0.004 (51/99)	0.004 (32/99)	0.002 (59/99)	495
Caesium (Cs)	XRF	0.004	0.004 (28/99)	0.005 (36/99)	0.005 (13/99)	0.005 (37/99)	0.003 (22/99)	495
Barium (Ba)	XRF	0.004	0.004 (85/99)	0.006 (88/99)	0.006 (89/99)	0.006 (84/99)	0.003 (88/99)	495
Platnium (Pt)	XRF	0.020	0.018 (62/99)	0.022 (63/99)	0.024 (43/99)	0.022 (66/99)	0.013 (58/99)	495
Mercury (Hg)	XRF	0.021	0.018 (53/99)	0.023 (69/99)	0.025 (41/99)	0.024 (63/99)	0.013 (65/99)	495
Lead (Pb)	XRF	0.033	0.045 (41/99)	0.058 (63/99)	0.059 (61/99)	0.059 (30/99)	0.032 (62/99)	495

[a] IC: Ion Chromatography.
AC: Automated Colorimetry.
TMO: Thermal Manganese Oxidation.
XRF: X-Ray Fluorescence.

[b] Minimum Detectable Limits (MDL) is the concentration at which instrument response equals three times the standard deviation of the response to a known concentration of zero. Sample volume varies from channel to channel for different sampling periods. Typical sample volumes are 8.4 m^3 for a sampling period of four hours.

[c] Lower Quantifiable Limit (LQL) is defined as the average of the precisions ($\overline{\sigma_{C_i}}$) for which the concentration of the measurement (C_i) is less than its corresponiding uncertainty (σ_{C_i}) where:

$$\overline{\sigma_{C_i}} = \frac{1}{n}\sum_{i=1}^{n} \sigma_{C_i} \text{ for } C_i < \sigma_{C_i}$$

C_i = concentration of species i

σ_{C_i} = uncertainty of C_i

[d] Countess (1989).
[e] Collins and Fujita (1989).
[f] Kellogg (1989).
[g] Number of samples is greater than LQL versus total number of valid samples.

Table 3-7

Analytical Specifications of Diurnal $PM_{2.5}$ Measurements Between 11/11/87 and 12/11/87 at Six SCAQS Sites

Species	Analysis Method	MDL ($\mu g/m^3$)[b]	LOL[c] ($\mu g/m^3$) 0000-0600 PST	0600-1000 PST	1000-1400 PST	1400-1800 PST	1800-2400 PST	Valid Samples
Mass	Gravimetric	0.6[d]	2.876 (36/36)[e]	4.351 (36/36)	4.350 (35/36)	4.338 (36/36)	2.780 (35/36)	180
HNO_3	IC	0.04[d]	1.163 (8/35)	1.723 (12/36)	1.726 (29/36)	1.752 (26/36)	1.205 (19/36)	179
NH_3	AC	0.12[d]	0.306 (36/36)	0.460 (36/36)	0.420 (34/36)	0.430 (33/36)	0.305 (36/36)	180
SO_2	IC	0.06[d]	0.086 (27/27)	0.110 (26/26)	0.113 (26/26)	0.117 (26/26)	0.084 (25/25)	130
Chloride (Cl^-)	IC	0.04[d]	0.080 (31/35)	0.118 (25/36)	0.119 (9/36)	0.119 (18/36)	0.080 (31/36)	179
Nitrate (NO_3^-)	IC	0.04[d]	0.325 (33/35)	0.503 (33/36)	0.515 (34/36)	0.525 (34/36)	0.340 (35/36)	179
Sulfate ($SO_4^=$)	IC	0.04[d]	0.157 (35/35)	0.239 (36/36)	0.241 (36/36)	0.239 (36/36)	0.160 (35/36)	179
Ammonium (NH_4^+)	AC	0.03[d]	0.100 (33/34)	0.140 (33/36)	0.145 (33/35)	0.150 (35/36)	0.100 (35/36)	177
Organic Carbon (OC)	TMO	0.2[e]	1.475 (36/36)	1.872 (36/36)	1.658 (36/36)	1.608 (35/35)	1.451 (35/36)	179
Elemental Carbon (EC)	TMO	0.2[e]	0.534 (36/36)	0.717 (36/36)	0.373 (36/36)	0.302 (36/36)	0.452 (35/36)	180
Sodium (Na)	XRF	0.024[f]	0.065 (30/36)	0.083 (28/36)	0.080 (27/36)	0.086 (29/36)	0.073 (30/36)	180
Magnesium (Mg)	XRF	0.003[f]	0.006 (36/36)	0.009 (36/36)	0.009 (36/36)	0.009 (36/36)	0.008 (36/36)	180
Aluminum (Al)	XRF	0.024[f]	0.012 (36/36)	0.019 (36/36)	0.017 (36/36)	0.017 (36/36)	0.015 (36/36)	180
Silicon (Si)	XRF	0.009[f]	0.023 (36/36)	0.040 (36/36)	0.035 (36/36)	0.034 (36/36)	0.029 (36/36)	180
Phosphorus (P)	XRF	0.003[f]	0.006 (36/36)	0.008 (36/36)	0.007 (34/36)	0.007 (35/36)	0.006 (36/36)	180
Sulfur (S)	XRF	0.021[f]	0.081 (36/36)	0.090 (36/36)	0.105 (36/36)	0.110 (36/36)	0.094 (36/36)	180
Chlorine (Cl)	XRF	0.007[f]	0.065 (34/36)	0.044 (36/36)	0.014 (36/36)	0.014 (36/36)	0.045 (35/36)	180
Potassium (K)	XRF	0.006[f]	0.013 (36/36)	0.013 (36/36)	0.010 (36/36)	0.011 (36/36)	0.012 (36/36)	180
Calcium (Ca)	XRF	0.002[f]	0.035 (34/36)	0.054 (36/36)	0.032 (36/36)	0.024 (36/36)	0.026 (36/36)	180
Titanium (Ti)	XRF	0.002[f]	0.004 (36/36)	0.005 (36/36)	0.005 (36/36)	0.005 (36/36)	0.004 (36/36)	180
Vanadium (V)	XRF	0.005[f]	0.004 (8/36)	0.005 (11/36)	0.006 (11/36)	0.006 (17/36)	0.005 (23/36)	180
Chromium (Cr)	XRF	0.018[f]	0.016 (16/36)	0.025 (14/36)	0.021 (14/36)	0.023 (9/36)	0.016 (19/36)	180
Manganese (Mn)	XRF	0.013[f]	0.020 (28/36)	0.026 (28/36)	0.021 (20/36)	0.019 (21/36)	0.020 (25/36)	180
Iron (Fe)	XRF	0.006[f]	0.029 (36/36)	0.046 (36/36)	0.040 (36/36)	0.040 (36/36)	0.035 (36/36)	180
Cobalt (Co)	XRF	0.005[f]	0.004 (13/36)	0.006 (17/36)	0.006 (18/36)	0.006 (16/36)	0.004 (17/36)	180
Nickel (Ni)	XRF	0.005[f]	0.004 (5/36)	0.006 (11/36)	0.006 (12/36)	0.006 (6/36)	0.004 (8/36)	180
Copper (Cu)	XRF	0.005[f]	0.020 (30/36)	0.019 (33/36)	0.020 (33/36)	0.026 (35/36)	0.018 (33/36)	180
Zinc (Zn)	XRF	0.006[f]	0.023 (36/36)	0.024 (36/36)	0.023 (36/36)	0.026 (36/36)	0.019 (36/36)	180

Table 3-7 (continued)

Analytical Specifications of Diurnal $PM_{2.5}$ Measurements Between 11/11/87 and 12/11/87 at Six SCAQS Sites

Species	Analysis Method	MDL ($\mu g/m^3$)[b]	LQL[c] ($\mu g/m^3$) 0000-0600 PST	0600-1000 PST	1000-1400 PST	1400-1800 PST	1800-2400 PST	Valid Samples
Arsenic (As)	XRF	0.008[f]	0.008 (15/36)	0.010 (12/36)	0.011 (12/36)	0.010 (8/36)	0.008 (15/36)	180
Selenium (Se)	XRF	0.009[f]	0.007 (13/36)	0.011 (8/36)	0.012 (14/36)	0.011 (13/36)	0.007 (18/36)	180
Bromine (Br)	XRF	0.010[f]	0.007 (36/36)	0.010 (36/36)	0.012 (28/36)	0.012 (27/36)	0.007 (36/36)	180
Strontium (Sr)	XRF	0.019[f]	0.017 (9/36)	0.026 (8/36)	0.027 (11/36)	0.026 (7/36)	0.017 (8/36)	180
Molybdenum (Mo)	XRF	0.045[f]	0.036 (9/36)	0.053 (8/36)	0.058 (13/36)	0.056 (11/36)	0.037 (9/36)	180
Cadmium (Cd)	XRF	0.002[f]	0.002 (36/36)	0.002 (33/36)	0.002 (29/36)	0.002 (29/36)	0.002 (32/36)	180
Tin (Sn)	XRF	0.007[f]	0.006 (15/36)	0.009 (13/36)	0.009 (13/36)	0.008 (9/36)	0.006 (12/36)	180
Antimony (Sb)	XRF	0.003[f]	0.003 (17/36)	0.004 (12/36)	0.004 (11/36)	0.004 (8/36)	0.003 (9/36)	180
Caesium (Cs)	XRF	0.004[f]	0.003 (18/36)	0.004 (15/36)	0.004 (16/36)	0.004 (14/36)	0.003 (13/36)	180
Barium (Ba)	XRF	0.004[f]	0.007 (33/36)	0.010 (35/36)	0.009 (33/36)	0.008 (29/36)	0.007 (32/36)	180
Platinum (Pt)	XRF	0.019[f]	0.015 (15/36)	0.022 (20/36)	0.022 (17/36)	0.022 (18/36)	0.015 (16/36)	180
Mercury (Hg)	XRF	0.020[f]	0.015 (17/36)	0.023 (19/36)	0.023 (16/36)	0.023 (17/36)	0.015 (16/36)	180
Lead (Pb)	XRF	0.032[f]	0.025 (35/36)	0.035 (36/36)	0.037 (29/36)	0.038 (26/36)	0.025 (31/36)	180

[a] IC: Ion Chromatography.
AC: Automated Colorimetry.
TMO: Thermal Manganese Oxidation.
XRF: X-Ray Fluorescence.

[b] Minimum Detectable Limits (MDL) is the concentration at which instrument response equals three times the standard deviation of the response to a known concentration of zero. Sample volume varies from channel to channel for different sampling periods. Typical sample volumes are 8.4 m^3 for a sampling period of four hours.

[c] Lower Quantifiable Limit (LQL) is defined as the average of the precisions ($\overline{\sigma_{C_i}}$) for which the concentration of the measurement (C_i) is less than its corresponiding uncertainty (σ_{C_i}) where:

$$\overline{\sigma_{C_i}} = \frac{1}{n}\sum_{i=1}^{n} \sigma_{C_i} \text{ for } C_i < \sigma_{C_i}$$

C_i = concentration of species i

σ_{C_i} = uncertainty of C_i

[d] Countess (1989).

[e] Collins and Fujita (1989).

[f] Kellogg (1989).

[g] Number of samples is greater than LQL versus total number of valid samples.

Table 3-8

Analytical Specifications of Diurnal PM_{10} Measurements Between 11/11/87 and 12/11/87 at Six SCAQS Sites

Species	Analysis Method	MDL ($\mu g/m^3$)[b]	LQL[c] $\mu g/m^3$ 0000-0600 PST	0600-1000 PST	1000-1400 PST	1400-1800 PST	1800-2400 PST	Total Number of Valid Samples
Mass	Gravimetric	0.6[d]	3.121 (36/36)[e]	4.356 (36/36)	4.364 (36/36)	4.339 (36/36)	2.998 (36/36)	180
Chloride (Cl^-)	IC	0.04[d]	0.070 (34/36)	0.112 (30/36)	0.113 (20/36)	0.118 (31/36)	0.080 (35/36)	180
Nitrate (NO_3^-)	IC	0.04[d]	0.320 (35/36)	0.460 (34/36)	0.480 (34/36)	0.500 (35/36)	0.320 (35/36)	180
Sulfate ($SO_4^=$)	IC	0.04[d]	0.110 (36/36)	0.148 (36/36)	0.153 (36/36)	0.150 (36/36)	0.106 (36/36)	180
Ammonium (NH_4^+)	AC	0.03[d]	0.130 (33/35)	0.195 (28/36)	0.198 (31/35)	0.200 (33/35)	0.135 (34/36)	177
Organic Carbon (OC)	TMO	0.2[e]	1.679 (36/36)	2.119 (36/36)	1.871 (36/36)	1.837 (35/35)	1.710 (36/36)	179
Elemental Carbon (EC)	TMO	0.2[e]	0.627 (36/36)	0.880 (36/36)	0.451 (36/36)	0.380 (36/36)	0.548 (35/36)	180
Sodium (Na)	XRF	0.025[f]	0.088 (35/36)	0.102 (33/36)	0.102 (30/36)	0.123 (35/36)	0.106 (35/36)	180
Magnesium (Mg)	XRF	0.003[f]	0.019 (36/36)	0.025 (36/36)	0.021 (36/36)	0.025 (36/36)	0.025 (36/36)	180
Aluminum (Al)	XRF	0.030[f]	0.052 (36/36)	0.074 (36/36)	0.055 (36/36)	0.057 (36/36)	0.064 (36/36)	180
Silicon (Si)	XRF	0.013[f]	0.133 (36/36)	0.184 (36/36)	0.126 (36/36)	0.130 (36/36)	0.150 (36/36)	180
Phosphorus (P)	XRF	0.003[f]	0.008 (36/36)	0.011 (36/36)	0.009 (36/36)	0.009 (36/36)	0.009 (36/36)	180
Sulfur (S)	XRF	0.021[f]	0.100 (36/36)	0.106 (36/36)	0.115 (36/36)	0.126 (36/36)	0.110 (36/36)	180
Chlorine (Cl)	XRF	0.003[f]	0.102 (34/36)	0.064 (36/36)	0.029 (36/36)	0.048 (35/36)	0.107 (35/36)	180
Potassium (K)	XRF	0.008[f]	0.029 (36/36)	0.034 (36/36)	0.026 (36/36)	0.029 (36/36)	0.033 (36/36)	180
Calcium (Ca)	XRF	0.001[f]	0.235 (36/36)	0.226 (36/36)	0.093 (36/36)	0.078 (36/36)	0.124 (36/36)	180
Titanium (Ti)	XRF	0.001[f]	0.010 (36/36)	0.013 (36/36)	0.012 (36/36)	0.013 (36/36)	0.012 (36/36)	180
Vanadium (V)	XRF	0.005[f]	0.005 (16/36)	0.006 (11/36)	0.006 (13/36)	0.007 (20/36)	0.006 (28/36)	180
Chromium (Cr)	XRF	0.019[f]	0.017 (24/36)	0.026 (23/36)	0.024 (18/36)	0.025 (19/36)	0.019 (28/36)	180
Manganese (Mn)	XRF	0.013[f]	0.026 (34/36)	0.038 (33/36)	0.028 (30/36)	0.029 (27/36)	0.027 (32/36)	180
Iron (Fe)	XRF	0.006[f]	0.108 (36/36)	0.154 (36/36)	0.107 (36/36)	0.113 (36/36)	0.129 (36/36)	180
Cobalt (Co)	XRF	0.005[f]	0.004 (13/36)	0.006 (17/36)	0.006 (17/36)	0.006 (17/36)	0.004 (14/36)	180
Nickel (Ni)	XRF	0.005[f]	0.005 (15/36)	0.006 (5/36)	0.006 (5/36)	0.007 (5/36)	0.005 (13/36)	180
Copper (Cu)	XRF	0.005[f]	0.014 (35/36)	0.017 (34/36)	0.017 (32/36)	0.019 (32/36)	0.016 (35/36)	180
Zinc (Zn)	XRF	0.006[f]	0.021 (36/36)	0.025 (36/36)	0.024 (36/36)	0.025 (36/36)	0.019 (36/36)	180

Table 3-8 (continued)
Analytical Specifications of Diurnal PM_{10} Measurements Between 11/11/87 and 12/11/87 at Six SCAQS Sites

Species	Analysis Method	MDL ($\mu g/m^3$)[a]	LQL[c] $\mu g/m^3$ 0000-0600 PST	0600-1000 PST	1000-1400 PST	1400-1800 PST	1800-2400 PST	Total Number of Valid Samples
Arsenic (As)	XRF	0.008[f]	0.008 (16/36)	0.011 (14/36)	0.011 (12/36)	0.011 (15/36)	0.008 (15/36)	180
Selenium (Se)	XRF	0.009[f]	0.008 (10/36)	0.011 (9/36)	0.011 (14/36)	0.011 (13/36)	0.007 (14/36)	180
Bromine (Br)	XRF	0.010[f]	0.007 (36/36)	0.010 (36/36)	0.013 (23/36)	0.012 (27/36)	0.007 (35/36)	180
Strontium (Sr)	XRF	0.019[f]	0.017 (11/36)	0.027 (8/36)	0.024 (13/36)	0.025 (9/36)	0.017 (11/36)	180
Molybdenum (Mo)	XRF	0.045[f]	0.036 (11/36)	0.056 (12/36)	0.052 (11/36)	0.054 (8/36)	0.036 (7/36)	180
Cadmium (Cd)	XRF	0.002[f]	0.002 (33/36)	0.003 (35/36)	0.003 (34/36)	0.002 (32/36)	0.002 (34/36)	180
Tin (Sn)	XRF	0.007[f]	0.007 (17/36)	0.009 (15/36)	0.009 (10/36)	0.008 (11/36)	0.006 (12/36)	180
Antimony (Sb)	XRF	0.004[f]	0.004 (27/36)	0.006 (22/36)	0.004 (13/36)	0.005 (16/36)	0.004 (25/36)	180
Caesium (Cs)	XRF	0.004[f]	0.003 (19/36)	0.004 (16/36)	0.004 (19/36)	0.004 (16/36)	0.003 (18/36)	180
Barium (Ba)	XRF	0.004[f]	0.011 (36/36)	0.016 (36/36)	0.013 (36/36)	0.013 (35/36)	0.012 (35/36)	180
Platinum (Pt)	XRF	0.020[f]	0.015 (14/36)	0.023 (18/36)	0.022 (16/36)	0.022 (14/36)	0.015 (15/36)	180
Mercury (hg)	XRF	0.021[f]	0.016 (15/36)	0.024 (17/36)	0.023 (19/36)	0.023 (16/36)	0.016 (15/36)	180
Lead (Pb)	XRF	0.033[f]	0.025 (36/36)	0.035 (36/36)	0.038 (31/36)	0.042 (29/36)	0.027 (34/36)	180

[a] IC: Ion Chromatography.
AC: Automated Colorimetry.
TMO: Thermal Manganese Oxidation.
XRF: X-Ray Fluorescence.

[b] Minimum Detectable Limits (MDL) is the concentration at which instrument response equals three times the standard deviation of the response to a known concentration of zero. Sample volume varies from channel to channel for different sampling periods. Typical sample volumes are 8.4 m^3 for a sampling period of four hours.

[c] Lower Quantifiable Limit (LQL) is defined as the average of the precisions ($\overline{\sigma_{C_i}}$) for which the concentration of the measurement (C_i) is less than its corresponiding uncertainty (σ_{C_i}) where :

$$\overline{\sigma_{C_i}} = \frac{1}{n}\sum_{i=1}^{n} \sigma_{C_i} \text{ for } C_i < \sigma_{C_i}$$

C_i = concentration of species i

σ_{C_i} = uncertainty of C_i

[d] Countess (1989).

[e] Collins and Fujita (1989).

[f] Kellogg (1989).

[g] Number of samples is greater than LQL versus total number of valid samples.

3.4.2a $PM_{2.5}/PM_{10}$ Ratios

Both the $PM_{2.5}$ mass and chemical species concentrations should be less than or equal to the corresponding PM_{10} concentrations. The analysis of the $PM_{2.5}$ to PM_{10} ratios also provides insight to the validity of the data base. Samples for which $PM_{2.5}$/ PM_{10} ratios are greater than unity within two propagated precision intervals have been identified and summarized in Appendix A. Figures 3-3a to 3-3g display scatterplots of PM_{10} versus $PM_{2.5}$ mass, silicon, sulfate, nitrate, ammonium, organic carbon, and elemental carbon. These chemical species were selected because they are the most prominent components of the $PM_{2.5}$ and/or PM_{10} mass, and they represent different types of chemical analysis method on different filter media within the sampling system. Linear regression statistics are also reported for each of these scatterplots with $PM_{2.5}$ as the independent variable and PM_{10} as the dependent variable. The vertical error bars on these figures represent the measurement uncertainties associated with PM_{10} mass and chemical species. The uncertainties for $PM_{2.5}$ measurements, although not shown in these figures, are similar in magnitude. The top six scatterplots in Figures 3-3a to 3-3g include both the summer (11 episode days between 6/19/87 and 9/3/87) and fall (6 episode days between 11/11/87 and 12/11/87) measurements at the Burbank, Downtown Los Angeles, Hawthorne, Long Beach, Anaheim, and Riverside sites. The bottom three scatterplots in Figures 3-3a to 3-3g include only the summer measurements at the San Nicolas Island, Azusa, and Claremont sites.

The $PM_{2.5}$ to PM_{10} mass ratios are generally below the one-to-one lines as shown in Figure 3-3a. The top six scatterplots in Figure 3-3a display a consistent regression line (slope$=1.0\pm0.1$) with a significant intercept, ranging from 17.4 ± 1.8 $\mu g/m^3$ at the Long Beach site to 32.8 ± 4.7 $\mu g/m^3$ at the Rubidoux site. The constant slope of approximately one with a typical intercept of 20 ± 2 $\mu g/m^3$ and high correlation coefficient (r) of $\geq$ 0.97 for the summer and fall measurements implies that coarse particle (PM_{10} minus $PM_{2.5}$) mass stayed rather constant during the study period, while $PM_{2.5}$ mass concentrations were the driving force for the low or high PM_{10} concentrations.

This is not true however, for the summer measurements at the Azusa and Claremont sites. While the intercepts were similar to those of summer and fall measurements at the other six sites, the slope of PM_{10} versus $PM_{2.5}$ mass increased to 1.3 and 1.4, indicating increasing quantities of coarse particle mass during the summer campaign. The plot for the San Nicolas Island site showed a much greater scatter (r=0.60) and a lower slope (0.7 ± 0.1). Even though the mass concentrations (approximately 15 to 20 $\mu g/m^3$) at this background site are a factor of 3 to 5 lower than the other sites, they are well above the LQLs of 2 to 3 $\mu g/m^3$ stated in Tables 3-5 and 3-6 for gravimetric analysis. The specific discrepancies are identified in Appendix A.

Silicon concentrations are acquired by the x-ray fluorescence analysis on Teflon-membrane filters. Silicon is known to be enriched in coarse particle geological material. The scatterplots of PM_{10} versus $PM_{2.5}$ silicon in Figure 3-3b show poor correlations ($0.25 \leq r \leq 0.77$) with very low (≤ 2 $\mu g/m^3$) $PM_{2.5}$ silicon concentrations. As expected, PM_{10} silicon generally exceeds $PM_{2.5}$ silicon by large amounts. The majority of the $PM_{2.5}$ silicon at the San Nicolas Island site are below the LQLs of 0.06 to 0.12 $\mu g/m^3$.

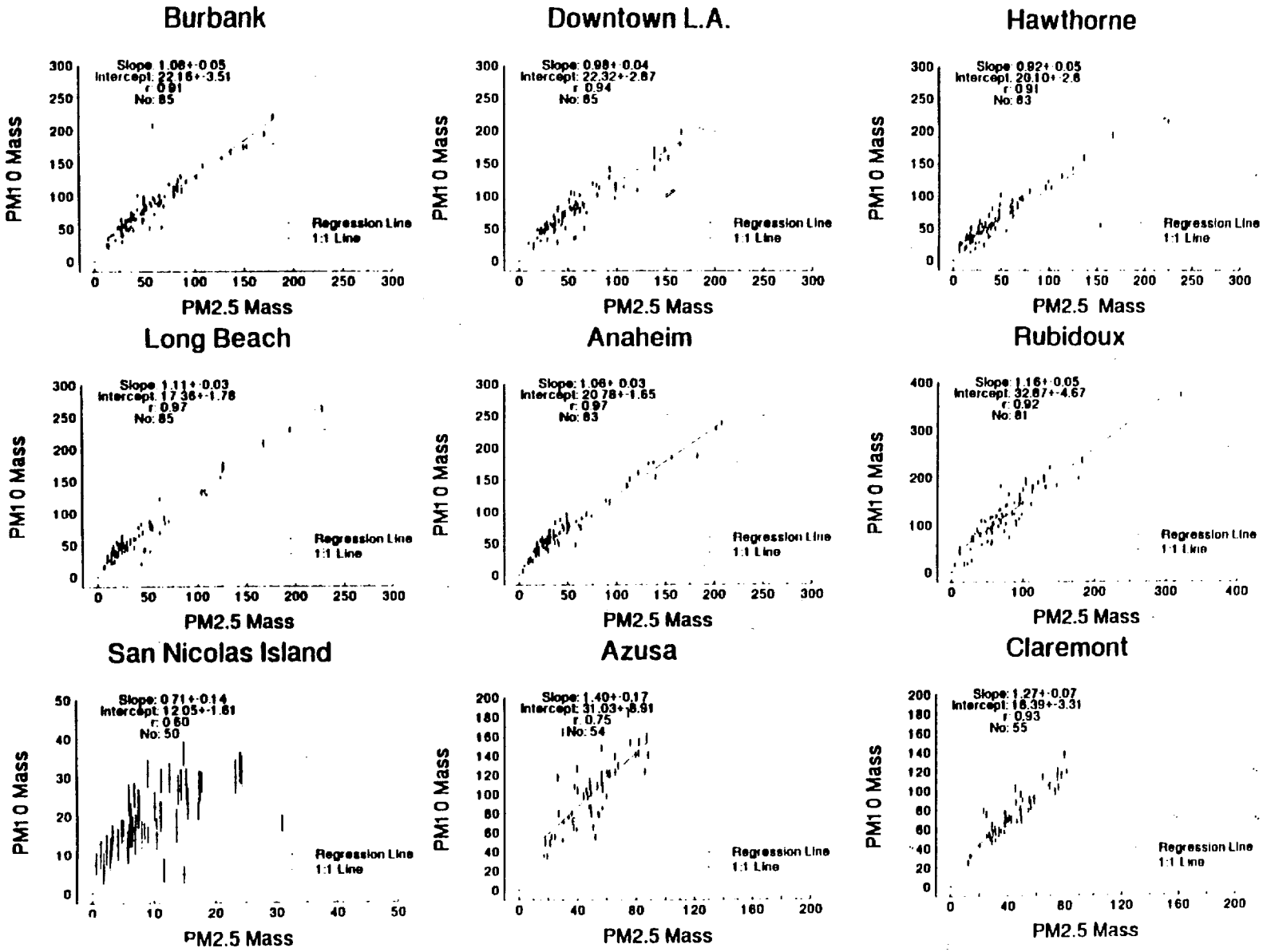

Figure 3-3a. Scatterplots of PM_{10} Versus $PM_{2.5}$ Mass at All SCAQS Sites During the Summer and Fall Campaigns

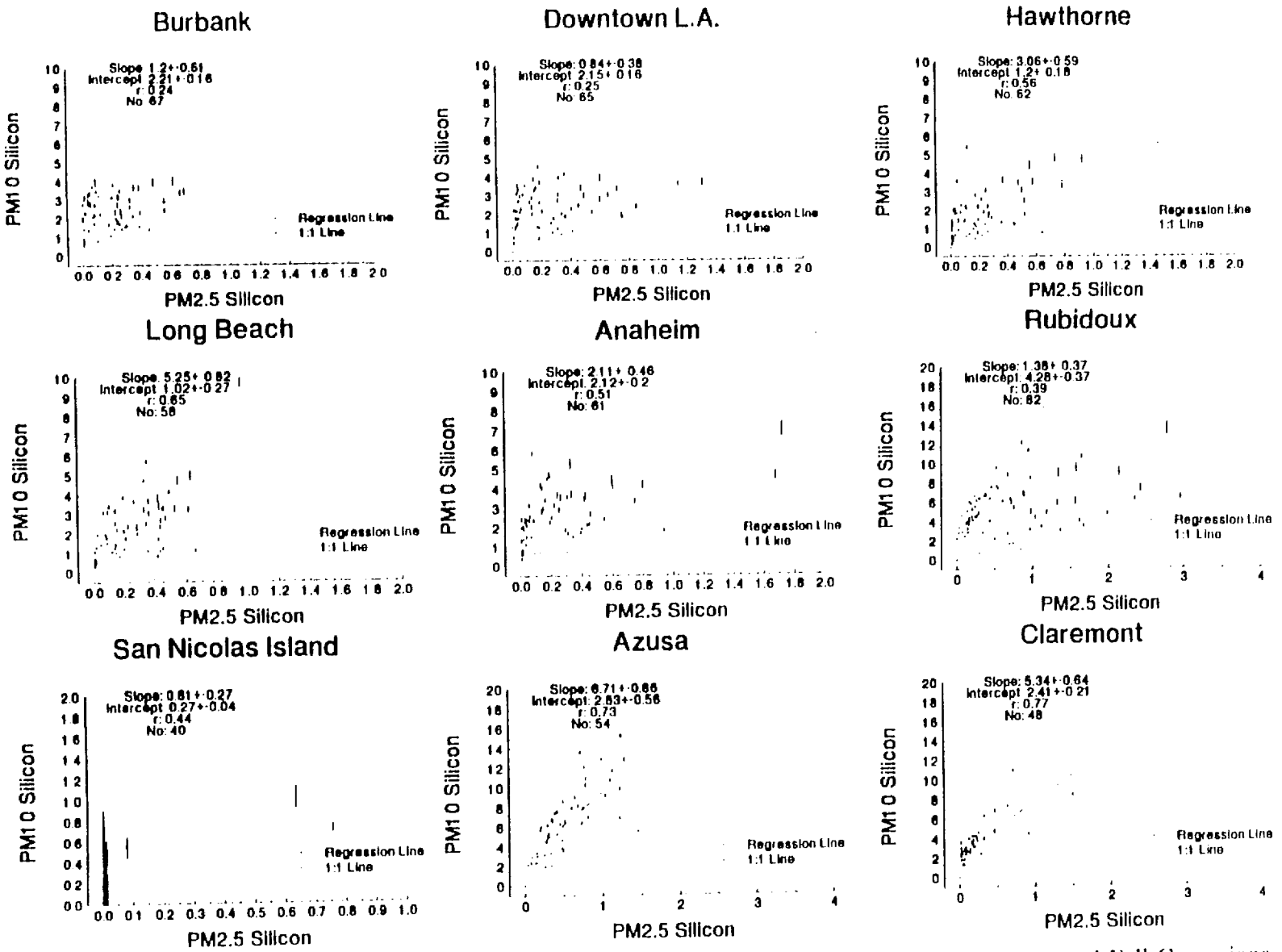

Figure 3-3b. Scatterplots of PM_{10} Versus $PM_{2.5}$ Silicon at All SCAQS Sites During the Summer and Fall Campaigns

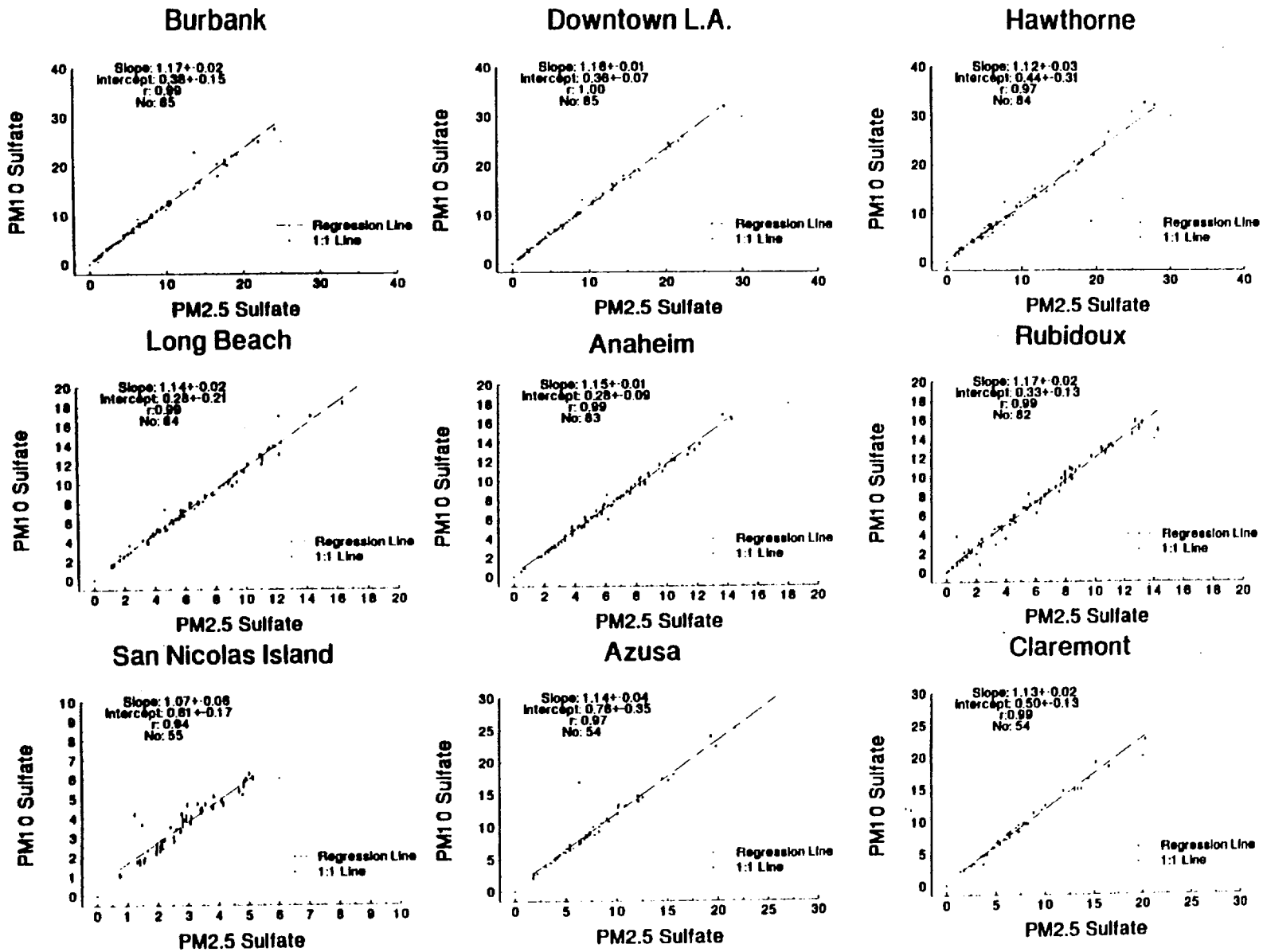

Figure 3-3c. Scatterplots of PM_{10} Versus $PM_{2.5}$ Sulfate at All SCAQS Sites During the Summer and Fall Campaigns

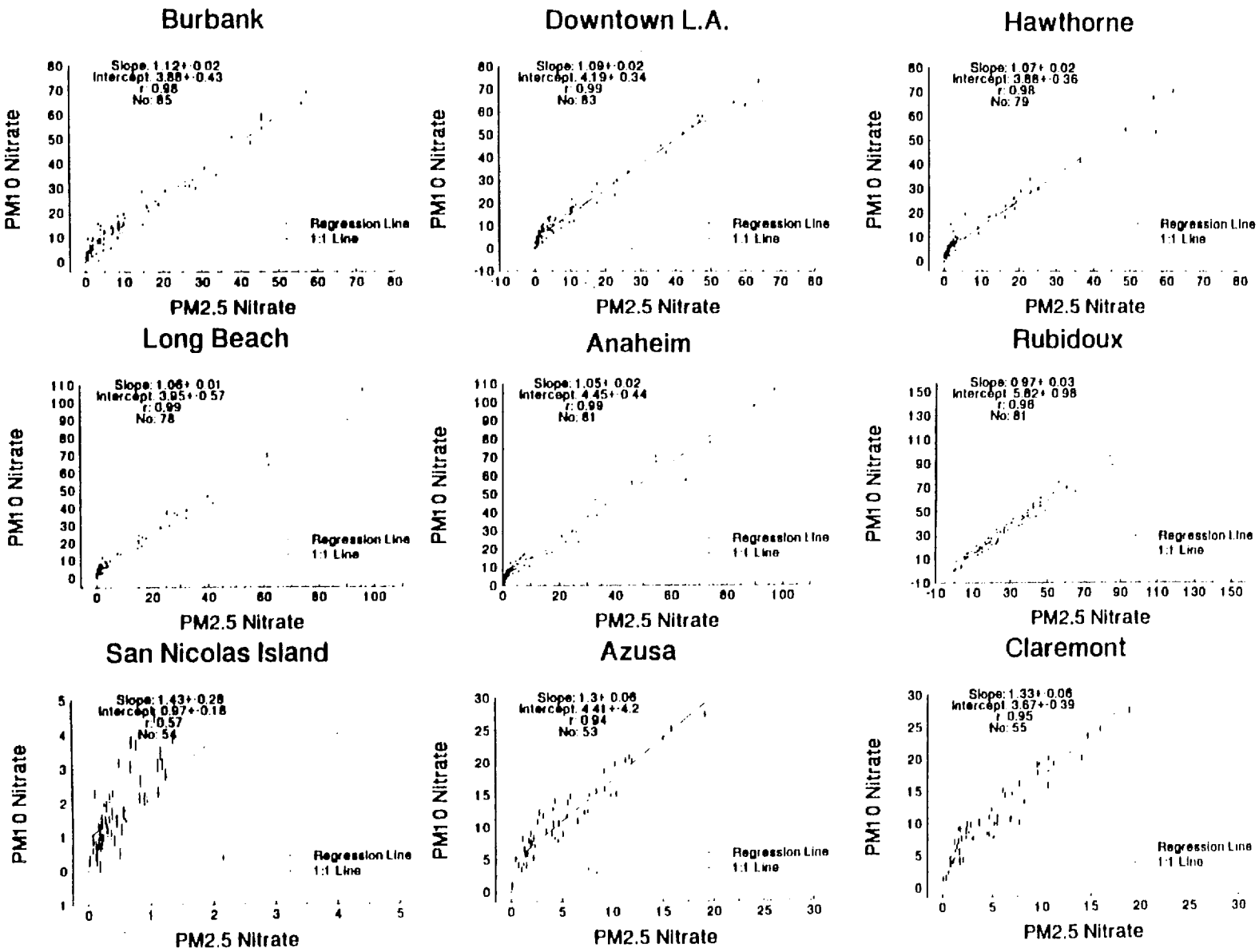

Figure 3-3d. Scatterplots of PM_{10} Versus $PM_{2.5}$ Nitrate at All SCAQS Sites During the Summer and Fall Campaigns

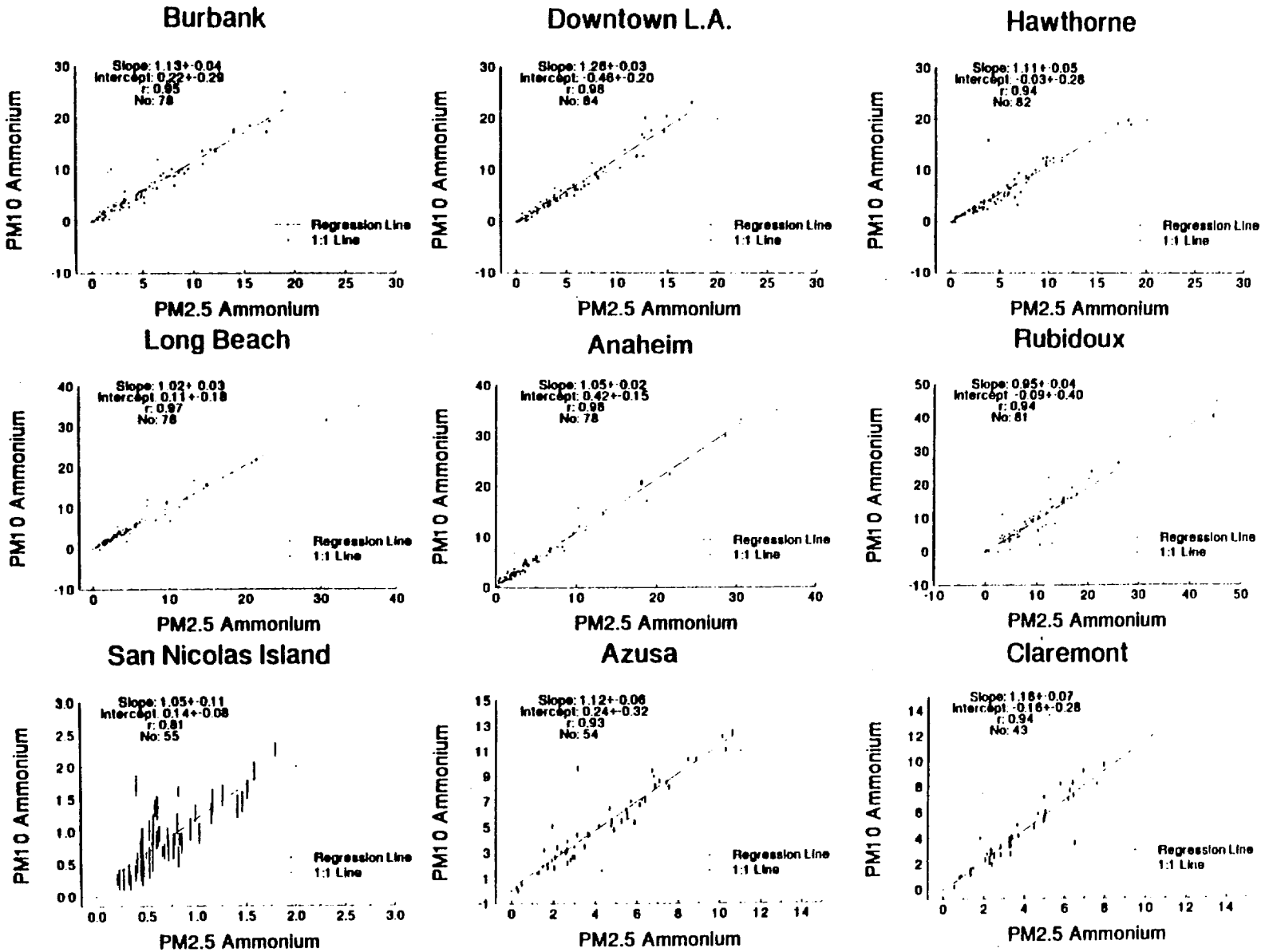

Figure 3-3e. Scatterplots of PM_{10} Versus $PM_{2.5}$ Ammonium at All SCAQS Sites During the Summer and Fall Campaigns

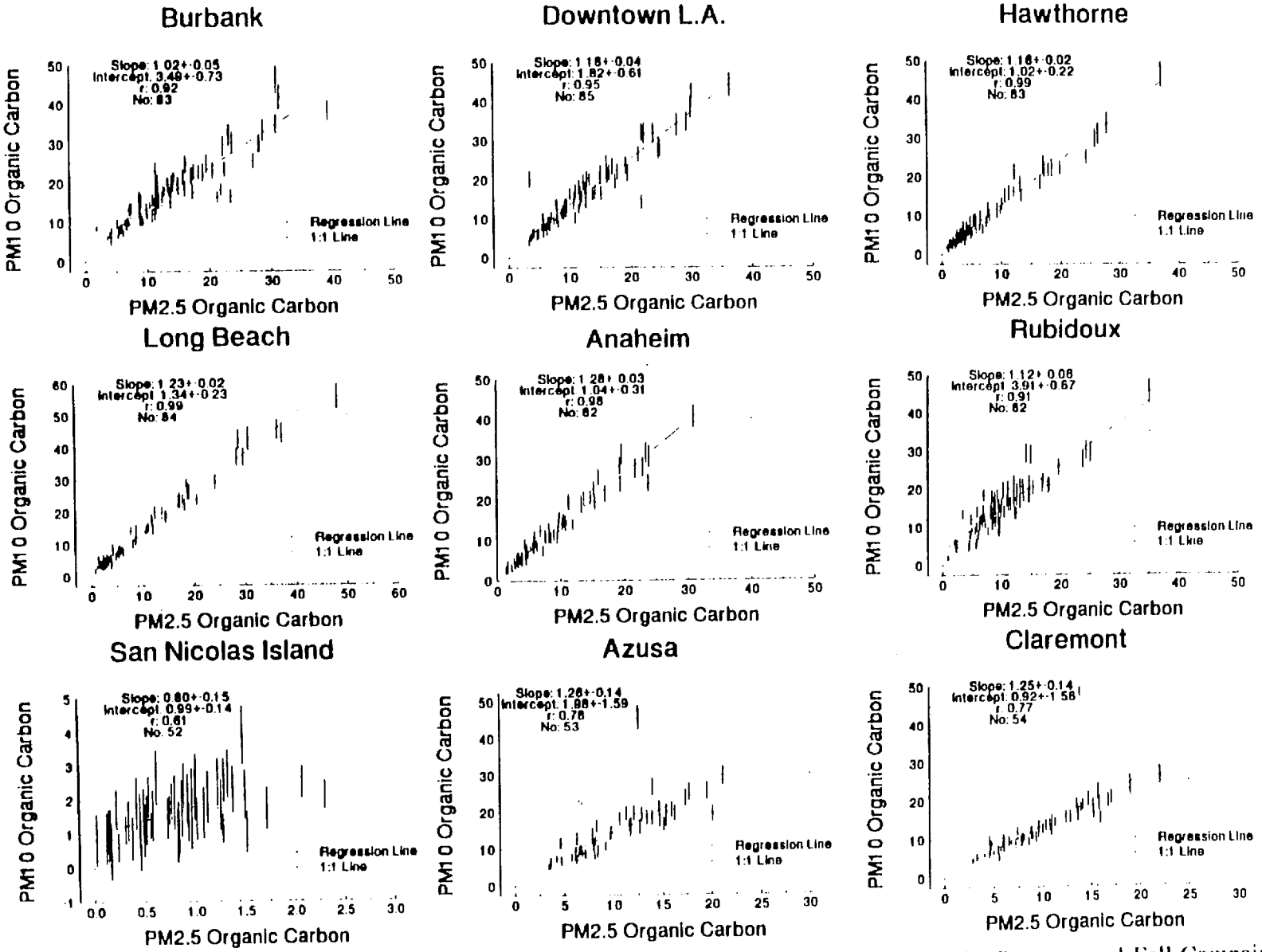

Figure 3-31. Scatterplots of PM_{10} Versus $PM_{2.5}$ Organic Carbon at All SCAQS Sites During the Summer and Fall Campaigns

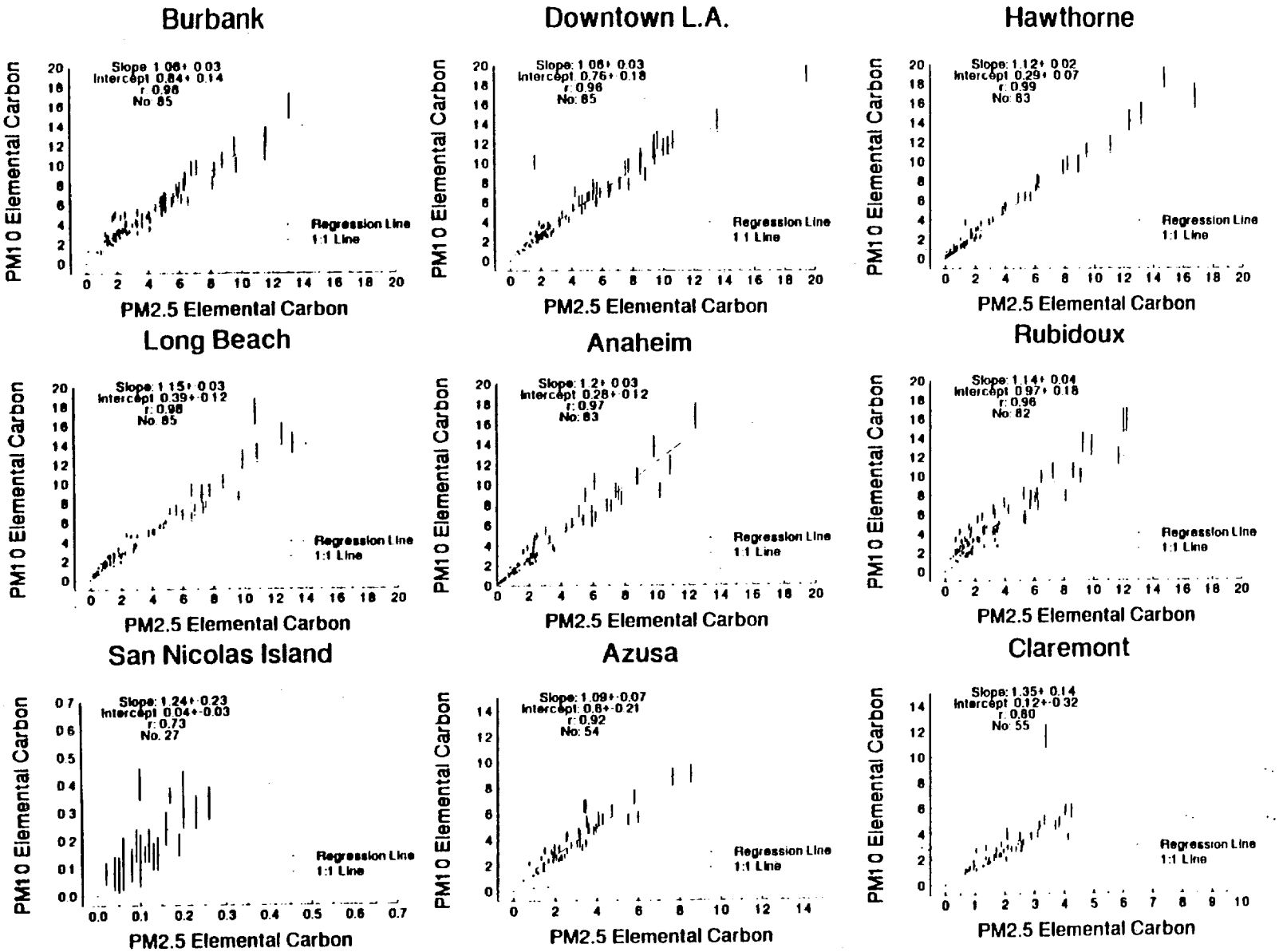

Figure 3-3g. Scatterplots of PM_{10} Versus $PM_{2.5}$ Elemental Carbon at All SCAQS Sites During the Summer and Fall Campaigns

Sulfate and nitrate concentrations were acquired from the ion chromatographic analysis on Teflon-membrane filter extracts. Excellent agreement is found for PM_{10} versus $PM_{2.5}$ sulfate. As shown in Figure 3-3c, the regression analysis resulted in high correlations ($r \geq 0.97$) and low ($< 0.8 \pm 0.4$ $\mu g/m^3$) intercepts. The slopes on these plots are very consistent, typically 1.15 ± 0.02, with a lower slope (1.07 ± 0.06) reported at the San Nicolas Island site. The majority ($\sim$ 90%) of the PM_{10} sulfate is found in the $PM_{2.5}$ fractions. Coarse particle sulfate such as sodium sulfate (Na_2SO_4) is probably present at the coastal sites, but not in great amounts.

Similar correlations ($r \geq 0.96$) are found in Figure 3-3d for the PM_{10} versus $PM_{2.5}$ nitrate plots. For the six sites during the summer and fall campaigns, the slopes are typically $\sim 1.1 \pm 0.02$ with intercepts of 4 to 5 $\mu g/m^3$; the Rubidoux site, however, shows a lower slope (0.97 ± 0.03) and higher ($\sim$ 1 $\mu g/m^3$) intercept. Coarse particle nitrate (i.e., $NaNO_3$) is more abundant than coarse particle sulfate as shown in Figure 3-3c.

The slopes of PM_{10} versus $PM_{2.5}$ nitrate at the Azusa and Claremont sites during the summer campaign are approximately 15% higher than at the other sites, ranging from 1.3 ± 0.06 to 1.33 ± 0.06. Coarse particle nitrate is more significant at the San Nicolas Island site which yields the highest slope (1.43 ± 0.3) among all the plots.

The ammonium concentrations are acquired from the automated colorimetric analysis of Teflon-membrane filter extracts. Figure 3-3e displays scatterplots of PM_{10} versus $PM_{2.5}$ ammonium concentrations. The regression lines are expected to be close to unity showing the majority of ammonium in the $PM_{2.5}$ fraction. A few outliers have been identified in these plots and excluded from the final regression calculations. $PM_{2.5}$ and PM_{10} ammonium concentrations at the San Nicolas Island site are typically less than 2.0 $\mu g/m^3$. The error bars on this plot are quite large and many values are below the one-to-one line. These data are further identified in Appendix A.

Organic and elemental carbon concentrations are acquired from TMO analysis of quartz-fiber filters. The majority of organic and elemental carbon is expected to be in the $PM_{2.5}$ fraction, except at those sites with greater geological source influences, where organic carbon is one of the soil components. The top six plots in Figure 3-3f show high correlations ($r \geq 0.91$) of PM_{10} versus $PM_{2.5}$ organic carbon, with slopes of 1.0 to 1.3 and intercepts of 1.0 ± 0.3 to 3.9 ± 0.7 $\mu g/m^3$ for the summer and fall campaigns. The correlations for the summer sites are much lower ($r \leq 0.78$), with noticeable outliers at the Azusa and Claremont sites. Most of the organic carbon concentrations at the San Nicolas Island site are below the LQLs (0.4 to 1.6 $\mu g/m^3$) with error bars often exceeding $\pm 30\%$. The lower than unity slope (0.8 ± 0.2) and low correlation coefficient (0.61) are indicative of the high uncertainties for these measurements.

The PM_{10} versus $PM_{2.5}$ elemental carbon comparisons in Figure 3-3g exhibit patterns similar to those of organic carbon with high correlations ($r \geq 0.96$), low intercepts (< 1.0 $\mu g/m^3$) and close to unity slope at the six summer and fall sites. The lower correlation ($r = 0.8$) and higher slope (1.3 ± 0.1) at the Claremont site reflects the outliers shown in the plot. The

majority of the elemental carbon values are below the LQLs (0.04 to 0.5 $\mu g/m^3$) at the San Nicolas Island site. The error bars on this plot are quite high ($\pm 50\%$).

The examples given in Figures 3-3a to 3-3g show how the data validation process provides explanations for physical inconsistencies in the data set. Appendix A documents the sampling site, date, period, and the suspect chemical species concentrations which have been discovered to be inconsistent in the data base.

3.4.2b Sum of Chemical Species Versus Measured Mass

The sum of the individual chemical concentrations for $PM_{2.5}$ and PM_{10} should be less than or equal to the corresponding mass loadings measured by gravimetric analysis. The sum of chemical species is calculated as a direct sum of Teflon-membrane filter (Channels 8 and 9 in Component two and Channels 11 and 12 in Component three) and front quartz-fiber filter (Channel 7 in Component two and Channel 10 in Component three) species concentrations. Chemical species measured more than once by different chemical analysis methods, such as soluble chloride, soluble sodium, and elemental sulfur, are excluded from the sum. No weighting was applied in these calculations since weighting the sum by converting metals to their respective oxides and organic carbon to some "typical" molecular weight compound imposes unnecessary assumptions for validation purposes. The scatterplots for each site (not shown here) were examined for $PM_{2.5}$ and PM_{10} size fractions and no significant differences were found. Therefore, Figure 3-4 shows the scatterplots of $PM_{2.5}$ and PM_{10} sum of species versus mass at all sites. Each plot contains a line indicating the 1:1 relationship as well as regression statistics with mass as the independent variable and sum of species as the dependent variable. The sum of chemical species is expected to be less than total mass since several important species (e.g., oxygen, hydrogen) have not been measured.

These figures show similar relationships for both $PM_{2.5}$ and PM_{10} at all sites. The correlation coefficients are greater than 0.97 in all cases. The outliers identified on Figure 3-3 were eliminated from the final regression calculations. The sum of species at these sites is consistently 20% to 30% lower than the measured mass, particularly at higher concentrations, where organic carbon and crustal elements constitute a large fraction of the mass. These ratios are, in general, 10% to 15% lower than the ratios found in other SoCAB aerosol studies (e.g., Solomon *et al.*, 1989, Chow *et al.*, 1992). The inhomogeneous sample deposits on the SCAQS samples described in Section 3.2 are suspected as the cause of this discrepancy. Even though universal correction factors shown in Table 3-4 have been applied to these elements, and several punches from the center, middle, and edge of the 47mm disc have been selected for carbon analysis, the elemental and carbon concentrations are, in general, lower limits of the elemental and carbon constituents on these filters. Besides the inhomogeneity of the sample deposits, metal shavings were found on the filter deposits for other studies such as the 1988 Rubidoux neighborhood study (Chow *et al.*, 1992) and 1988/1989 Valley Air Quality Study (Chow *et al.*, 1993a) where SCAQS samplers were used. These brass fittings could result in higher than actual mass concentrations.

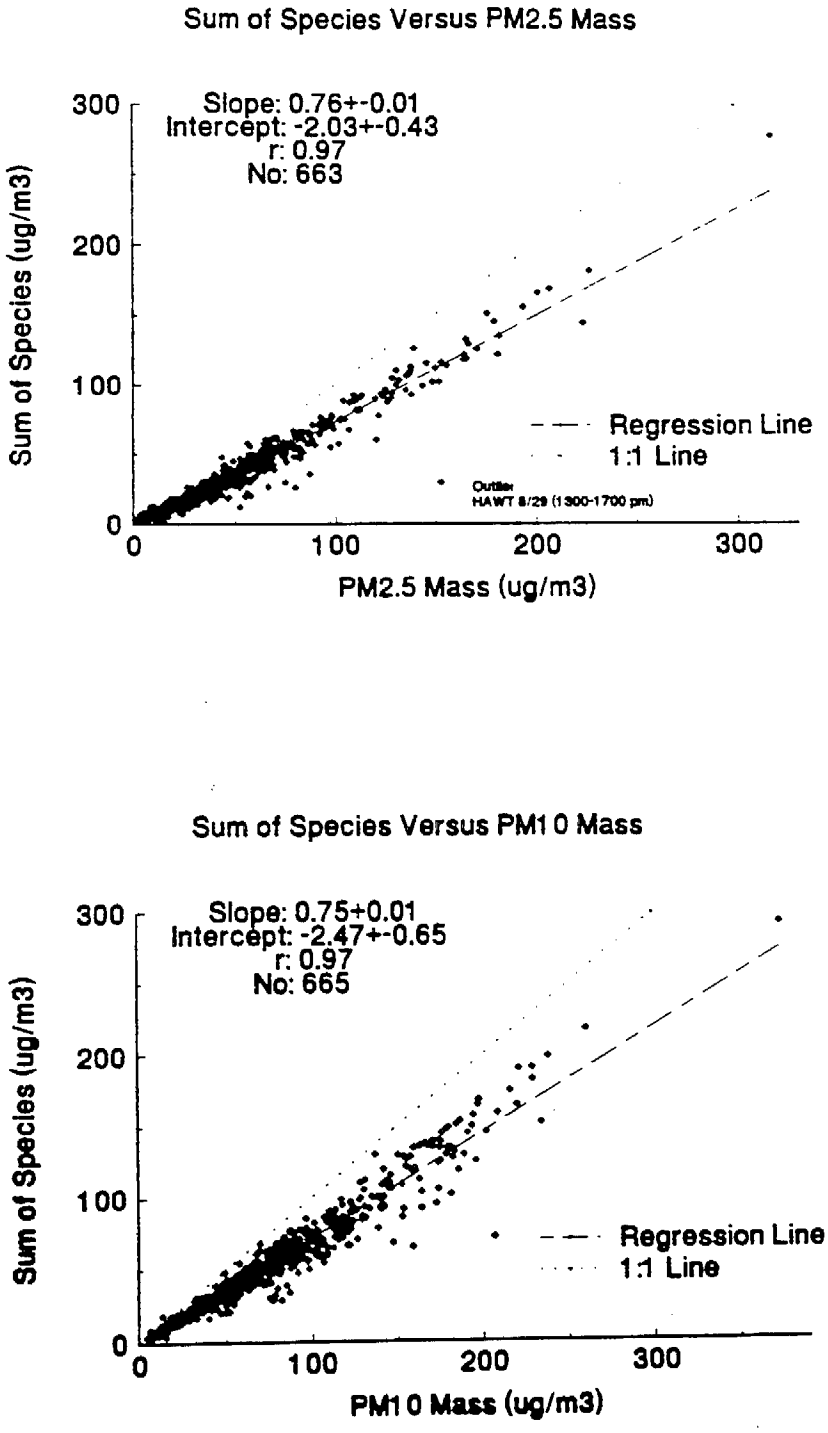

Figure 3-4. Scatterplots of $PM_{2.5}$ and PM_{10} Sum of Species Versus Mass at All SCAQS Sites Between 6/19/87 and 12/11/87.

3.4.2c Physical Consistency

Composition of chemical species concentrations measured by different methods can be examined for a few cases. Sulfate ($SO_4^=$) acquired by ion chromatographic analysis on Teflon-membrane filters on Channels 8 and 11 can be composed of elemental sulfur (S) obtained by x-ray fluorescence analysis on Teflon-membrane filters on Channels 9 and 12 of the SCAQS samplers (Figure 3-2) for $PM_{2.5}$ and PM_{10} size fractions. The $SO_4^=$ to S ratio should equal "three" if all of the elemental sulfur is present as soluble sulfate. Figure 3-5 shows scatterplots of sulfate versus sulfur for $PM_{2.5}$ and PM_{10} measurements at all sites. Excellent correlations ($r > 0.99$) are found on these measurements with a near zero intercept and higher than expected slope (3.4 ± 0.02). This observation supports the contention in the previous section that sulfur measurements are biased ($\sim$ 13%) low due to the inhomogeneity of the sample deposit. This bias is similar for the $PM_{2.5}$ and PM_{10} sulfur measurements. Soluble sodium versus total sodium comparisons were made for $PM_{2.5}$ and PM_{10} and soluble chloride versus chlorine comparisons were made for $PM_{2.5}$ and PM_{10} (not shown here). Higher than expected soluble to total ratios were found for those measurements, also supporting the hypothesis that elemental concentrations by XRF analysis, after the recommended corrections, are biased low.

Channel 9 of the SCAQS sampler (Figure 3-2) measures $PM_{2.5}$ nitrate from the Teflon-membrane filter, while Channel 3 measures $PM_{2.5}$ particulate nitrate from the Teflon/nylon filter packs which were preceded with nitric acid denuders. The nylon backup filters installed in Channel 3 were intended to capture the volatilized particulate nitrate disassociated from the front Teflon-membrane filters. Theoretically, the nitric acid denuded nitrate (Channel 3) should be greater than or equal to the $PM_{2.5}$ nitrate (Channel 9), depending on the extent of volatilization.

Figure 3-6 shows scatterplots of $PM_{2.5}$ particulate nitrate versus nitric acid denuded nitrate for the summer and fall campaigns at all sites. As discussed in Section 2.3, secondary ammonium nitrate is not a stable compound. Its equilibrium with gaseous ammonia and nitric acid is strongly influenced by temperature and relative humidity. The dissociation of particulate nitrate from the front Teflon-membrane filters is higher in the summer time when temperatures are higher. Figure 3-6 yields a slope of 0.62 ± 0.02 for the summer campaign and 0.92 ± 0.02 for the fall campaign with a zero to $\sim$ -1 $\mu g/m^3$ intercept. Approximately 40% of the particulate nitrate from the Teflon-membrane filters seem to have volatilized during summer. This volatilization decreases to 10% during the fall when temperatures are lower. The variations in volatilization are greater in the summer ($r=0.84$) as compared to the fall ($r=0.97$). Volatilized nitrate is not part of the measured $PM_{2.5}$ mass. PM_{10} measurements from long-term monitoring networks underestimate the actual PM_{10} concentrations during summer, but they are probably reasonably accurate during the fall and winter.

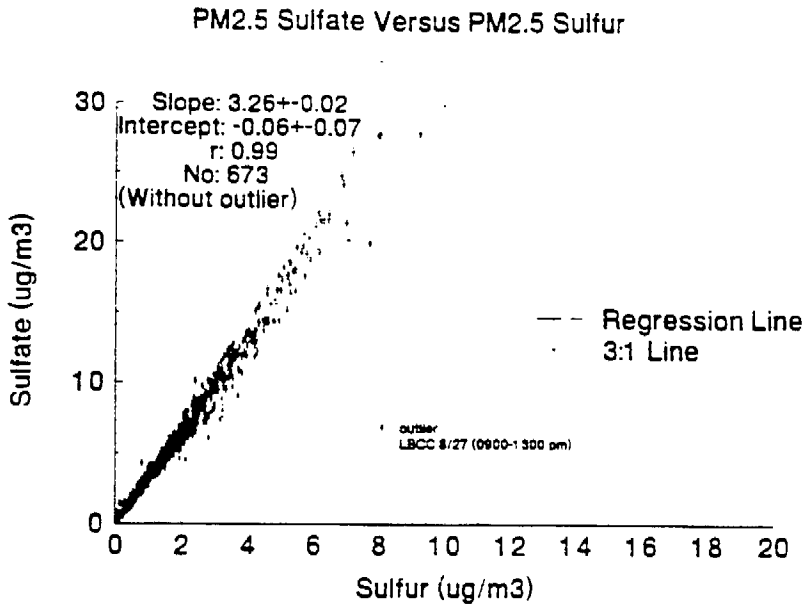

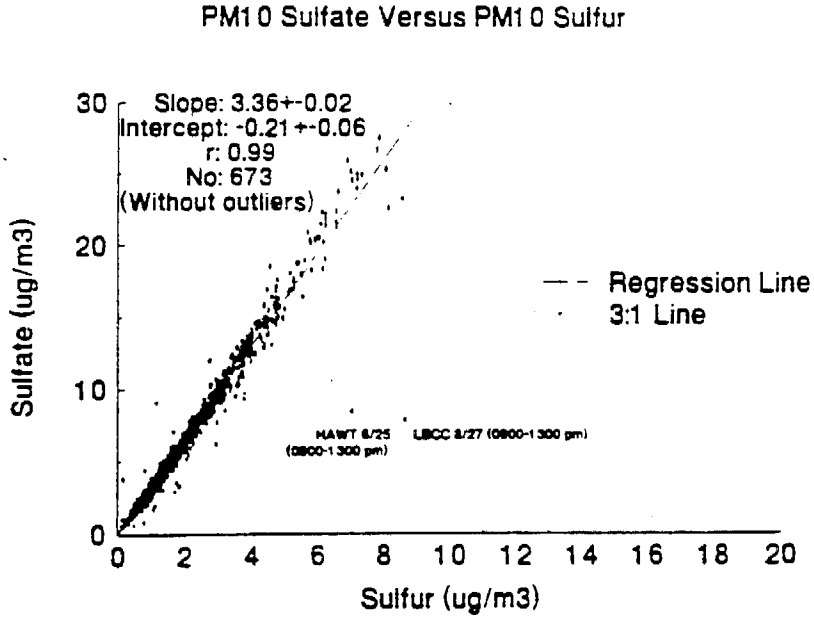

Figure 3-5. Scatterplots of Sulfate Versus Sulfur for $PM_{2.5}$ and PM_{10} Measurements at All SCAQS Sites Between 6/19/87 and 12/11/87

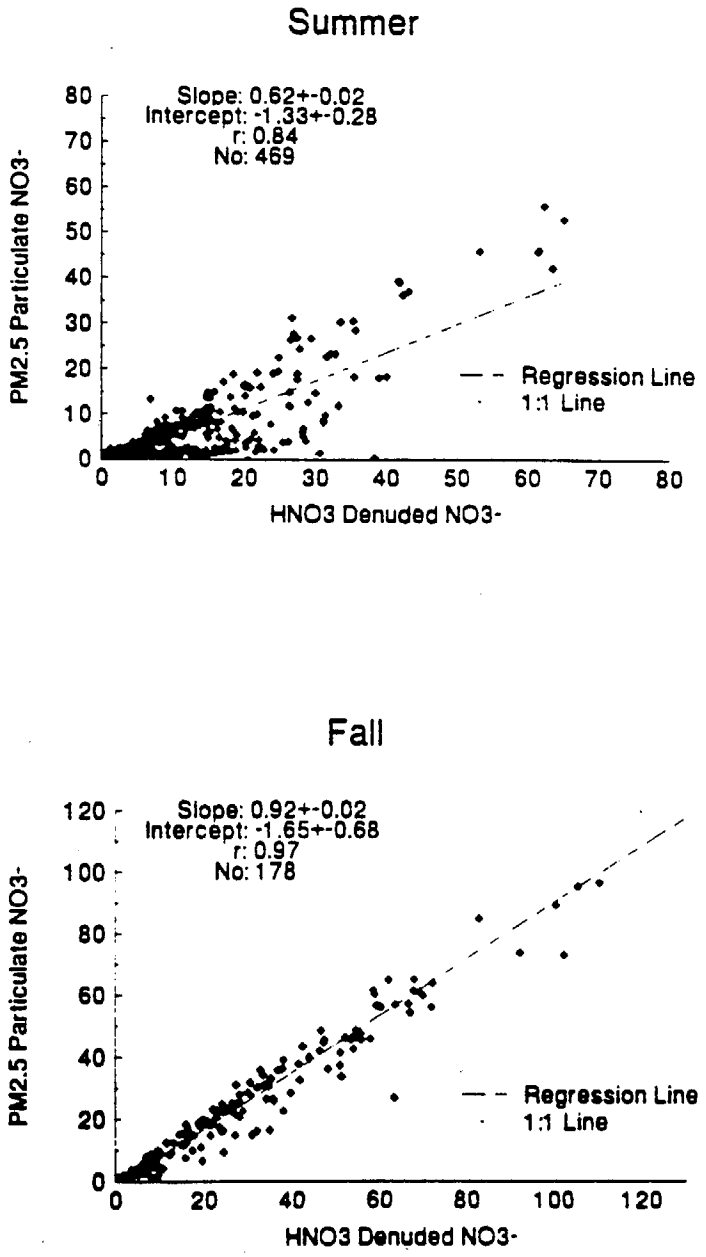

Figure 3-6. Scatterplots of $PM_{2.5}$ Nitrate Versus Nitric Acid Denuded Nitrate at All SCAQS Sites Between 6/19/87 and 12/11/87

3.4.2d Ion Balances

As discussed in Section 2.3, ammonium nitrate (NH_4NO_3), sodium nitrate ($NaNO_3$), sodium sulfate (Na_2SO_4), ammonium sulfate ($(NH_4)_2SO_4$), and ammonium bisulfate (NH_4HSO_4) are the most likely nitrate and sulfate compounds in the SoCAB. Ammonium (NH_4^+) can be calculated based on the stoichiometric ratios of the different compounds and compared with that which was measured.

Two hypothetical cases were tested for the ammonium balance:

- Case I: where nitrate and sulfate or bisulfate are balanced by equivalent ammonium.

- Case II: where some of the sulfate, calculated from soluble or elemental sodium, is assumed to come from sea salt and some of the nitrate is associated with sea salt sodium (Na^+) in an amount equivalent to the reduction of chloride (Cl^-) from its seawater Cl^-/Na^+ ratio.

"Case I" assumes that sulfate is either ammonium sulfate or ammonium bisulfate, and that all of the particulate nitrate is in the form of ammonium nitrate. Measured ammonium concentrations should equal those calculated from ammonium bisulfate or ammonium sulfate and ammonium nitrate on a molar to molar basis. The following steps were applied in these calculations:

- Assuming all sulfate is ammonium sulfate:

$$\text{calculated ammonium} = 0.38 \times \text{sulfate} + 0.29 \times \text{nitrate}$$

- Assuming all sulfate is ammonium bisulfate:

$$\text{calculated ammonium} = 0.192 \times \text{sulfate} + 0.29 \times \text{nitrate}$$

The ammonium, nitrate, and sulfate concentrations used in these comparisons are those measured on the front Teflon-membrane filters (Channel 9 in Component two for $PM_{2.5}$ and Channel 12 in Component three for PM_{10}). The above comparisons assume that nitrate lost by volatilization of ammonium nitrate from the front Teflon-membrane filter depletes both particulate ammonium and nitrate.

Measured and calculated ammonium are plotted in the left half of Figures 3-7a to 3-7i for $PM_{2.5}$ and PM_{10} size fractions at each of the nine sites. Each figure contains calculated ammonium based for both the ammonium sulfate (◆) and ammonium bisulfate (◇) cases. Three types of ion balances are exhibited in these figures:

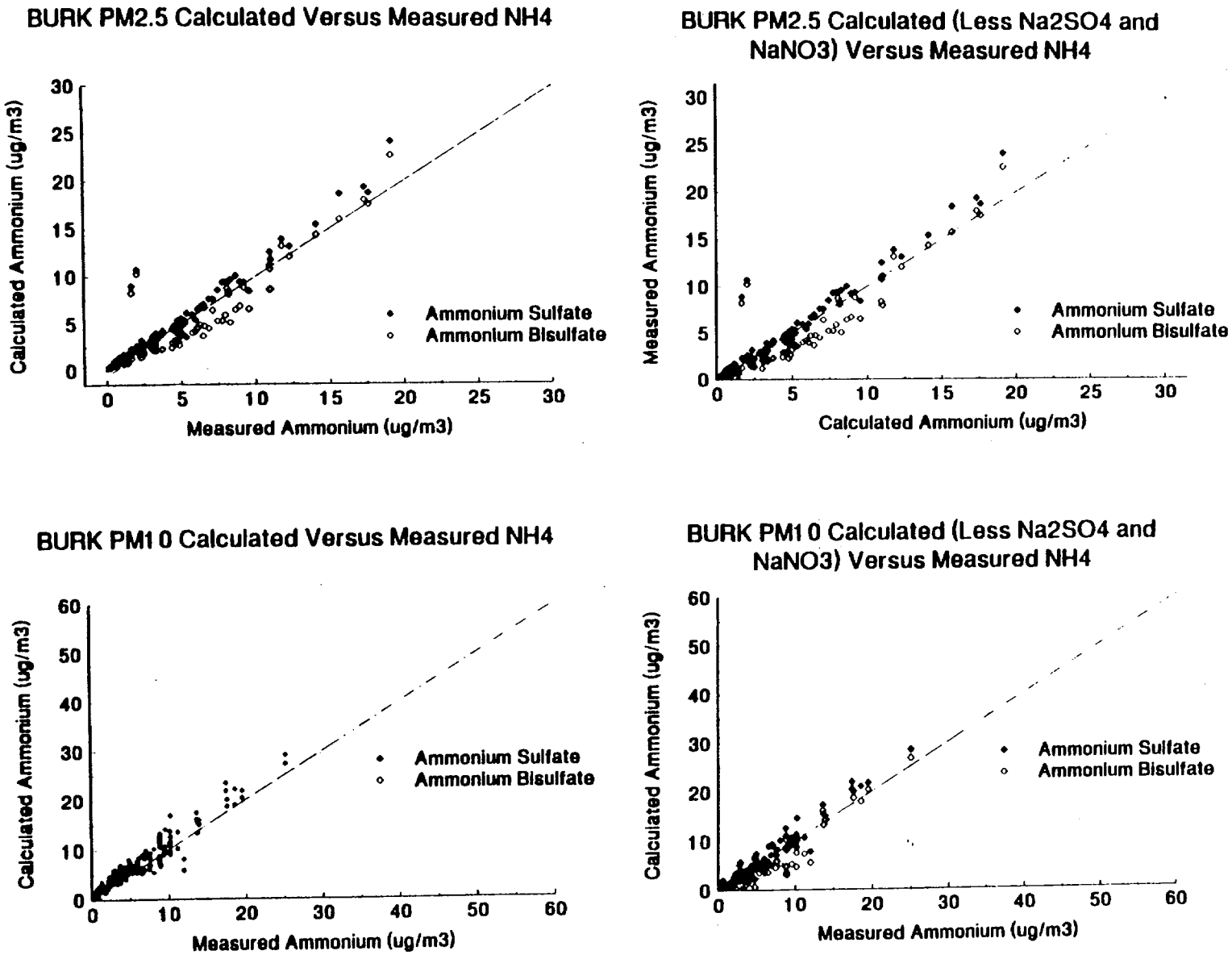

Figure 3-7a. Scatterplots of $PM_{2.5}$ and PM_{10} Calculated Versus Measured Ammonium at the Burbank Site During the Summer and Fall Campaigns

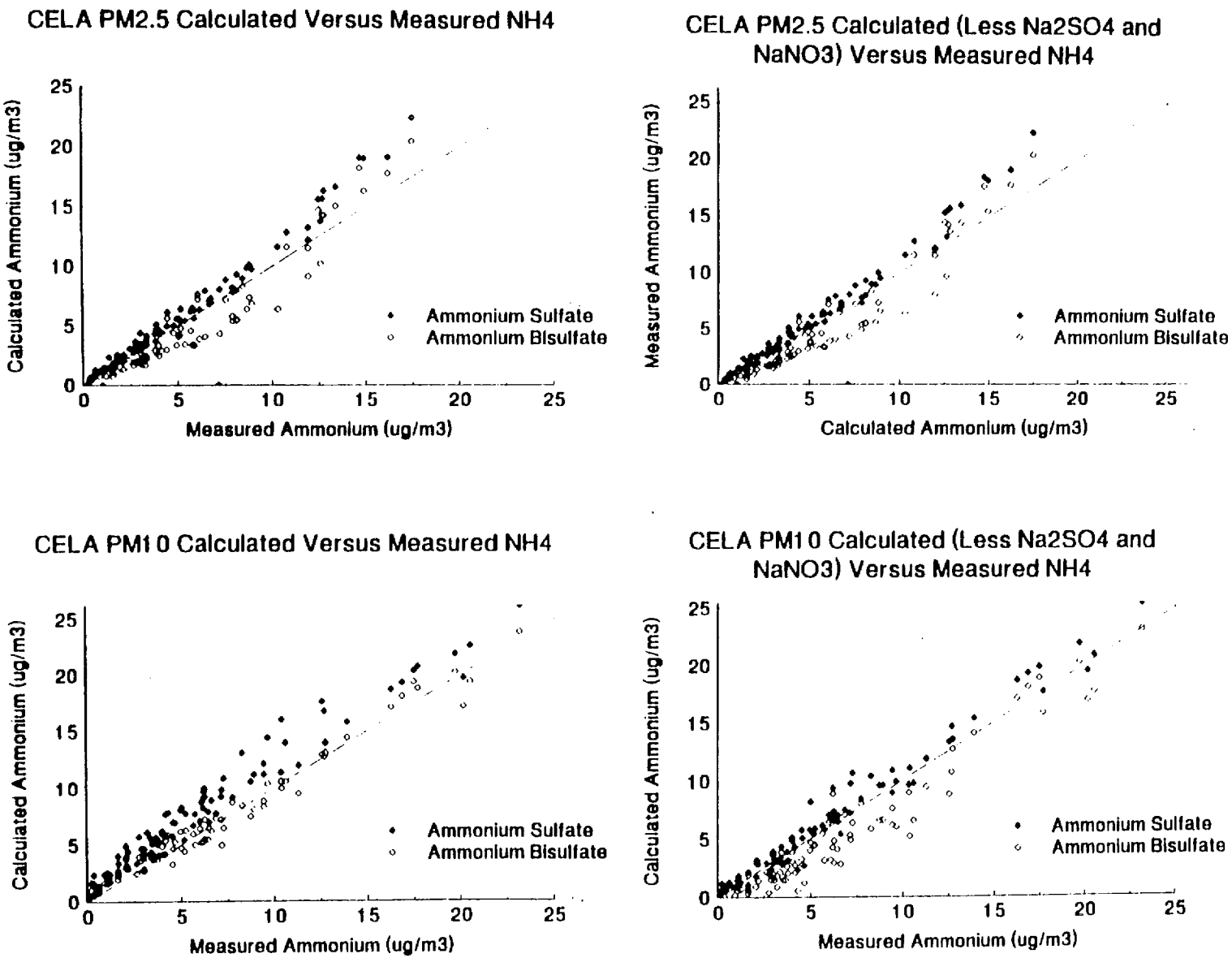

Figure 3-7b. Scatterplots of $PM_{2.5}$ and PM_{10} Calculated Versus Measured Ammonium at the Downtown Los Angeles Site During the Summer and Fall Campaigns

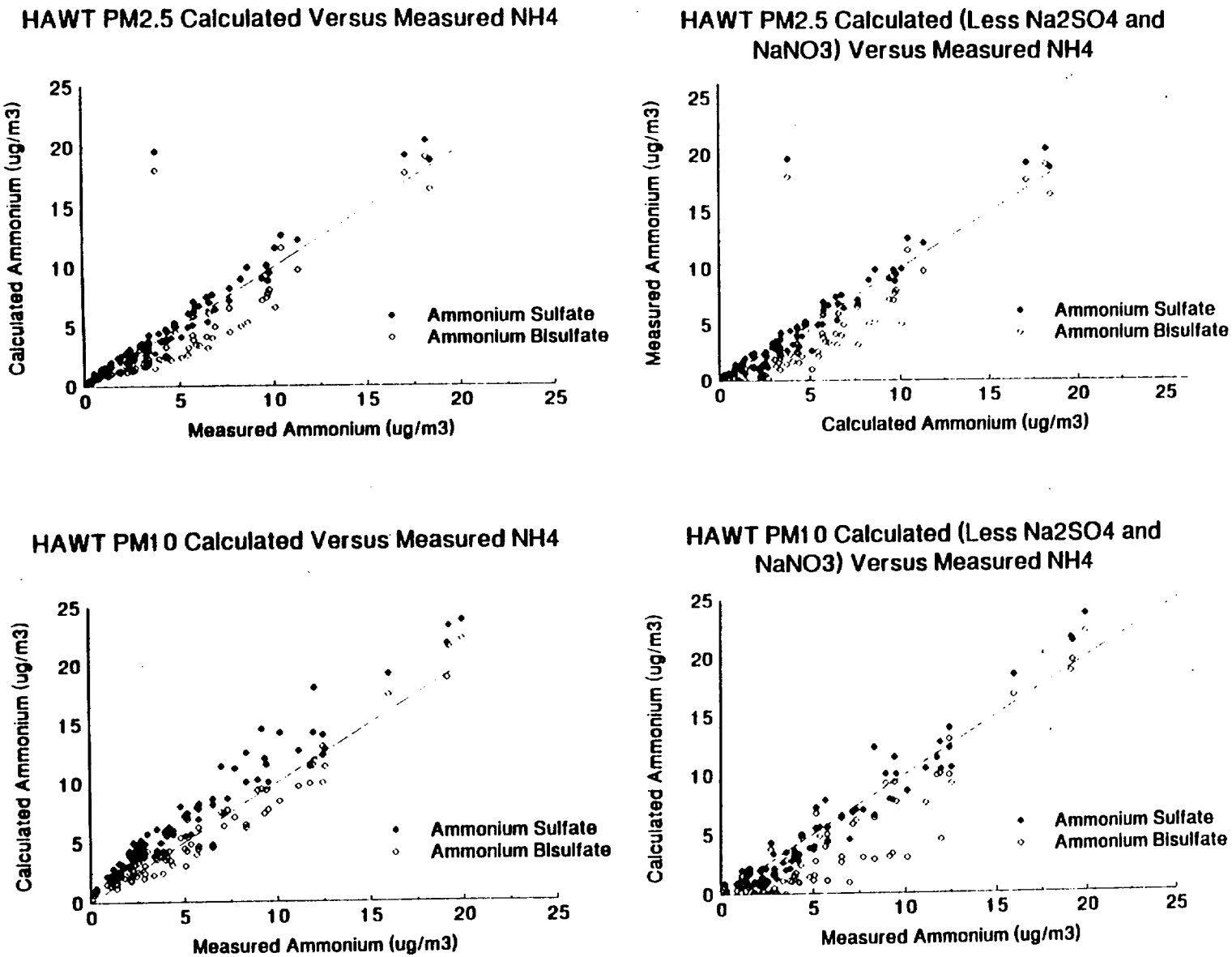

Figure 3-7c. Scatterplots of $PM_{2.5}$ and PM_{10} Calculated Versus Measured Ammonium at the Hawthorne Site During the Summer and Fall Campaigns

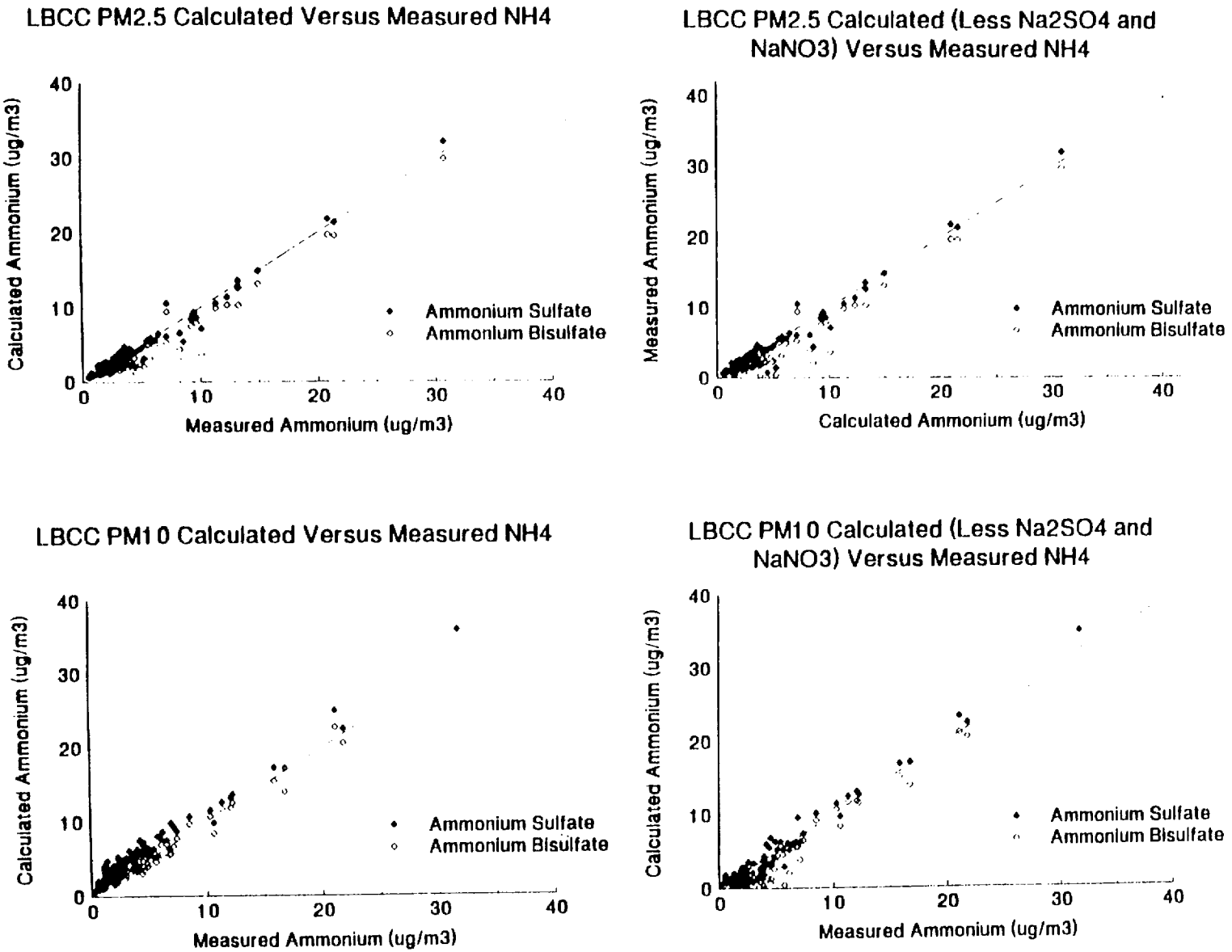

Figure 3-7d. Scatterplots of $PM_{2.5}$ and PM_{10} Calculated Versus Measured Ammonium at the Long Beach Site During the Summer and Fall Campaigns

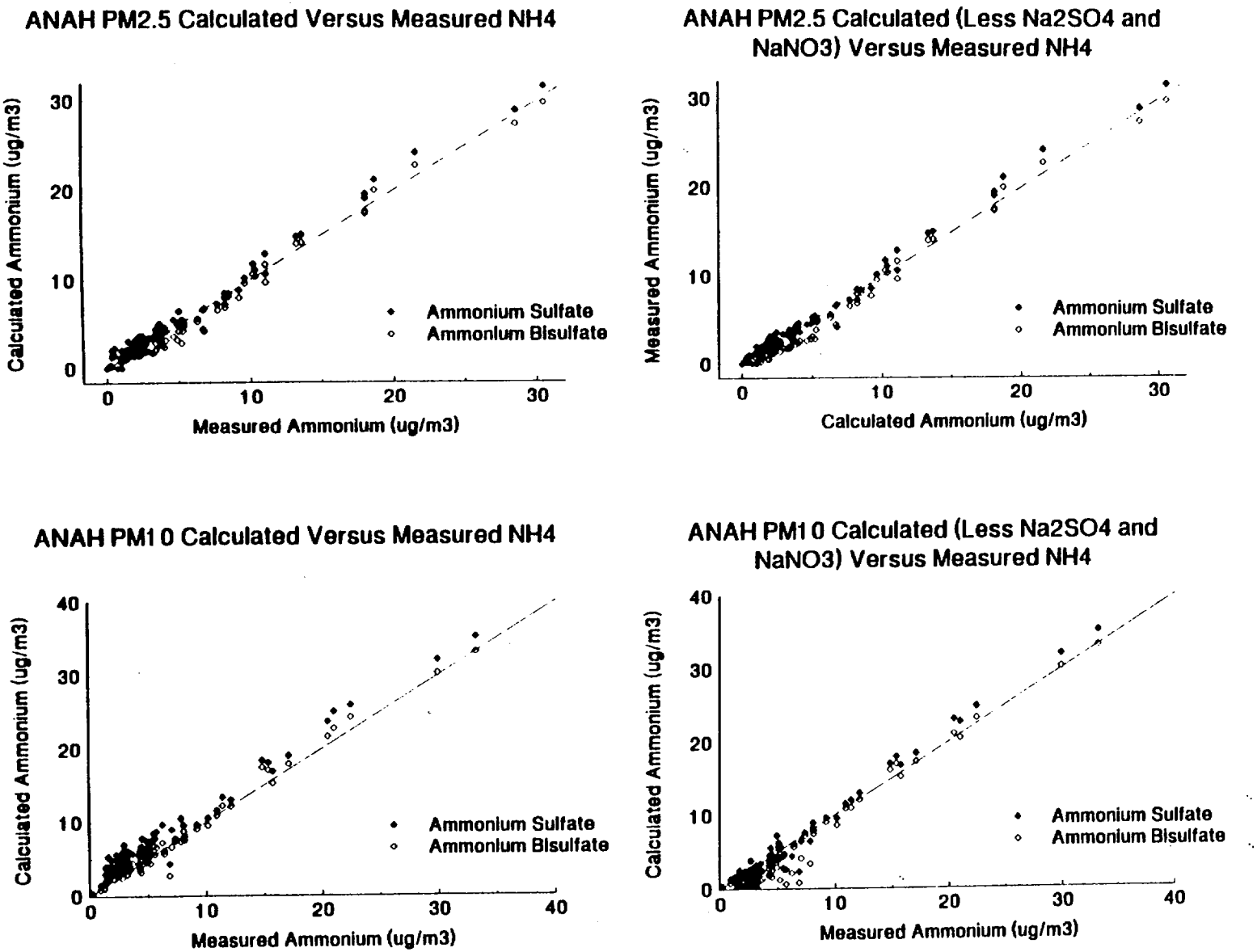

Figure 3-7e. Scatterplots of $PM_{2.5}$ and PM_{10} Calculated Versus Measured Ammonium at the Anaheim Site During the Summer and Fall Campaigns

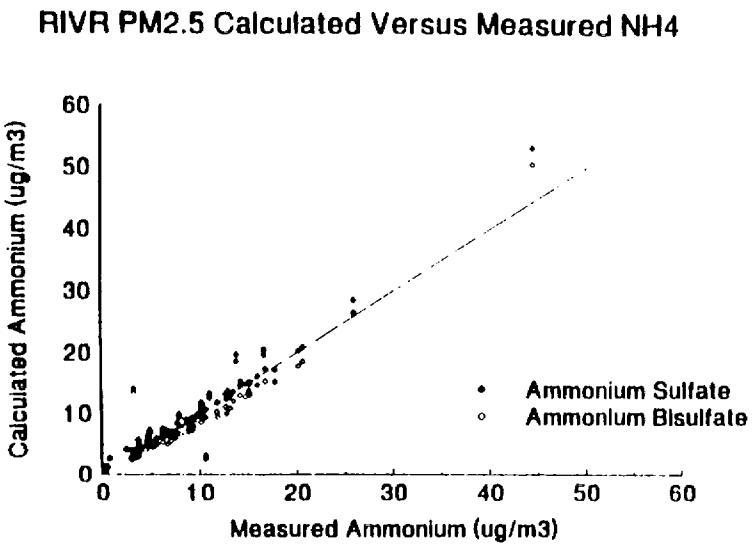

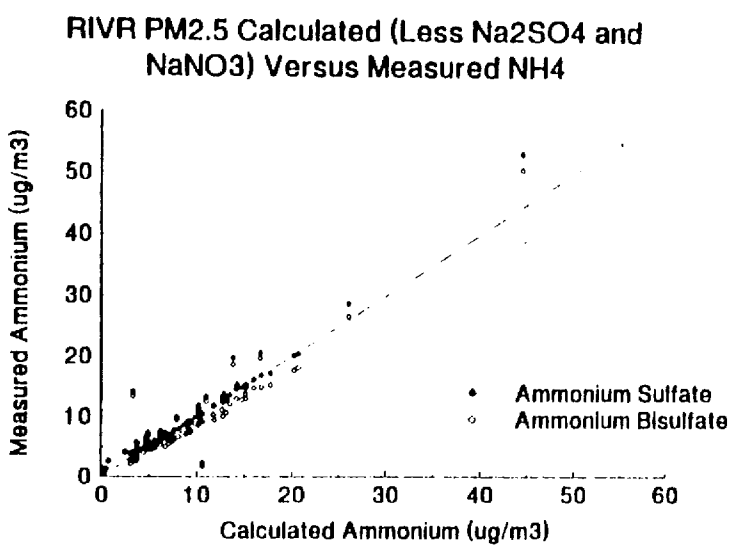

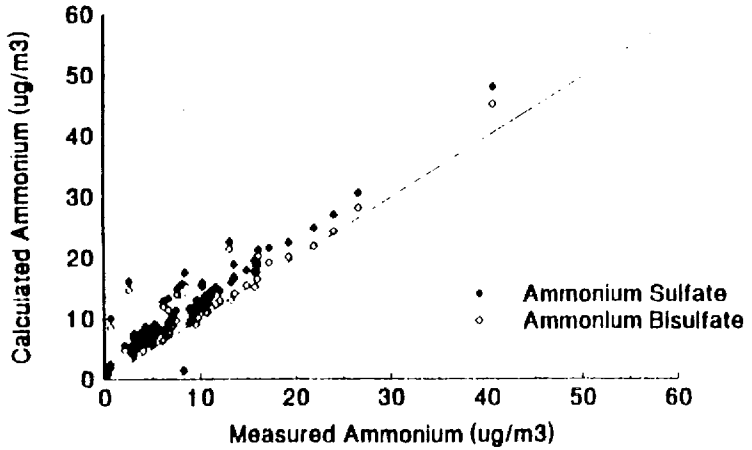

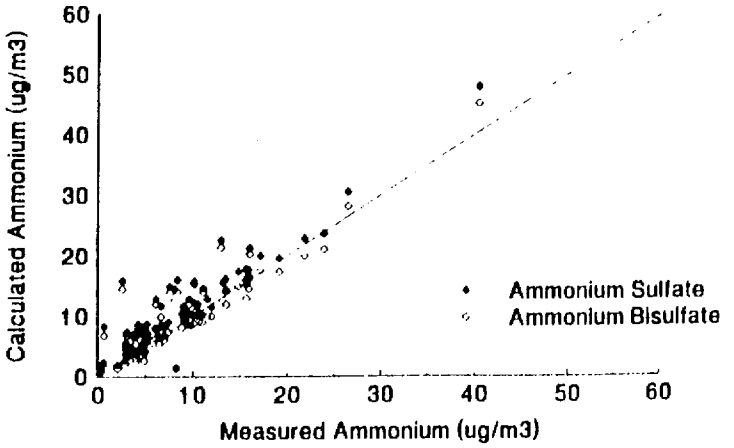

Figure 3-7f. Scatterplots of $PM_{2.5}$ and PM_{10} Calculated Versus Measured Ammonium at the Rubidoux Site During the Summer and Fall Campaigns

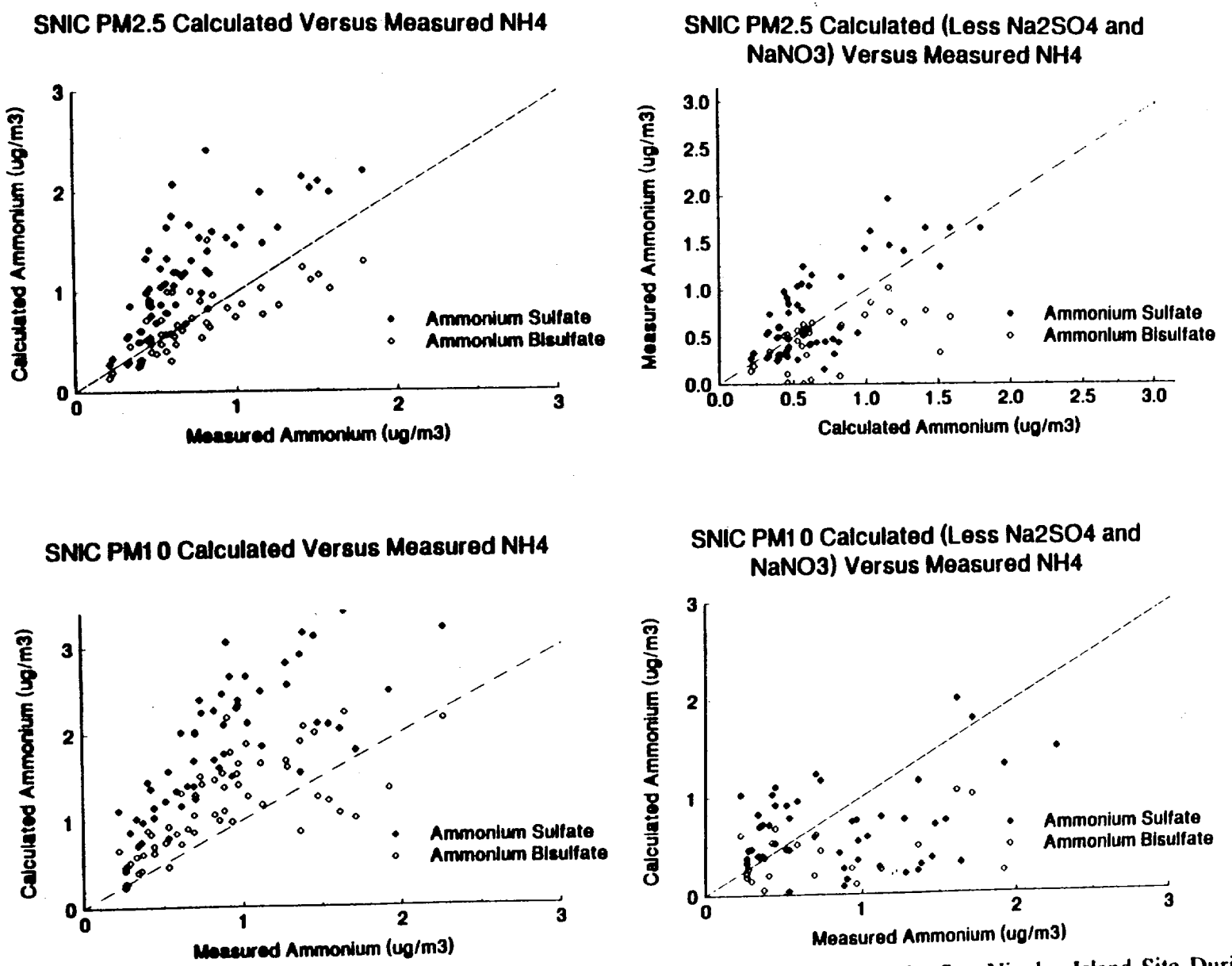

Figure 3-7g. Scatterplots of $PM_{2.5}$ and PM_{10} Calculated Versus Measured Ammonium at the San Nicolas Island Site During the Summer Campaign

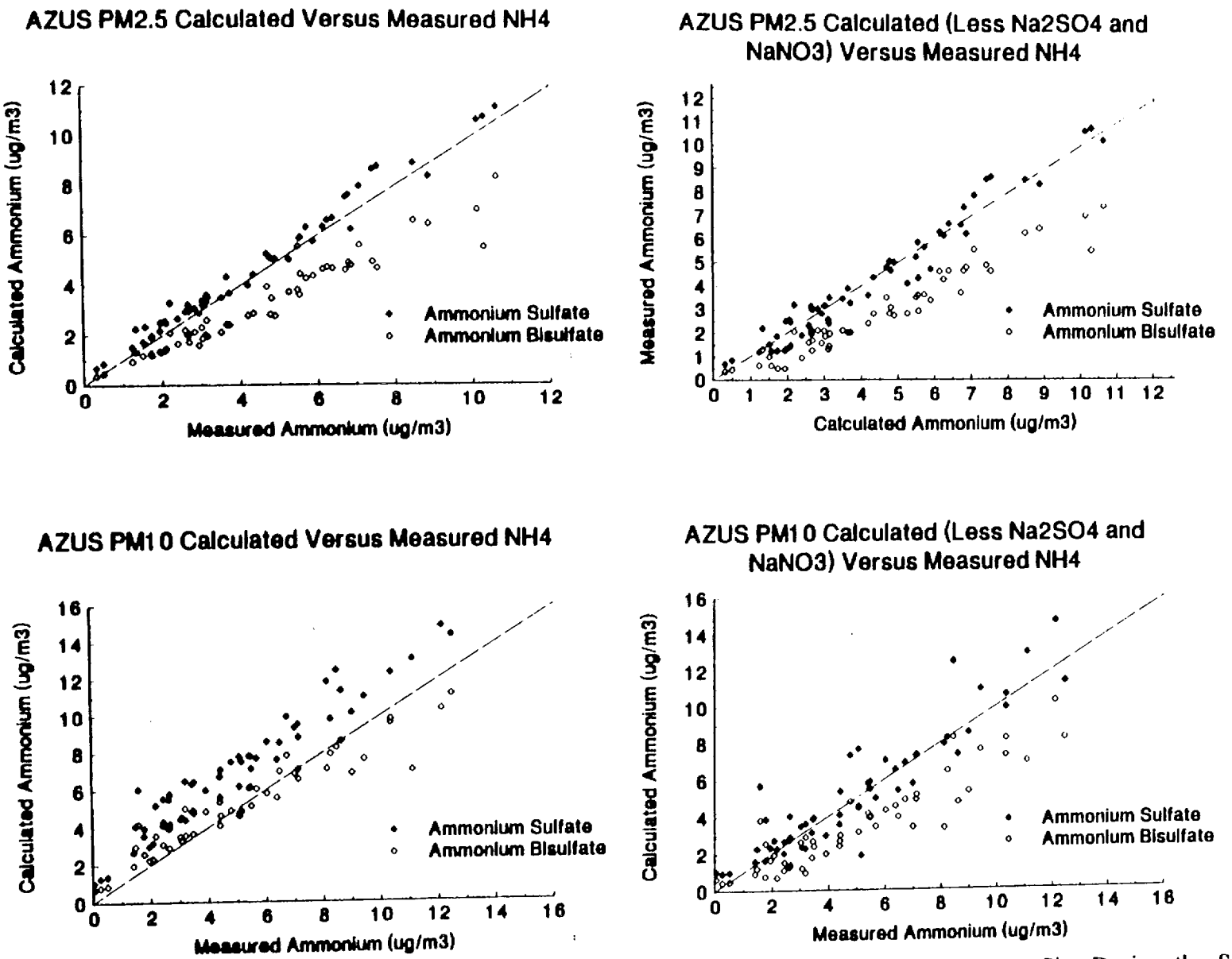

Figure 3-7h. Scatterplots of $PM_{2.5}$ and PM_{10} Calculated Versus Measured Ammonium at the Azusa Site During the Summer Campaign

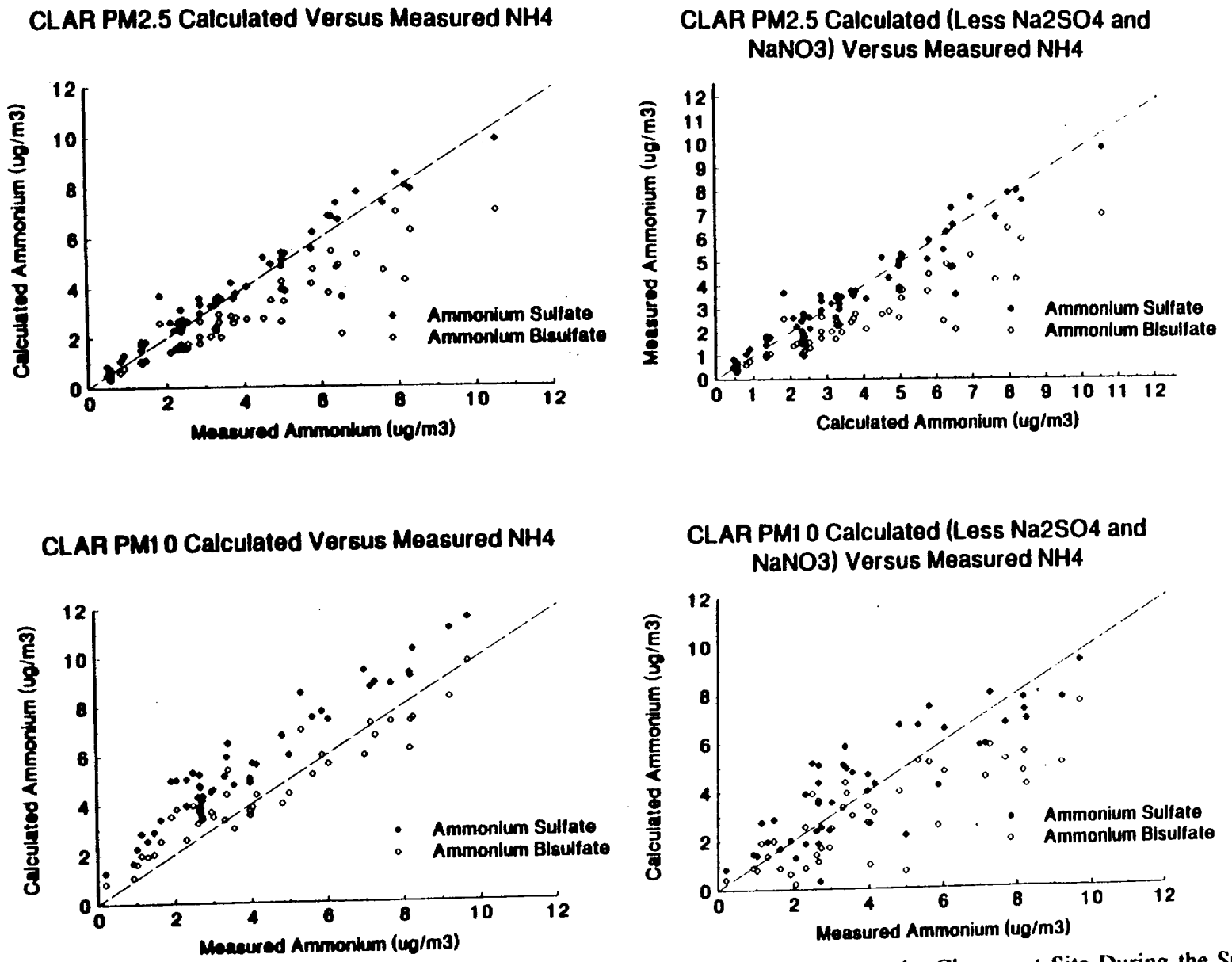

Figure 3-7i. Scatterplots of $PM_{2.5}$ and PM_{10} Calculated Versus Measured Ammonium at the Claremont Site During the Summer Campaign

- The majority of the ammonium bisulfate points are on the 1:1 line. This suggests that ammonium bisulfate is the dominant species and most of the sulfuric acid was not completely neutralized by ammonia. The PM_{10} ion balances at the Downtown Los Angeles (Figure 3-7b), San Nicolas Island (Figure 3-7g), Azusa (Figure 3-7h), and Claremont (Figure 3-7i) sites show this tendency.

- The majority of the ammonium sulfate points are on the 1:1 line. This suggests that ammonium sulfate is the dominant species at the sampling site. The $PM_{2.5}$ ion balance at the Claremont site (Figure 3-7i) shows this tendency.

- The 1:1 line lies between the ammonium sulfate and ammonium bisulfate points. This suggests a mixture of ammonium sulfate and ammonium bisulfate in the environment. The $PM_{2.5}$ ion balances at the Burbank (Figure 3-7a), Downtown Los Angeles (Figure 3-7b), Hawthorne (Figure 3-7c), Anaheim (Figure 3-7e), Rubidoux (Figure 3-7f) and San Nicolas Islands (Figure 3-7g) sites show this tendency.

Figures 3-7a to 3-7i indicate that points are above the 1:1 line for PM_{10} relative to $PM_{2.5}$ at the Burbank (Figure 3-7a), Downtown Los Angeles (Figure 3-7b), Hawthorne (Figure 3-7c), Long Beach (Figure 3-7d), San Nicolas Island (Figure 3-7g), Azusa (Figure 3-7h), and Claremont (Figure 3-7i) sites. This suggests that coarse aerosol at these sites is either more acidic (i.e., sulfate is present as bisulfate or sulfuric acid) and/or that coarse particle nitrate is associated with cations other than ammonium, such as sodium. Sea salt aerosol may react with nitric acid to produce coarse particle ammonium nitrate. This upward shift in the PM_{10} plots in Figure 3-7g is most dramatic for the PM_{10} fraction at the San Nicolas Island site, which is the site most influenced by marine aerosol. Soluble Na^+ and Cl^- concentrations are high at this site.

In "Case II", the ammonium balance is refined by subtracting sulfate and nitrate which might occur as sodium sulfate (Na_2SO_4) or sodium nitrate ($NaNO_3$) . This can occur by reaction of sulfuric and nitric acids with sodium chloride (NaCl). If this is the case, the sulfate (i.e., Na_2SO_4) concentration is equal to $0.25 \times Na^+$ (Pytcowicz and Kester, 1971). The following steps were applied to re-calculate ammonium by subtracting for sodium sulfate:

- Calculate sulfate in sodium sulfate as $0.25 \times Na^+$;

- Convert the sulfate as sodium sulfate to equivalents of ammonium, as ammonium bisulfate or ammonium sulfate according to the relationships given in "Case I"; and

- Subtract this ammonium equivalent from the total calculated ammonium.

Steps were also taken to estimate the amount of nitrate associated with sodium nitrate:

- Calculate the chloride deficit (Cl_d) for sodium chloride as $1.8 \times Na^+$ minus Cl^-;

- If Cl^-_d is less than zero, sodium nitrate is zero; if Cl^-_d is greater than zero, calculate an equivalent nitrate concentration corresponding to the chloride deficit as $2.7 \times Cl^-_e$ where 2.7 is the stoichiometric ratio of nitrate to sodium in sodium nitrate;

- Convert this sodium nitrate to an ammonium equivalent using the relationships given in "Case I"; and

- Subtract this ammonium equivalent from the total calculated ammonium.

For comparison, the right half of Figures 3-7a to 3-7i displays the calculated ammonium (less sodium sulfate and sodium nitrate) versus measured ammonium for $PM_{2.5}$ and PM_{10} size fractions at all sites. These figures show that subtracting the calculated ammonium for sodium nitrate and sodium sulfate has two effects: 1) it considerably reduces the scatter in the ion balance; 2) it shifts the points downward so that the ammonium sulfate points line up along the 1:1 line; and 3) coarse particle nitrate and sulfate corrections change the PM_{10} plots more than they change the $PM_{2.5}$ plots. The effects are least evident for $PM_{2.5}$ at the Rubidoux (Figure 3-7f), Azusa (Figure 3-7h), and Claremont (Figure 3-7i) sites, which are the sites furthest from the coast. Figures 3-7a to 3-7i thus suggest that ammonium sulfate is the dominant compound in most cases and that sulfate and nitrate from marine aerosol are significant components of PM_{10} in the SoCAB. Calculated and measured PM_{10} ammonium at the San Nicolas Island and Claremont sites experienced the greatest scatter, even after corrections for coarse particle sulfate and nitrate.

These cation/anion balances support the accuracy and precision of the nitrate, sulfate, and ammonium measurements on $PM_{2.5}$ and PM_{10} front Teflon-membrane filters, since such close agreement would not be found if these analyses were questionable. This balance also demonstrates that most of the nitrate and sulfate present in these particle samples occurs as ammonium nitrate and ammonium sulfate. The decision not to measure hydrogen ion in SCAQS is justified, since the potentially acidic particles appear to be entirely neutralized.

3.4.2e Carbon Variations in Ambient and Source Data Base

Discussions in Section 2.5 indicated that different carbon analysis methods such as thermal manganese oxidation (TMO, Fung, 1990), thermal/optical reflectance (TOR, Chow *et al.*, 1993b), and thermal/optical transmission (TOT, Cary, 1990) may have yielded different fractions of organic and elemental carbon.

The 1982 study reported by Gray *et al.* (1986) and the South Coast Source Composition Library reported by Cooper *et al.* (1987) and NEA (1990a; 1990b; 1990c) used the TOR method, whereas the 1986 South Coast Air Basin Study reported by Solomon *et al.* (1989) used the TOT method, and the SCAQS used the TMO method.

The thermal/optical reflectance (TOR) method of carbon analysis developed by Huntzicker *et al.* (1982) has been adapted by several laboratories for the quantification of organic and elemental carbon on quartz-fiber filter deposits. While the principle used by these laboratories is identical to that of Huntzicker *et al.* (1982), the details differ with respect to calibration standards, analysis time, temperature ramping, and volatilization/combustion temperatures. A filter is submitted to volatilization at temperatures ranging from ambient to 550°C in a pure helium atmosphere, then to combustion at temperatures between 550°C and 800°C in a 2% oxygen and 98% helium atmosphere with several temperature ramping steps. The carbon which evolves at each temperature is converted to methane and quantified with a flame ionization detector.

The reflectance from the deposit side of the filter punch is monitored throughout the analysis. This reflectance usually decreases during volatilization in the helium atmosphere owing to the pyrolysis of organic material. When oxygen is added, the reflectance increases as the light-absorbing carbon is combusted and removed. Organic carbon is defined as that which evolves prior to re-attainment of the original reflectance, and elemental carbon is defined as that which evolves after the original reflectance has been attained. By this definition, "organic carbon" is actually organic carbon that does not absorb light at the wavelength used (632.8 nm) and "elemental carbon" is light-absorbing "organic" and "elemental" carbon. The TOT method (Cary, 1990; Turpin et al., 1990a) applies the same thermal/optical carbon analysis method except that the transmission instead of reflectance of the filter punch is measured.

The TMO method (Mueller *et al.*, 1982; Fung, 1990) uses manganese dioxide (MnO_2), present and in contact with the sample throughout the analysis as the oxidizing agent. Temperature distinguishes between organic and elemental carbon: carbon evolving at 525°C is classified as organic carbon, and carbon evolving at 850°C is classified as elemental carbon.

The major area of concern in thermal carbon analysis is that there are at present no common definitions of "organic" and "elemental" carbon. Each of the thermal carbon analysis methods divides the evolved carbon into segments which are defined by: 1) temperature; 2) rate of temperature increase; 3) composition of atmosphere surrounding the sample; and 4) method of optical correction for pyrolysis.

The definitions of organic and elemental carbon are, therefore, operational and reflect the method and purpose of measurement. For light extinction budgets, light-absorbing carbon is a more useful concept than "elemental" carbon. Light-absorbing carbon is not entirely constituted by graphitic carbon, since there are many tarry organic materials which absorb light. Even the "graphitic" black carbon in the atmosphere has only a poorly developed graphitic structure with abundant surface chemical groups such as hydroxyl. For source apportionment by receptor models, one would want to have several distinct fractions of carbon in both source and receptor samples. Differences in ratios of the carbon concentrations in these fractions form part of the source profile which distinguishes the contribution of one source from the contributions of other sources.

The Carbonaceous Species Methods Comparison Study (CSMCS, Hering *et al.*, 1990; Lawson and Hering, 1990) compared results from several variations of the thermal (T), thermal/optical reflectance (TOR, Chow *et al.*, 1993b), thermal/optical transmission (TOT), and thermal manganese oxidation (TMO) methods for organic and elemental carbon; spiking experiments for elemental carbon; and elemental carbon by optical absorption (OA), photoacoustic spectroscopy, and nonextractable mass. The thermal (T) methods, as distinct from thermal/optical methods (TOR, TOT), have no optical correction for pyrolysis. The CSMCS included samples from woodburning-dominated environments, source samples from diesel and various types of spark-ignition vehicles, and a photolytic smog-chamber aerosol (Cadle and Mulawa, 1990; Countess, 1990; Fung, 1990; Shah and Rau, 1991; Turpin *et al.*, 1990a).

All of the carbon analysis methods — T, TOR, TOT, TMO — agree within 5 to 15% on the sum of organic and elemental carbon in ambient samples and source samples (Countess, 1990; Houck *et al.*, 1989; Kusko *et al.*, 1989; Shah and Rau, 1991) and, on the average, within 3% on standards. Evaluation of these methods then becomes a matter of assessing how they differentiate between organic and elemental carbon. Comparison with respect to elemental carbon alone is a convenient way to compare methods since organic carbon is essentially the complement of elemental carbon.

The TOR systems at OGI and DRI give similar splits between organic and elemental carbon (Countess, 1990; Shah and Rau, 1991), within ~ 12% referred to elemental carbon or a few percent referred to total carbon. Excellent agreement between OGI TOR elemental carbon and nonextractable (in toluene/*n*-propanol) mass has been obtained on diesel exhaust particulate matter (Japar *et al.*, 1984). Elemental carbon by DRI TOR is said (Allen, 1991) to agree fairly well with real-time optical transmission measurements on the Lawrence Berkeley Laboratory aethalometer (Hansen *et al.*, 1982) in the Harvard Uniontown (PA) Acidic Aerosol Study in July and August 1990.

There is good agreement between TOR and TOT in some studies but not in all. In the CSMCS ambient samples, collected in the Los Angeles air basin at Citrus College in Glendora, CA, the elemental carbon averages stood in the order TOR > OA > TMO ≈ T > TOT. The difference in elemental carbon between TOR and TOT was approximated by a factor of two; elemental carbon constituted ~ 20% of the carbon in these samples, so the disparity corresponds to ~ 14% of the total carbon. In the CSMCS source samples, TOR and TOT agreed within ~ 1% on diesel exhaust particulate matter (elemental carbon ≈ 80% of total carbon) but TOR exceeded TOT on the others, the worst being the woodsmoke-dominated samples where the disparity was four- to seven-fold in elemental carbon. Houck *et al.* (1989) found disparities in comparisons of nine different types of source samples and source-dominated samples, and reported elemental carbon ratios $\overline{TOR}/\overline{TMO}/\overline{TOT} \approx 1.6/1.35/1$; the comparison is discussed in more detail by Shah and Rau (1991).

Shah and Rau (1991) have suggested that in the TOR and TOT methods the reflectance of the filter surface regains its initial value before the transmittance does, because of unburned pyrolytic material beneath the surface, causing TOR to be undercorrected for pyrolysis and

hence to read erroneously high on elemental carbon while TOT is more nearly correct. Countess (1990) concluded that TOR underestimates the amount of charring compared to TOT, and support can be found in certain observations by Turpin *et al.* (1990a) regarding filter blackening. If TOR and TOT are equivalent, then TOR can be evaluated further through evaluation of TOT. Comparison of the TOT method (two laboratories) with photoacoustic spectroscopy gave excellent agreement on elemental carbon. This was established on Dearborn (MI) ambient aerosol in 1986 (Adams *et al.*, 1989) and at the Claremont site during SCAQS (Adams *et al.*, 1990; Turpin *et al.*, 1990b).

TOR and TMO agreed within a few percent in elemental carbon in the diesel exhaust particulate sample from the CSMCS. Elemental carbon in the smog-chamber aerosol read ~ 2% of total carbon by TOR/TOT, 8% by TMO, and presumably was in fact zero. Otherwise, TOR was consistently higher than TMO on elemental carbon, more so when elemental carbon was a small fraction of total carbon. In the ambient samples (elemental carbon ≈ 20% of total carbon), the disparity was a factor of 1.6 ± 1.2, or ~ 9% of the total carbon. The largest disparity was in the two woodsmoke-dominated samples (elemental carbon ≈ 11% of total carbon), with TOR/TMO ratios 8 and 53 — and with TMO lower by far than any other method (T, TOR, TOT, OA). TMO in one sample gave only 25% as much elemental carbon as the mean of the other methods and laboratories; and in the other sample, TMO gave only 4% as much.

Another factor that should be considered is that the TMO analytical conditions are derived based on properties of polycrystalline graphite as the elemental carbon. High-molecular weight material that is virtually elemental carbon in composition, or in general forms of "elemental carbon" less difficult to oxidize than polycrystalline graphite, will be classified as organic by the TMO method as presently calibrated.

The excellent agreement among TOR, TMO, and TOT on diesel exhaust particulate matter is informative when set against the situation on woodsmoke-dominated samples. There is very little polymeric or light-absorbing organic material in diesel exhaust particulate matter (Szkarlat and Japar, 1983). Most of the light-absorbing carbon exhibits a weakly ordered structure approaching that of polycrystalline graphite (Rosen and Novakov, 1977; Rosen *et al.*, 1978, 1979, 1982). For chemical reactivity purposes this structural description may be misleading. It is more appropriate to think of the material as consisting of assemblies of large (~ 130 carbon atoms) stacked polynuclear aromatic hydrocarbon molecules of dimensions ~ 2 nm x 2 nm, six layers per stack, with reactive chemical groups on many or most of the edge carbons (Ebert, 1990). Possibly this material would evolve at high enough temperatures to be classified as elemental carbon by all methods, whereas some of the light-absorbing carbon in woodsmoke-dominated samples may evolve under conditions (525°C in the presence of oxidant) which in the TMO method would classify it as organic but which in the TOR method would classify it as elemental. Also, pyrolysis should be relatively unimportant in diesel exhaust particulate matter.

In general, the TMO method used for SCAQS carbon analysis will provide total carbon similar to that measured by other carbon analysis methods. The TMO method generally

attributes more of the total carbon to organic carbon and less to elemental carbon than the thermal/optical methods (TOR, TOT) which have been applied in prior ambient sampling and source characterization studies in the SoCAB. Therefore, direct comparisons of SCAQS organic and elemental carbon concentrations with those from other studies should not be made. Only total carbon levels should be compared.